ASSESSING CYANOBACTERIA IN A SMALL RESERVOIR USING UNMANNED AERIAL VEHICLE SYSTEMS (UAVs): A CASE STUDY OF HIGH FLIGHT FARM DAM

by

Nobubelo Ngwenya

Submitted in fulfilment of the academic requirements of

Master of Science in Hydrology

in

Centre for Water Resources Research

School of Agricultural, Earth and Environmental Sciences

College of Agriculture, Engineering and Science

University of KwaZulu-Natal

Pietermaritzburg

South Africa

January 2025

PREFACE

The research contained in this thesis was completed by the candidate while based in the Discipline of Hydrology, School of Agricultural, Earth and Environmental Sciences of the College of Agriculture, Engineering and Science, University of KwaZulu-Natal, Pietermaritzburg Campus, South Africa. The research was financially supported by the Water Resource Commission of South Africa.

The contents of this work have not been submitted in any form to another university and, except where the work of others is acknowledged in the text, the results reported are due to investigations by the candidate.

Signed: Prof. T. Mabhaudhi

Date: 28 January 2025

Signed: Dr. T. Bangira

Date: 28 January 2025

DECLARATION 1: PLAGIARISM

I, Nobubelo Ngwenya declare that:

(i) the research reported in this thesis, except where otherwise indicated or acknowledged, is my original work;

(ii) this thesis has not been submitted in full or in part for any degree or examination to any other university;

(iii) this thesis does not contain other persons' data, pictures, graphs or other information, unless specifically acknowledged as being sourced from other persons;

(iv) this thesis does not contain other persons' writing, unless specifically acknowledged as being sourced from other researchers. Where other written sources have been quoted, then:

a) their words have been re-written but the general information attributed to them has been referenced;

b) where their exact words have been used, their writing has been placed inside quotation marks, and referenced;

(v) where I have used material for which publications followed, I have indicated in detail my role in the work;

(vi) this thesis is primarily a collection of material, prepared by myself, published as journal articles or presented as a poster and oral presentations at conferences. In some cases, additional material has been included;

(vii) this thesis does not contain text, graphics or tables copied and pasted from the Internet, unless specifically acknowledged, and the source being detailed in the thesis and the References sections.

Signed: Nobubelo Ngwenya

Date: 28 January 2025

DECLARATION 2: PUBLICATIONS

The role of the student in each paper and presentation is indicated. The * indicates the corresponding author.

Chapter 3

1. Ngwenya, N*., Bangira, T., Sibanda, M., Gurmessa, S.K. and Mabhaudhi, T., 2025. UAV-based remote sensing of chlorophyll-a concentrations in inland water bodies: A systematic review. Geocarto International. https://doi.org/10.1080/10106049.2025.2452246.

The research in this paper is based on the systematic review that the student carried out under the supervision of Prof Tafadzwanashe Mabhaudhi, Dr. Tsitsi Bangira, Dr. Mbulisi Sibanda, and Prof. Seifu Kebede Gurmessa. The student designed the review framework, collected and analysed the relevant literature, and authored the manuscript. This work would not have been possible without the guidance and insights provided of the student's supervisors, whose expertise significantly contributed to the development and completion of this study.

Chapter 4

2. Ngwenya, N*., Bangira, T., Sibanda, M., Gurmessa, S.K., Gokool, S. and Mabhaudhi, T. (2025), (*in press)* Assessing cyanobacteria in a small reservoir using unmanned aerial vehicle systems (UAVs).

This paper presents an analysis of in situ water quality data collected by the student at High Flight Farm Dam. The student was responsible for field sampling, laboratory analysis, and manuscript preparation. The UAV images used in this study were collected with assistance from Dr. Shaeden Gokool. The paper is based on Chapter 4 of the student's research and is under review. The collaboration and technical expertise of the co-authors significantly contributed to the successful completion of this work.

[redacted]

Signed: Nobubelo Ngwenya

Date: 28 January 2025

ABSTRACT

Monitoring water quality, particularly chlorophyll-a (chl-a) concentrations, is critical for managing irrigation water, as excessive chl-a can degrade aquatic ecosystems and reduce water availability. While multispectral satellite-based remote sensing is widely used, its spatial resolution is inadequate for small water bodies, which are crucial to smallholder farmers. Unmanned Aerial Vehicles (UAVs) offer high-resolution, near-real-time data, presenting a promising solution. This thesis investigates UAV-based multispectral imaging for chl-a estimation in small reservoirs through an empirical study in South Africa, supported by a background systematic review of existing literature. The empirical study integrates UAV-based multispectral data from April, June, and July 2024 with in-situ measurements of chl-a, total nitrogen (TN), total phosphorus (TP), and dissolved oxygen (DO). The machine learning models tested include Artificial Neural Networks (ANN), Random Forest (RF), Support Vector Machine (SVM), and Extreme Gradient Boost (XGBoost), K-Nearest Neighbours (KNN), with ANN consistently outperforming the others and achieving the highest R^2 values across the three sampling periods: 0.949 (April), 0.991 (June), and 0.734 (July). The green, red, and red-edge bands were the most sensitive for chl-a estimation. Seasonal patterns emerged, with high chl-a concentrations in April and June, followed by a decline in July due to reduced water levels. Strong correlations were found between chl-a and nutrient parameters, particularly TP (R^2 = 0.879) and TN (R^2 = 0.711) in July. This study highlights the potential of UAV-based remote sensing for high-resolution chl-a monitoring in small water bodies. This study demonstrates the potential of UAV-based remote sensing for accurate, localized, and detailed chl-a monitoring in small water bodies, offering valuable insights for water resource management in smallholder agricultural systems worldwide.

ACKNOWLEDGEMENTS

I would like to express my sincere gratitude to the Lord Almighty for His guidance throughout this academic journey. I am deeply thankful to my supervisors, Dr. Tsitsi Bangira and Dr. Mbulisi Sibanda, for their consistent support, guidance, and constructive feedback. I also appreciate Dr. Shaeden Gokool for assisting with UAV image acquisition. Special thanks go to Prof. Seifu Kebede Gurmessa for guidance during lab preparations and analyses, and to Prof. Tafadzwanashe Mabhaudhi and the Water Research Commission (WRC) for financial support and assistance with fieldwork logistics. I acknowledge the support of Celuxolo Dlamini, Kuhlekonke Mathenjwa, Thulani Mnguni, and Khayelihle Msomi during field data collection. I am also grateful to the laboratory staff; Brice Gijsbertsen, Vivek Naiken, Khulekani Mkhonza, Busisiwe Mazibuko, Thokozani Nkosi, and the late Wilson Sikhakhane for their technical assistance. A special thanks to my colleague Shannyn Pillay for her collaboration and my peers, including Nqobile Nkomo, Joseph Fukaleza, Ayanda Luthuli, and Anita Masenyama, for their valuable support during various stages of this work. I would like to thank my family for their unwavering support: my husband, Bongani Mpofu, for his patience and understanding throughout this process, and my daughter, Emihle Nkanyezi Mpofu, for her presence and joy. To my parents, Sikhangele Moyo and Wilfred Ngwenya, your encouragement has been instrumental in my journey. Lastly, I appreciate the assistance provided by the School's administrative staff, particularly Noxolo Mncwabe, Pamela Mkhize, and Noluthando.

TABLE OF CONTENTS

Page

LIST OF FIGURES

Figure **Page**

LIST OF TABLES

Table **Page**

CHAPTER 1: INTRODUCTION

1.1 Background

The quality of water in reservoirs is affected by changes in land use and cover due to human activities (Meneses *et al.*, 2015; Hua, 2017; Tahiru *et al.*, 2020). Agriculture is the dominant land use globally, covering nearly half of the earth's surface and consuming the majority of freshwater resources (Schürings *et al.*, 2022). This extensive land use is vital for ensuring food security. In South Africa, with a population exceeding 60 million (Worldometers.info, 2023), the increasing demand for agricultural production has led to higher usage of fertilisers and pesticides to boost crop yields (Baiphethi and Jacobs, 2009; Davis *et al.*, 2017). This intensified agricultural activity, along with urbanisation and industrialisation, contributes to significant nitrogen and phosphorus runoff, which accelerates nutrient pollution in freshwater resources (Bashir *et al.*, 2020). Furthermore, mining, deforestation, and stream bank cultivation exacerbate water quality degradation, driving eutrophication in water bodies (Banda and Kumarasamy, 2020; Bashir *et al.*, 2020; Sun *et al.*, 2022). Climate change further compounds these challenges, resulting in more unpredictable weather patterns and increased water stress.

South Africa, with an annual average precipitation of 464 mm, less than half the global average, is classified as water-stressed (Otieno and Ochieng, 2004; Du Plessis, 2017). The country faces a significant water scarcity issue (Lade *et al.*, 2014; Peace and Muhammad, 2020). To mitigate this challenge, South Africa relies heavily on small (1 m^2) and large (surface area > 20,000 m^2) reservoirs to secure water supply. However, while these reservoirs play a critical role in addressing water shortages, their water quality is increasingly at risk due to human activities, particularly nutrient pollution from agriculture. Fertilisers often used to boost crop yields, introduce nitrogen and phosphorus into water bodies, creating conditions that significantly degrade water quality. Studies have further detected harmful levels of herbicides like 2,4-D and glyphosate in water samples from agricultural regions, highlighting their potential threat to aquatic ecosystems (Carnie, 2019; Horn *et al.*, 2019).

This nutrient enrichment leads to eutrophication, a process that triggers harmful algal blooms (HABs), primarily cyanobacteria, in water bodies. These blooms severely impact water quality by increasing turbidity, reducing dissolved oxygen, and lowering water transparency (Downing *et al.*, 2001; Falconer, 2001). Additionally, climate change exacerbates cyanobacteria proliferation by altering weather patterns and increasing water temperatures (Rankinen *et al.*,

2019). The consequences of HABs extend beyond water quality, as they also threaten irrigation systems by clogging filters, which hampers crop growth and in turn, compromises food security (Jeong *et al.*, 2016; NSWG, 2017; Singh *et al.*, 2018). Given these challenges, water management authorities emphasise the importance of routinely monitoring cyanobacteria at both temporal and spatial scales to understand better and manage their impacts (Palmer *et al.*, 2015; Banda and Kumarasamy, 2020). One widely used method for assessing eutrophication and detecting HABs is measuring chlorophyll-a (chl-a), a primary indicator of phytoplankton biomass (Matthews, 2017; Liu *et al.*, 2019).

Traditionally, chl-a has been measured through in situ sampling and subsequent laboratory analysis, but these methods are time-intensive and costly and lack the spatial and temporal coverage needed for effective monitoring (Modiegi *et al.*, 2020). Given these limitations, remote sensing platforms such as ground-based, airborne, and spaceborne systems, offer efficient solutions for large-scale water quality monitoring. These platforms are equipped with advanced sensors, including hyperspectral and multispectral instruments, which enhance the precision of detecting chl-a as well as other water quality indicators. Remote sensing provides extensive spatial and temporal coverage, enabling continuous and dynamic monitoring of water bodies (Yang *et al.*, 2022; Tian *et al.*, 2023; Bangira *et al.*, 2024). Chl-a can be detected through remote sensing owing to its distinctive optical properties, characterised by the absorption of light in the red and blue wavelengths and reflection in the green and near-infrared regions (Wu *et al.*, 2010; Gao *et al.*, 2015).

While hyperspectral sensors offer high accuracy in detecting chl-a, their high costs and computational demands limit widespread application (Cao *et al.*, 2021). Multispectral satellite data, such as from Medium Resolution Imaging Spectrometer (MERIS), Sentinel-2, and Landsat 8-9, provide a more accessible alternative, offering improved spatial and spectral resolutions for large-scale applications (Matthews *et al.*, 2010; Saberioon *et al.*, 2020). Despite the advantages of satellite-based remote sensing, challenges such as coarse resolution and limited control over data collection persist (Yang *et al.*, 2022). To address these gaps, UAVs emerge as a promising alternative platform for multispectral sensors, delivering higher spatial resolution, controlled data collection, and flexibility in timing, making them ideal for monitoring small water bodies with precision and at a relatively low cost (Xiang *et al.*, 2019; Yao *et al.*, 2019).

A wide range of studies have demonstrated the effectiveness of UAVs in detecting chl-a in inland water bodies (Cillero Castro *et al.*, 2020; Ahn, 2021; Xiao, 2022). However, the majority of these studies have focused on larger reservoirs in developed countries, leaving a gap in understanding their applicability in smaller reservoirs. Many of these studies have also utilised machine learning algorithms (MLAs) to enhance chl-a estimation accuracy, highlighting their potential for integrating UAV-derived multispectral data. This study aims to assess the effectiveness of UAV multispectral data for monitoring chl-a levels in small water bodies in South Africa, while also exploring the role of MLAs in improving prediction models.

1.2 Rationale for the Research (nature and scope)

South Africa, like many developing countries, faces increasing challenges in managing its water resources due to a rising population and land use activities. Agricultural practices, such as using nitrogen, phosphorus, and potassium (NPK) fertilisers, and urbanisation contribute to nutrient-rich effluent discharge, leading to eutrophication. Climate change exacerbates this issue by creating conditions favourable for algal blooms, which degrade water quality. Cyanobacteria blooms harm the environment and cause practical issues, such as clogged irrigation systems and reduced crop yields. The ability of UAVs to capture high-resolution and site-specific data, makes them an ideal tool for monitoring water quality in smaller water bodies. This research demonstrates the feasibility of UAV technology for collecting high-resolution imagery to monitor chl-a levels in small water bodies. Machine learning algorithms such as Artificial Neural Networks (ANN), Extreme Gradient Boosting (XGBoost), and Random Forest (RF) will be employed to construct and evaluate chl-a estimation models using UAV-derived multispectral data. The findings aim to enhance water resource management by informing decision-making, improving water treatment and irrigation maintenance, and supporting agricultural sustainability and food security.

1.3 Aim

To assess the impacts of eutrophication in small water bodies used for irrigation purposes within the Umgeni catchment using UAV remotely sensed data.

1.4 Objectives

- To use the Preferred Reporting Items for Systematic Reviews and Meta-Analysis (PRISMA) method to systematically review the literature on UAV-based remote sensing of chlorophyll-a concentrations in inland water bodies.

- To estimate the spatiotemporal variability of chlorophyll-a concentrations in a reservoir using UAV data and different machine learning algorithms.
- To assess the potential of remotely sensing chlorophyll-a as a proxy for total nitrogen (TN), total phosphorus (TP), and dissolved oxygen (DO) using UAV remotely sensed data.

1.5 Research Questions

- What are the key findings and trends in the existing literature regarding the use of UAV-based remote sensing for assessing chlorophyll-a concentrations in inland water bodies?
- To what extent can remotely sensed predicted chlorophyll-a concentrations effectively serve as a proxy for assessing Total Nitrogen (TN), Total Phosphorus (TP), and Dissolved Oxygen (DO) in inland lakes?

1.6 Dissertation Outline

This thesis consists of five chapters.

Chapter 1 outlines the general introduction of the study, the rationale of the research, the aim, objectives, and research questions.

Chapter 2 gives a literature review of the factors that lead to eutrophication and ultimately impact irrigation water quality. It also discusses the parameters, focusing on chl-a and nutrients used to assess levels of eutrophication, as well as the methods with a special highlight of the UAV technology. Additionally, this chapter also gives a summary of the case studies that utilised UAVs to monitor chl-a in small water bodies. Lastly, it outlines the gap, challenges, and opportunities.

Chapter 3 gives a systematic review of the studies that have used sensors onboard UAVs to monitor Chl-a on inland lakes.

Chapter 4 focuses on the utilisation of remotely sensed data collected by multispectral cameras onboard UAVs to monitor Chl-a at a small water body in High Flight Farm. It narrates the laboratory methods employed to analyse chl-a, total nitrogen, total phosphorus, and dissolved oxygen and the processing of the UAV image for chl-a retrieval. The results on the

spatiotemporal variability of chl-a and the possibility of using chl-a as a proxy for nutrients and dissolved oxygen in aquatic systems is also discussed.

The final chapter, Chapter 5, integrates the work conducted in Chapters 3 and 4 and then provides conclusions and future research possibilities.

CHAPTER 2: LITERATURE REVIEW

This chapter begins by examining Land use and land cover (LULC) changes in the Umgeni catchment, highlighting their impact on ecological systems and water quality. It then delves into the aspect of eutrophication which is a result of LULC changes, its causes, effects, and prevalence in South African water bodies. The review also explores the role of cyanobacteria as an indicator of eutrophication and its connection to nutrient enrichment and climate change. Lastly, the chapter emphasises the advancements in remote sensing technologies, such as satellite systems and unmanned aerial vehicles (UAVs), for monitoring chl-a concentrations, addressing the limitations of traditional methods, and enhancing water quality assessment in inland waters.

2.1 Land Use and Land Cover Changes in Umgeni Catchment

Land use and land cover (LULC) changes result from intricate interactions between human activities and the environment, potentially impacting ecosystem services (Fan *et al.*, 2016). Several studies have recorded land use changes in the KwaZulu-Natal province of South Africa, where the Umgeni catchment is situated. Before exploring specifics about the Umgeni catchment, it is pertinent to discuss the broader context of land use in KwaZulu-Natal. Between 1994 and 2011 in KwaZulu, the naturally vegetated land area decreased from 73% to 53%, driven by increased urbanisation, agriculture, and commercial plantations (Fairbanks and Everard, 2000; Bulcock and Jewitt, 2012). A recent study also examined land use and land cover changes in KwaZulu Natal from 1995 to 2020. The findings revealed irregular variations in cultivated areas, a decline in forest and grassland, an increase in urban areas, and fluctuations in water and unused land. These changes were found to be predominantly driven by socio-economic factors, with the demand for growing sugarcane, tea, and pineapple motivating small-scale farmers to convert natural land to cultivation (Wang *et al.*, 2023).

A noteworthy portion of the KwaZulu Natal population resides in the Umgeni catchment, heavily relying on water supplies from its upstream regions. As a result, human activities are causing ecological disturbances in the catchment (Beires, 2010). A study by Namugize *et al.* (2018) noted that in 2011, cultivation, forest plantations, and natural vegetation covered approximately 85% of the Umgeni catchment, specifically upstream of the Albert Falls Dam. More so, the natural vegetation land area decreased between 1994 and 2011 owing to urban expansion and other land uses. Also, sub-catchments around the Midmar Dam (upper of

Umgeni catchment), marked by high urbanisation as a result of high population density, experienced changes in land use, and land cover. This study also highlighted a significant observation of increased nutrient levels in Umgeni catchment water bodies, particularly during the rainy season, attributed to LULC changes within the catchment. These shifts in land use and cover were identified as a major contributor to the degradation of water quality. This underscores the critical need to understand and manage the impacts of land use on nutrient loading at a catchment level as this aids in improving water quality downstream of streams and rivers (Brion *et al.*, 2011; Ding *et al.*, 2016).

2.2 Eutrophication in Upper Umgeni Catchment

Literature notes that the excessive use of pesticides and fertilisers contributes to nutrient loading, specifically phosphorus, and nitrogen, in water bodies, a phenomenon known as eutrophication (Serediak *et al.*, 2014; Gao *et al.*, 2015; Dlamini *et al.*, 2016). Farmers, aiming to enhance production, frequently utilise nitrogen and phosphorus-based fertilisers and pesticides (Baiphethi and Jacobs, 2009; Davis *et al.*, 2017). Some studies have recorded the highest loads of 4 602 kg/year of ammonia (NH_3), 7 998 kg/year of nitrate, and 800 kg/year of total phosphorus entering Midmar Dam (Van Deventer *et al.*, 2022). Additionally, eutrophication in the catchment is exacerbated by inadequate sanitation maintenance systems impacting water quality within the Midmar sub-catchment, as noted by Ramnath (2010).

The combination of high nutrient concentrations, elevated temperatures due to climate change, and light energy creates favourable conditions for algae proliferation in water bodies (Rankinen *et al.*, 2019; Paerl and Barnard, 2020). However, the flourishing algal blooms contribute to fluctuations in dissolved oxygen (DO) levels (Koparan *et al.*, 2018). Consequently, the alteration in DO emerges as a noteworthy outcome of eutrophication in water bodies (Omer, 2019; Zhao *et al.*, 2021). As a result of eutrophication in aquatic environments, there is a significant change in the levels of DO, which has been identified as a crucial indicator of biological activity and eutrophication (Chung and Yoo, 2015; Omer, 2019; Zhao *et al.*, 2021). It is crucial to emphasise that maintaining healthy water quality entails DO levels above the critical threshold of 4.5 mg/L (Banerjee *et al.*, 2019).

South Africa has witnessed a rapid increase in eutrophication, jeopardising its water bodies' functionality in the last decade (Van Ginkel, 2011). Harding (2015), reported that eutrophication affects 76% of South African dams. In addition, Matthews and Bernard (2015)

study in South Africa on the 50 largest water bodies revealed alarming statistics, with 62% of the dams showing high levels of nutrient enrichment and 52% experiencing cyanobacterial blooms. The South African government has thus been implementing measures to address eutrophication, such as the National Eutrophication Monitoring Programme (NEMP). This programme is currently operational in over 80 impoundments in the country (DWS, 2022). The NEMP programme has produced valuable data sets, such as the Cyanolakes website, focused on chlorophyll-a (chl-a) and cyanobacterial analyses. Despite the initial plans of the government to expand the network from 50 to 100 reservoirs by 2012 (DWAF, 2004), challenges, including funding constraints, have limited its reach. The efforts by the government, though commendable, indicate that more extensive research and proactive measures are required to combat eutrophication in South African water bodies.

2.3 Cyanobacteria (blue-green algae)

Cyanobacteria, formerly known as blue-green algae, are a diverse group of prokaryotic bacteria that can exist as single-celled or multicellular organisms and undergo photosynthesis as part of their metabolic processes (NEMP, 2002). These organisms thrive in environments with water, light, carbon dioxide, and inorganic substances, with optimal growth occurring at temperatures above 25ºC (Falconer *et al.*, 1999). Thus, climate change emerges as one of the significant drivers of cyanobacterial blooms, fueled by rising global temperatures and erratic rainfall patterns (Joehnk *et al.*, 2008; Paerl and Barnard, 2020). Cyanobacteria blooms indicate increased eutrophication rates (Van Ginkel, 2011) and pose adverse effects, forming toxic scum that can clog irrigation systems such as pumps and filters (DWAF, 2004).

To assess cyanobacteria algal levels, two common algal pigments, chl-a, and phycocyanin, are frequently employed (Kutser *et al.*, 2006; Urquhart *et al.*, 2017; Shi *et al.*, 2019). However, it is challenging to estimate phycocyanin in eutrophic water bodies because it is less sensitive to the currently available commercial equipment (Stumpf *et al.*, 2016; Fernandez-Figueroa *et al.*, 2022). Thus, chl-a serves as a widely used indicator parameter for eutrophication (Harvey *et al.*, 2015; Lins *et al.*, 2017; Rankinen *et al.*, 2019; McEliece *et al.*, 2020; Cao *et al.*, 2023) and functions as a proxy for algae (Schaeffer *et al.*, 2013; Kim and Ahn, 2022). Table 2.1 offers a summary of the target water quality range meanings of algae in a water body. Remote sensing is a valuable method for estimating chl-a as an important indicator for water quality, by utilising its optically active properties to monitor its presence.

Table 2.1: Target water quality range for algae (DWAF, 1996)

Range	Interpretations
$0 - 15\mu g/L$	No health effects
$15 - 30\mu g/L$	Algal scum is likely to occur, water may take a green colour resulting in reduced light penetration.
$> 30\mu g/L$	Water appears to have significant levels of algal scum and may present a considerable nuisance.

2.4 Remote Sensing of Chlorophyll-a (Chl-a) and Spectral Properties

Remote sensing is a process of collecting of information about an object, land region, or ecosystem process via a non-contact device (Lillesand *et al.*, 2015). Remote sensing is a cost-effective method that complements in-situ data (Li and Li, 2004). Remote sensing makes use of carriers known as platforms, which are equipped with sensors, to obtain data from a distance. There are three types of platforms: air-borne platforms (manned aircraft, unmanned aerial vehicles (UAVs)), ground-borne platforms (ground-based laser scanning (LiDAR), terrestrial photogrammetry), and space-borne platforms (low-earth orbit platforms, geostationary orbit platforms). In remote-sensed water quality, it is fundamental to understand the spectral properties of a parameter of interest.

Chl-a exhibits distinctive spectral properties crucial for its remote sensing and quantification. Chl-a is associated with four key bands: near-infrared (NIR), red (R), blue (B), and green (G) (Kabbara *et al.*, 2008; Chebud *et al.*, 2012). Research by Gitelson (1992) revealed that chl-a primarily absorbs and reflects light within the 400 nm and 500 nm wavelength ranges. It has a high absorption rate in the blue and red regions, particularly around 443 and 675 nm, respectively. It reflects strongly in the green and red-edge spectra, specifically in 550-555 nm and 685-710 nm, respectively (Gitelson, 1992; Kirk, 1994; Mobley, 1994). High concentrations of chl-a are observed by an increase in reflectance at bands G and R and a decrease in reflectance at band B (Pulliainen *et al.*, 2001). The maximum reflectance associated with chl-a is observed at 580 nm (Dekker, 1993), and peak reflection at 700 nm (Gitelson, 1992). Therefore, monitoring changes in reflectance within these bands, particularly increases in G and R and decreases in B, is instrumental in identifying high chl-a concentrations. Figure 2.1 shows the spectral absorbance graph of chl-a.

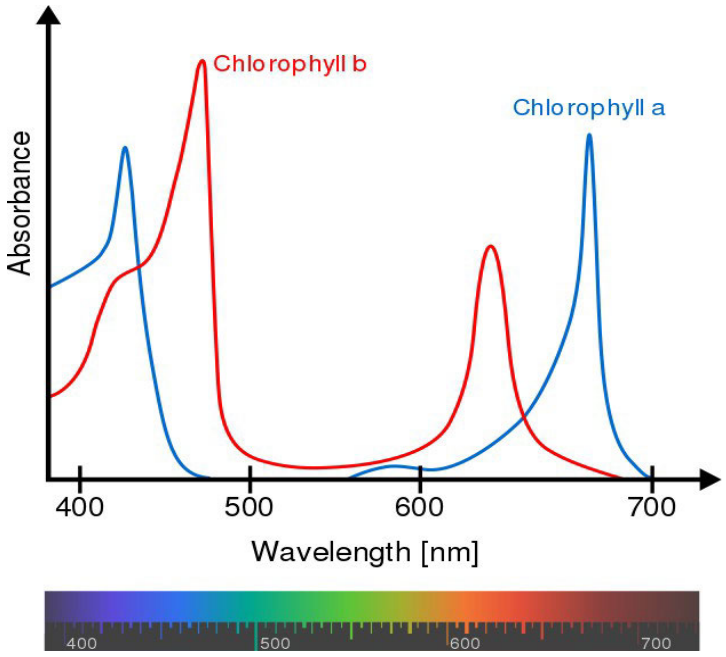

Figure 2.1: Spectral absorbance of chlorophyll-a (Pugliesi, 2012)

2.4.1 Remote Sensing of Chl-a using Satellites Borne Remotely Sensed Data

Satellite technology, when integrated with traditional monitoring methods, provides a valuable approach for assessing chl-a levels in aquatic systems. Globally, numerous studies have demonstrated the potential of satellite-based remote sensing for monitoring water quality, particularly chl-a concentrations. For instance, satellites like the Sentinel-2, Medium Resolution Imaging Spectrometer (MERIS), Landsat 8 OLI, and MODIS/AQUA have been widely used to derive spectral data linked to chl-a levels. These platforms provide significant advantages, including consistent temporal monitoring, broad spatial coverage, and cost-effectiveness, as they provide free access to historical and near real-time data (Torbick *et al.*, 2013; Matthews and Bernard, 2015; Lai *et al.*, 2021; Tian *et al.*, 2023). Applications extend to detecting harmful algal blooms (HABs) and monitoring biomass in large water bodies (Kutser *et al.*, 2006; Anderson, 2009). Studies, such as Harvey *et al.* (2015), have shown a strong correlation between satellite-derived chl-a measurements and field observations gathered within a 0–3 day time frame, achieving an RMSE of 64% and a mean normalised bias (MNB) of 17%. Similarly, Gohin *et al.* (2020) demonstrated the use of VIIRS/NPP, OLCI-A/Sentinel-3, and MODIS/AQUA in detecting chl-a, revealing consistent trends between satellite retrievals and in situ measurements.

Despite their global utility, satellite platforms face inherent challenges. These include limited spatial resolution, particularly problematic for smaller water bodies like rivers and ponds (Anderson and Gaston, 2013; Palmer *et al.*, 2015; Adjovu *et al.*, 2023), and data inconsistencies caused by the time lag between field sampling and satellite overpasses (Su and Chou, 2015; Lai *et al.*, 2021). Cloud cover further complicates data acquisition by obscuring optical signals, which impacts accuracy (Sagan *et al.*, 2020). Also, satellite platforms have image signal-to-noise ratio (SNR), data storage, and transmission problems (Cao *et al.*, 2021; Yang *et al.*, 2022). To overcome these limitations, recent advancements in remote sensing have shifted focus toward higher-resolution platforms, such as unmanned aerial vehicles (UAVs).

In South Africa, satellite-based remote sensing has been applied to monitor chl-a concentrations in various water systems, including dams, reservoirs, and wetlands. Studies have utilised platforms like Landsat 8 OLI, MERIS, and Sentinel-2 to assess water quality parameters, with some success in identifying patterns of eutrophication and cyanobacteria blooms (Matthews, 2014; Malahlela *et al.*, 2018; Sakuno *et al.*, 2018; Ali *et al.*, 2022; Dzurume *et al.*, 2022). These studies highlight the cost-effectiveness and practicality of satellite imagery for large-scale monitoring. However, research on smaller water bodies remains scarce, as the coarse-spatial resolution of satellites limits their applicability in such contexts. Additionally, many South African studies emphasise larger lakes, often overlooking the importance of monitoring smaller water bodies critical for agricultural irrigation and domestic use.

This gap in research underscores the need for innovative approaches like UAV technology, which can provide higher spatial resolution, greater flexibility in data acquisition, and enhanced accuracy for monitoring smaller inland water bodies. By complementing satellite-based observations, UAVs can bridge the gap in monitoring water quality across various scales, particularly in resource-constrained regions like South Africa.

2.4.2 Remote Sensing of Chl-a using UAVs

In the recent years, UAVs have proven to be a valuable real-time monitoring tool for remote sensing in small inland waters (Xiang *et al.*, 2019; Román *et al.*, 2022). This technology utilises a lightweight system equipped with a spectrometer, Lidar, infrared sensor, and multispectral camera (Sayyed *et al.*, 2015). UAV flights are strategically conducted below cloud cover and in favourable weather conditions to ensure accurate data collection and prevent equipment

damage or loss (Jeong *et al.*, 2016; Koparan *et al.*, 2018; McEliece *et al.*, 2020; Román *et al.*, 2022).

Real-time monitoring with multispectral UAVs offers significant advantages, including speed, cost-effectiveness, high-resolution imagery, widespread coverage, and the ability to assess variations in water quality (McEliece *et al.*, 2020; Román *et al.*, 2022; Sun *et al.*, 2022). Multispectral UAVs, equipped with sensors of varying wavelengths, are particularly effective in capturing high-resolution images of inland waters compared to satellite sensors (Zang *et al.*, 2012; Shi *et al.*, 2019). This process is not only time-efficient but also yields comprehensive data (Wang *et al.*, 2020a).

Chl-a retrieval is achieved using models constructed using either or both empirical and machine learning methods. Retrieval models are established using physically measured data and reflectance of the optimal bands or band combinations or vegetation indices of chl-a. Different UAV models and multispectral sensors comprising the green, blue, red, red-edge, and near-infrared (NIR) bands are frequently employed by many studies. These bands have been found to work best in studying chl-a, phytoplankton, and aquatic plants (Visser *et al.*, 2013; Flynn and Chapra, 2014; Rhee *et al.*, 2018b). Also, the red and NIR wavelength bands in band algorithms show promising results in the estimation of chl-a in eutrophic aquatic environments (Shi *et al.*, 2019).

Cillero Castro *et al.* (2020) studied a small reservoir (4.5ha) in Spain which was known to be affected by cyanobacteria. This investigation used an empirical approach with band indices and algorithms to assess chl-a retrieval. Similarly, a longitudinal study successfully demonstrated the utility of UAVs in chl-a estimation through machine learning models in two distinct regions—a dam and a lake in Brazil Silveira Kupssinskü *et al.* (2020). Various regression models, including Random Forest (RF), linear regression, K-Nearest Neighbours (KNN), Support Vector Regression (SVR), LASSO, and Artificial Neural Networks (ANN), were employed in the study and the Random Forest model yielded the best results. Also, in China, Xiao *et al.* (2022) conducted a study on the downstream of a river during two dry seasons, emphasising chl-a estimation for water and environmental conservation. Their research combined machine learning and traditional regression methods for chl-a retrieval.

Furthermore, Bunyon *et al.* (2023) studied six lakes in the USA using a MicaSense multispectral sensor mounted on a UAV to assess cyanobacteria. The study used simple linear regression to assess chl-a measured using in-situ methods. Reflectance values extracted from the UAV were used to calculate different bands and indices (see Table 2.2). The classification for UAV images and chl-a indices was performed using random forest. To improve the accuracy of chl-a retrieval, other studies have made use of stacked machine models as they have been discovered to give the best results as compared to single techniques (Xiao *et al.*, 2022). Overall, studies have demonstrated that best-performing models have high values of the coefficient of determination (R^2), low values of the Root Mean Square Error (RMSE), and Mean Absolute Error (MAE) gives a summary of some of the studies that have successfully used multispectral sensors carried on UAVs to measure chl-a.

Table 2.2: Case studies of remote sensing of chl-a using UAV multispectral in inland waters

UAV	Sensor	Method	Indices	Model/s	Accuracy	Study Area	Author/(s)
Octocopter Atyges FV8	Multispectral RedEdge Micasense sensor: blue, 475 nm (B1), red 560 nm (B2), green 668 nm (B3), red edge 717 nm (B5), NIR 840 nm (B4)	Linear regression	SABI NDCI NDVI 2BDA 3BDA 3BDA 2BDA B3B1 GB1 GR	Empirical	R^2: 0.982 Pearson r: 0.991	Small reservoir, Spain	Cillero Castro *et al.* (2020)
SenseFly, Swinglet CAM model	4 band multispectral sensor (Band 2 (Blue, 0.490 µm), Band 3 (Green, 0.560 µm), and band 8 (NIR, 0.842 µm)	Machine learning -IDW, kriging, stochastic models for interpolation	None	LASSO SVR KNN ANN RF linear regression	LASSO: R^2: 0.315-0.351 SVR: R^2 0.413-0.634 KNN: R^2 0.761-0.896 ANN: R^2 0.726-0.900 RF: R^2 0.823-0.900 Linear regression: R^2: 0.315-0.353	Unisinos Lake and Broa Dam, Brazil	Silveira Kupssinskü *et al.* (2020)
Phantom 4 Multispectral (P4M) DJI UAV	Multispectral six-camera array (1 high-definition color sensor and five sensors: R, G, B, RE, and NIR)	-Vegetation indices -Multiple regression -Machine learning	28 Common vegetation indices	SVM RF ELM CNN	CNN: R^2 = 0.792, RMSE = 8.766, and MRE = 0.246	Erhai Lake, China	Zhao *et al.* (2022)

UAV	Sensor	Method	Indices	Model/s	Accuracy	Study Area	Author/(s)
DJI P4 multispectral UAV	1 color sensor (RGB) and 5 monochromatic sensors (blue 450 nm, green 560 nm ± 16 nm, red 650 nm ± 16 nm, red edge 730 nm ± 16 nm, and near-infrared 840 nm ± 26 nm)	-Regression models -Spectral band indices -Stacked Machine learning	2BDA	RF BP MLR XGBoost Least Absolute Shrinkage and Selection Operator	XGBoost R^2 :0.958; RMSE: 0.801; MAE: 0.478 RF-XGB: $R^{2:}$ 0.999; RMSE: 0.019; MAE: 0.017 RF: R^2 :0.762; RMSE: 1.393; MAE: 1.087	Zhanghe River, China	Xiao *et al.* (2022)
DJI M300 RTK UAV	MicaSense 10-bands (Coastal Blue-444 nm, B–475 nm, G–531 nm, G–560nm, R–650 nm, R–668 nm, RE–705 nm, RE–717 nm, RE–740 nm, NIR–842 nm)	-Regression models -Machine learning -Derivative bands	NDVI NDRE BNDVI cBNDVI NGBDI NGRDI SABI SHI index CI	-Random forest	R^2 = 0.940	Six Lakes, USA	Bunyon *et al.* (2023)
DJ P4 Multispectral (P4M)	Single RGB visible band and five multispectral bands (blue, green, red, red-edge, and NIR)	-Correlation analysis between spectral indices and chl-a -Stepwise linear regression	G2B NDCI NDTI NDVI NFH560 Ocx SABI 2BDA	-Empirical	R^2 ~ 0.650 RMSE ~ 6.25 MAE ~ 5	River confluence, China	Xiao *et al.* (2023)

Notes* R- Red, G- green, B – blue, NIR –near infrared, LR – Linear regression, SVR - Support Vector Regression, KNN- K Nearest Neighbors, RF - Random Forest, ANN - Artificial Neural Networks, MLR - Multiple Linear Regression, BP - Backpropagation Neural Network, XGBoost - eXtreme Gradient Boosting, BDA - band algorithm, SABI - surface algal bloom index, NDVI – Normalised Difference Vegetation Index, GA_XGBoost - genetic algorithm_extreme gradient boosting, NDCI - Normalised Difference Chlorophyll Index, , ELM - extreme learning machine, NDTI - Normalised Difference Turbidity Index SVM - Support Vector Machine, MRE - Mean Relative Error, CNN - convolutional neural network, NGBDI - normalised green blue difference index, DNN - Deep Neural Network, GA_RandomForest - genetic algorithm_RandomForest, AdaBoost - adaptive boosting, SHI index (named after the author Kun Shi), GA_AdaBoost - genetic algorithm_adaptive boosting, NDRE - normalised difference red edge index, cBNDVI - coastal blue normalised difference vegetation index, , FLH Blue - florescence line height—blue, NGRDI - normalised green red difference index, and cyanobacteria index (CI)

2.5 Reported Impacts of Nutrient Pollution and Water Quality Degradation

Nutrient pollution has been widely associated with serious environmental consequences in small water bodies, particularly eutrophication and harmful algal blooms, as reported in multiple studies (Su and Chou, 2015; Kim, 2016; Choo, 2018; Cillero Castro *et al.*, 2020; Wu, 2023). For example, in a case study from China, historical data indicated that many small reservoirs were either eutrophic or hypereutrophic. In response, submarine pipeline projects were implemented to protect potable water sources from nutrient pollution (Su, 2017). In Brazil, nutrient enrichment was also found to negatively affect the quality of drinking water (Cillero Castro *et al.*, 2020). Another study from China highlighted broader socio-economic impacts: pollution of the Zhan Wei Xin River deprived local communities of clean drinking water, caused agricultural losses through toxic irrigation water that harmed crops and soils, and led to fish deaths and ecological degradation (Yi, 2023). These examples illustrate how nutrient pollution not only threatens aquatic ecosystems but also has direct consequences for human health, food security, and livelihoods, reinforcing the importance of water quality monitoring and management in small water bodies.

2.6 Gaps, Challenges, and Opportunities

- Existing studies in South Africa have primarily used satellite-based imagery, which has limitations due to its coarse resolution, particularly in overseeing smaller water bodies susceptible to eutrophication. Also, these studies have concentrated considerably on water bodies supplying drinking water, overlooking irrigation reservoirs crucial for smallholder farmers.
- The utility of UAVs and machine learning techniques for precise chl-a retrieval in small inland waters, vital to smallholder farmers, remains understudied.
- Insufficient studies exploring the correlation between chl-a concentrations and Dissolved Oxygen (DO), Total Nitrogen (TN), and Total Phosphorus (TP).
- Lack of research on the potential limitations or confounding factors affecting the reliability of chl-a as a proxy for multiple water quality parameters.
- Lack of standardised methodologies for UAV-based chl-a concentration assessments, insufficient exploration of technological advancements impacting remote sensing accuracy and reliability, and inadequate understanding of factors influencing spatiotemporal variability in chl-a concentrations.

- There is a noticeable lack of research in the southern part of Africa, of UAV multispectral image-based monitoring for chl-a, while it is widely conducted in Europe, America, and Asia.
- The use of hyperspectral sensors presents an alternative, yet prohibitive costs pose challenges.
- Accessibility challenges for data collectors in remote areas, where smallholder farms are often situated, hinder effective monitoring. Moreover, the technical expertise required for operating UAV technology is lacking among smallholder farmers. The moderately high cost of UAVs presents a financial barrier to the adoption of precision agriculture practices.
- There is an opportunity for collaboration among stakeholders, including policymakers, the private sector, the government, and farmers, to provide resources for effective water resource management.
- The proficiency of machine learning algorithms in handling extensive datasets creates an opportunity to establish correlations between UAV imagery data and in-situ measurements.

CHAPTER 3: UAV-BASED REMOTE SENSING OF CHLOROPHYLL-A CONCENTRATIONS IN INLAND WATER BODIES: A SYSTEMATIC REVIEW[1]

3.1 Abstract

Monitoring chlorophyll-a content is crucial for irrigation water quality, as excessive levels can harm water bodies and reduce their volumetric capacity due to algal growth. While satellite data enhances monitoring, its coarse resolution limits application in small water bodies. Unmanned Aerial Vehicles (UAVs) offer high-resolution, near-real-time data, bridging this gap. This review explores global progress, gaps, and recommendations on UAV-based chlorophyll-a monitoring in small inland water bodies, focusing on sensor characteristics, platforms, validation data and retrieval algorithms, using the Preferred Reporting Items for Systematic Reviews and Meta-Analysis (PRISMA) approach. Multispectral sensors onboard DJI UAVs are the most widely used and, machine learning methods like random forest dominate chlorophyll-a inversion models. However, gaps remain in Africa due to high UAV costs, limited expertise and stringent regulations. Additionally, a universal chlorophyll-a retrieval method is also lacking. This review serves as a reference for future studies, highlighting UAVs' potential in water quality monitoring.

Keywords*: chlorophyll-a, inland waters, remote sensing, systematic review, unmanned aerial vehicle*

3.2 Introduction

Small water bodies between 1 m^2 and 20,000 m^2 with a maximum depth of no more than 8m (Biggs *et al.*, 2005) support over 70% of the world's population in arid and semi-arid areas, and this proportion is increasing. These small inland water resources store scarce and reliable water for crop irrigation during dry spells (Wisser *et al.*, 2010a). They are among the most vulnerable ecosystems, and any changes due to anthropogenic activities can affect specific water uses and endanger aquatic habitats. The major water quality threat in small water bodies is the excessive growth of cyanobacteria. The disposal of phosphorous, nitrogen, and nutrients from rivers and

[1] **Ngwenya, N**., Bangira, T., Sibanda, M., Gurmessa, S.K. and Mabhaudhi, T., 2025. UAV-based remote sensing of chlorophyll-a concentrations in inland water bodies: A systematic review. *Geocarto International*. https://doi.org/10.1080/10106049.2025.2452246.

streams, as well as prolonged sunlight hours and warm temperatures, accelerates cyanobacteria blooms. Understanding the quantity of cyanobacteria, often referred to as blue-green algae, in inland water resources is essential for the level of treatment required for agricultural, domestic, and industrial use. Therefore, it is more important than ever to consider water quality and strictly monitor the number of harmful bacteria in inland water bodies.

Cyanobacteria is a photosynthetic and toxin-producing bacteria that significantly impairs water quality (Aranda *et al.*, 2023). These bacteria are characterised by their single chlorophyll type, termed chlorophyll-a (chl-a) and a variety of carotenoids, including the blue pigment phycobilin and the red pigment phycoerythrin. Chl-a is commonly used as a proxy of phytoplankton biomass (Gregor and Maršálek, 2004; Søndergaard *et al.*, 2011; Stengel *et al.*, 2023). Cyanobacteria are the predominant form of phytoplankton responsible for harmful algal blooms (HABs) in freshwater environments (Cook *et al.*, 2023). This issue has escalated into a global concern, as emphasised by Paerl and Barnard (2020), necessitating increased attention and efforts to mitigate its impacts. Climate change-induced factors like elevated temperatures and erratic rainfall further exacerbate cyanobacteria blooms (Rankinen *et al.*, 2019). Cyanobacteria blooms can severely degrade water quality, causing increased turbidity, reduced dissolved oxygen levels, and decreased water transparency (Liu and Qiu, 2007). Therefore, monitoring chl-a levels, a reliable proxy for estimating cyanobacteria, is essential, as demonstrated by numerous studies (Song, 2022; Zhao, 2022a; Bunyon, 2023). Chl-a is widely employed as a proxy for assessing cyanobacterial harmful algal blooms (cyano-HABs) due to its role as a primary pigment in photosynthetic organisms. However, accurately discriminating cyanobacteria from other phytoplankton often requires complementary approaches, such as phycocyanin and green algae detection (Schalles, 2006; Hunter *et al.*, 2008; Salmi *et al.*, 2021; Cook *et al.*, 2023).

Moreover, chl-a may not always accurately represent cyano-HABs, particularly in systems with mixed algal communities or during bloom phases characterised by low pigment concentrations (Becker *et al.*, 2009; Paerl *et al.*, 2011; Adejimi *et al.*, 2023; Li *et al.*, 2023; Pamula *et al.*, 2023; Fournier *et al.*, 2024). Furthermore, challenges inherent to inland waters, including high turbidity, interference from dissolved organic matter (DOM), and overlapping pigment signatures, can complicate chl-a sensing (Kutser, 2009; Matthews, 2011).

Traditional methods for determining chl-a levels involve collecting field samples and conducting laboratory analysis (Ritchie *et al.*, 2003; Batur and Maktav, 2018; Morgan *et al.*, 2020), a time-consuming, labour-intensive, and costly process. Moreover, these in situ techniques are limited in their ability to provide comprehensive spatial and temporal coverage, hindering the issuance of timely warnings for intense blooms (Kuhn *et al.*, 2019; Modiegi *et al.*, 2020). Due to their reliance on point sampling, these methods lack spatial representativeness, highlighting the need for robust, spatially explicit, and synoptic approaches to detect and monitor chl-a concentrations as a proxy for water quality.

Remote sensing is one approach that is robust and spatially explicit and has been used to estimate chl-a (Su, 2015; Arango, 2019; Xiao, 2022). Chl-a exhibits unique optical and spectral properties that enable its detection through remote sensing technologies (Wu *et al.*, 2010; Gao *et al.*, 2015). Remote sensing offers several advantages for measuring chl-a concentration, including extensive coverage, cost-effectiveness, and capturing temporal, spatial, and dynamic changes, making it an effective method for comprehensive monitoring (Yang *et al.*, 2022; Tian *et al.*, 2023). Research has shown that chl-a has distinct optical properties, with high absorption rates at 443 nm and 665 nm (Gilerson *et al.*, 2010; Gurlin *et al.*, 2011; Yu *et al.*, 2014; Johan *et al.*, 2018; Warren *et al.*, 2021; Wang *et al.*, 2022), and high reflectance in the green and red-edge spectra 550-555 nm and 685-710 nm, respectively (Gitelson, 1992; Kirk, 1994; Mobley, 1994). High chl-a concentrations are characterised by increased reflectance in the green (G) and red (R) bands and decreased reflectance in the blue (B) band (Pulliainen *et al.*, 2001). The maximum reflectance associated with chl-a occurs at 580 nm (Dekker, 1993), and peak reflection at 700 nm (Gitelson, 1992). Therefore, monitoring changes in reflectance within these specific bands can effectively identify high concentrations of chl-a.

Numerous studies have successfully utilised airborne hyperspectral data to estimate chl-a levels in inland waters (Moses *et al.*, 2012; Pyo *et al.*, 2018; Kolluru *et al.*, 2023). However, airborne hyperspectral sensors are expensive, limiting their adoption for small water bodies. The freely available multispectral satellite data has been utilised to estimate chl-a concentration in large aquatic systems using ocean chlorophyll wavelength-based algorithms (412, 443, 490, 510, 555 nm). These algorithms were originally developed for oceanic monitoring and have since been adapted for use in inland water bodies. The foundation of chl-a algorithms emanated from satellite data and oceans as the primary study area, as reflected in key studies (O'Reilly *et al.*, 1998; O'Reilly *et al.*, 2000; Lins *et al.*, 2017; Markogianni *et al.*, 2018; O'Reilly and

Werdell, 2019; Cao *et al.*, 2020; Lai *et al.*, 2021; Kolluru and Tiwari, 2022). On the other hand, freely available multispectral satellite data has limitations such as coarse resolution, limited data control, and untimely collection (Yang *et al.*, 2022). Unmanned aerial vehicles (UAVs) provide a promising alternative, enabling remote monitoring of chl-a in small water bodies with higher spatial resolutions, controlled temporal scales, and flexible data collection at a relatively low cost (Wu *et al.*, 2019; Xiang *et al.*, 2019; Yao *et al.*, 2019). UAVs address satellite-based limitations, providing enhanced precision and flexibility for effective cyanobacteria monitoring in small water bodies like lakes, rivers, dams, reservoirs, streams, and wetlands (Cillero Castro, 2020; Silveira Kupssinskü, 2020; Xiao, 2022; Fu, 2023; Lo, 2023). Studies have demonstrated UAV-acquired remote sensing data's potential in detecting and monitoring chl-a with high accuracy, including (Cillero Castro, 2020), who used empirical approaches and band indices to detect chl-a in a Spanish reservoir, and Silveira Kupssinskü (2020), who employed machine-learning models in Brazil. Similarly, Xiao (2022) estimated chl-a downstream of a river using machine learning and traditional regression. Fu (2023) estimated chl-a levels in a Chinese karst wetland using partial least squares and adaptive ensemble algorithms. These studies showcase UAV-acquired remote sensing data's promise in accurately detecting and monitoring chl-a in small water reservoirs.

While there is evidence of using UAVs to monitor chl-a in small water bodies, there is a notable gap in the assessment of existing literature. Little research has focused on systematically and comprehensively assessing studies that monitored chl-a in small water bodies using UAVs. A comprehensive review is required to assess, evaluate, and select the most appropriate method that can be used for chl-a approximation in small inland waters using UAVs. To boost and enhance the knowledge on using UAVs to monitor chl-a levels in small inland waters, this paper took the initiative to track and evaluate the existing literature and document the current progress, challenges, and opportunities centred around this subject. The objectives of this paper were to (1) identify and systematically review the literature on UAV remote sensing of chl-a concentrations in small water bodies, (2) evaluate and analyse the methodologies and technologies employed in UAV-based remote sensing for measuring chl-a concentrations, including sensor types, imaging techniques, and data processing methods, and (3) assess the progress, opportunities, gaps, and challenges in using UAV technology for monitoring chl-a in small inland water bodies. Addressing this gap is important for establishing efficient monitoring and management strategies for water resources.

3.3 Materials and Methods

3.3.1 Literature Search Strategy

A literature search was conducted to find global studies on estimating chl-a in small water bodies using UAVs. The first step entailed identifying and compiling keywords and phrases commonly used in the previous UAV remote sensing studies of chl-a. The following key terms were used in the search string: “Unmanned aerial vehicle” OR Drone OR “unmanned aerial systems” AND “remote sensing” AND “chlorophyll-a” OR “algae" OR "phytoplankton" OR cyanobacteria blooms" AND "inland waters" OR "lakes" OR "reservoir". A database was then constructed by searching these key terms from research databases: Science Direct, Scopus, Web of Science (WOS), IEEE Xplore, and Google Scholar. While the publication end date of papers searched was restricted to December 31, 2023, the publication start date was unrestricted. All articles with a published status were considered, regardless of their geographical location. Due to the variations in the configuration settings in Scopus and Web of Science, the key search strings were slightly different (Table 3.1).

Table 3.1: Number of articles retained using five search engines

Search Engine	Search Criterion	Number of articles retained
Web of Science	All fields (“Unmanned aerial vehicle” OR “Drone”) AND (“remote sensing”) AND (“chlorophyll-a”) AND (“algae") AND ("phytoplankton") AND ("cyanobacteria”) AND (“inland waters”) AND ("lakes") AND (“small water bodies”) AND ("multispectral")	2262
Google Scholar	(“Unmanned aerial vehicle” OR Drone OR “unmanned aerial systems”) AND (“remote sensing”) AND (“chlorophyll-a” OR “algae" OR "phytoplankton" OR "cyanobacteria”) AND (“inland waters”)	900
Science Direct	TITLE-ABS-KEY (“Unmanned aerial vehicle” OR Drone OR “unmanned aerial systems”) AND (“remote sensing”) AND (“chlorophyll-a” OR “algae" OR "phytoplankton" OR "cyanobacteria”) AND (“inland waters”)	84
Scopus	TITLE-ABS-KEY ("Unmanned aerial vehicles" OR "drone") AND ("remote sensing") AND ("chlorophyll-a" OR "algae" OR "phytoplankton" OR "cyanobacteria blooms") AND ("inland waters" OR "lakes" OR "reservoir")	44
IEEE Xplore	ALL METADATA (“Unmanned aerial vehicle” OR Drone AND “remote sensing” AND chlorophyll-a OR algae OR phytoplankton OR “cyanobacteria blooms” AND “inland waters” OR lakes OR reservoir)	5

3.3.2 Screening and Selection Strategy

A total of 3295 studies were retrieved: 2262 from WOS, 900 from Google Scholar, 84 from Science Direct, 44 from Scopus, and 5 from IEEE Xplore. Retrieved articles were then exported in the Endnote software, where the bibliographic information of articles, including the year, article title, name of the journal, author names, abstract, keywords, Digital Object Identifier (DOI), and Uniform Resource Locator (URL) was compiled. The search was refined by screening titles and abstracts using relevant keywords. The Preferred Reporting Items for Systematic Reviews and Meta-Analysis (PRISMA) reporting checklist (https://www.prisma-statement.org/, accessed 20 February 2024) was used as a guide to eliminate bias reporting and

structure the review. The articles that qualified for the meta-analysis were those that met the following criteria:

(1) The scope of the study focused on the estimation of chl-a or assessment of cyanobacteria in a small water body
(2) The study utilised data from UAV-based remotely sensed data
(3) The results of the study and the accuracy assessment are clearly stated
(4) The study is from an accredited journal and is peer-reviewed
(5) The study paper is written in English.

The first exclusion step was to remove duplicates. In total, 132 articles were removed as duplicates. The remaining 3163 articles were screened using titles and abstracts to determine their eligibility for this study. Three thousand one hundred twenty-two articles were excluded at this stage for one of the following reasons: beyond the scope of the review, not peer-reviewed, missing full article, and imprecise or not clearly stated results. Finally, the remaining 41 studies and 14 studies obtained from backward referencing (Horsley et al., 2011) underwent full-text assessment for eligibility. In total, 55 studies met the final selection criteria and were carried on to the data extraction step. The selection process and screening outcomes are illustrated in a PRISMA flowchart, as shown in Figure 3.1.

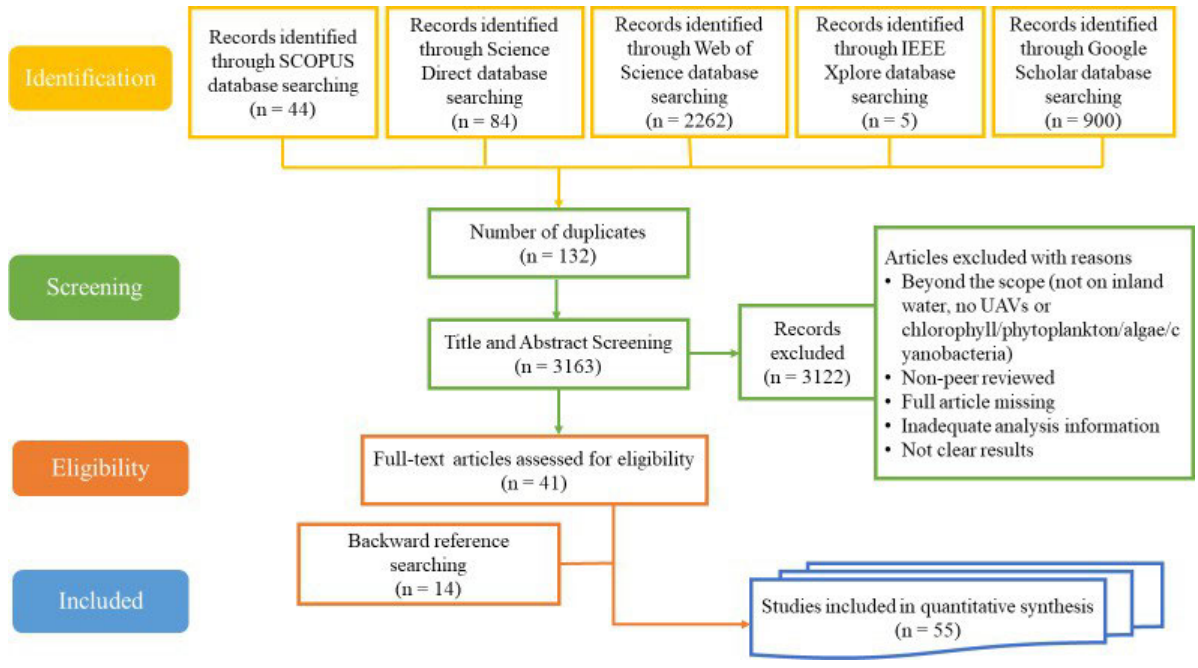

Figure 3.1: PRISMA flow diagram indicating the article selection process

The selected articles were exported from Endnote to Microsoft Excel and downloaded as PDF documents to extract comprehensive data. In addition to the bibliometric data from Endnote, details such as the year and country of study, type of water body, eutrophication water quality parameter monitored, sensor and UAV platform characteristics, vegetation indices, regression models, and remote sensing algorithms were retrieved. These categorical attributes were subsequently transformed into measurable variables in preparation for the data analysis phase, and the relevance of the systematic review was evaluated by assessing the quality of the articles. The coefficient of determination (R^2) was extracted from each study for the accuracy assessment, as it measures the goodness fit between predicted and observed values.

3.3.3 Data Analysis

In this review paper, qualitative and quantitative analyses were performed on the extracted data. Statistical frequencies and trend analysis were employed to determine the progress of using UAVs to monitor water quality, specifically chl-a in inland water bodies. Microsoft Excel was used to delineate the statistical frequencies (Carlberg and Carlberg, 2014). Additionally, a bibliometric analysis identified trends in the co-occurrence of key terms and interlinkages between keywords related to monitoring chl-a in small water bodies using UAV-derived data. The VOSviewer software (https://www.vosviewer.com/) was used to mine text and quantitatively examine the occurrence and co-occurrence of keywords in the titles and abstracts of the reviewed studies (Van Eck and Waltman, 2007). VOSviewer also illustrated the evolution of concepts and topics related to the remote sensing of chl-a in small water bodies. Although bias is common in literature analysis, a specific bias assessment was not performed since the focus was on the occurrence, co-occurrence, and frequency distribution of key terms.

To meet the research objectives, this review was divided into two sections. The first section explored the spatial distribution of studies, keyword analysis, types of water bodies and their uses, parameters, and quantitative analysis of the algorithms, sensors, platforms, and indices employed by the reviewed studies. The second section outlined the opportunities, gaps, and challenges identified in the reviewed literature on estimating chl-a using UAV remotely sensed data in small inland waters.

3.4 Results

3.4.1 Evolution and Analysis of Keywords in UAV-Derived Chl-a Literature

In assessing the evolution and topical concepts of monitoring chl-a in small water bodies using UAV-derived data, the results showed that “unmanned aerial vehicle”, “chlorophyll”, “algae”, “reservoir”, and “multispectral imagery” were the most utilised keywords around 2019 (Figure 3.2). This indicates the wide use of multispectral cameras during that time to monitor algae in water bodies such as reservoirs. The period between 2020 and 2021 indicates the wide application of remote sensing in water quality to monitor chl-a leveraging on the reflection of water bodies such as rivers. This period also represents the introduction of deep learning algorithms in water quality monitoring. The 2021 to 2022 period was marked by keywords such as “hyperspectral imaging”, “machine learning, “multispectral image”, “uav remote sensing”, “water quality monitoring”, “linear regression”, “cyanobacteria”, and “inland waters”. This highlights the growing trend of using UAVs for water quality monitoring, the adoption of advanced methods for model development such as machine learning, and the investment into high-resolution sensors such as hyperspectral cameras. This significant evolution of key terms can be attributed to the recent technological advancements in analysis techniques and the widespread application of UAVs in monitoring chl-a.

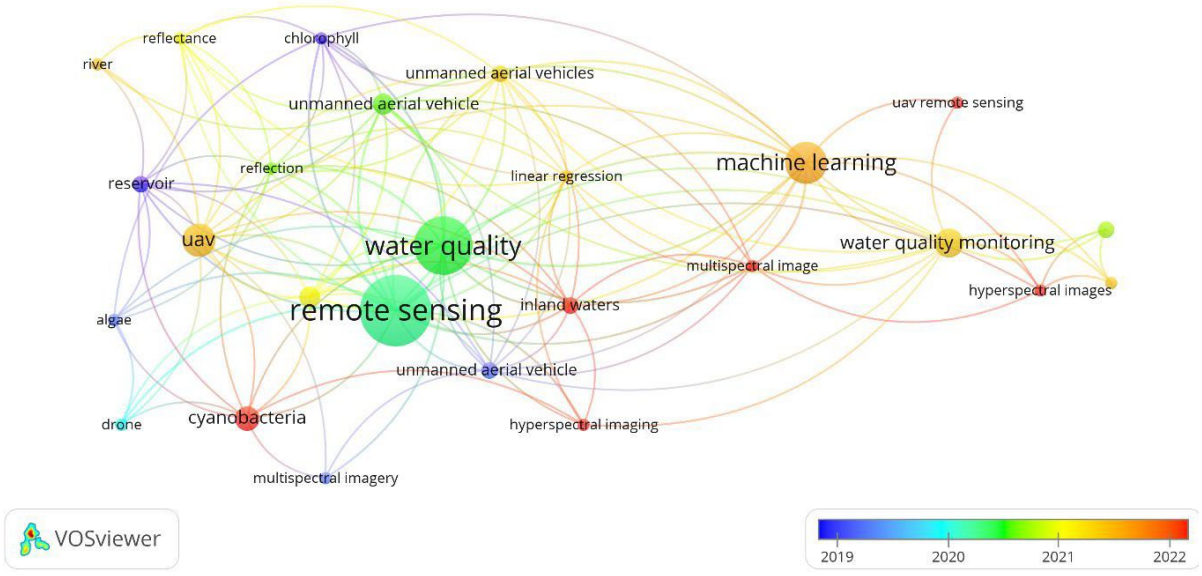

Figure 3.2: Evolution and direction of topical concepts on chl-a monitoring in small water bodies using UAV remote sensing, derived from abstracts, titles, and keywords of the selected literature

A total of 303 keywords were identified from the reviewed literature. To analyse the trends, the minimum number of occurrences was set to three, which narrowed the number of keywords to a threshold of 23. These keywords were then grouped into five clusters: red, purple, green, blue, and yellow (Figure 3.3). The red cluster emerged as the biggest, representing the keywords most used during the search period. It comprised the keywords such as “remote sensing”, “reflection”, “chlorophyll”, “cyanobacteria”, and “drone”. This also shows the interlinkages between the water quality parameters, water body, and imagery. The second cluster (purple) had the following key terms, “water quality”, “multispectral imagery”, and “unmanned aerial vehicle”, indicating a strong association between the use of UAVs equipped with multispectral imaging sensors for monitoring water quality. The third cluster (green) had the keywords “machine learning”, “water quality monitoring”, “UAV remote sensing”, “multispectral image”, and “hyperspectral images”. This highlights integrating cutting-edge remote sensing technologies, including multispectral and hyperspectral imaging, with machine learning algorithms to monitor water quality. The blue cluster had the following key terms, “uav”, “reservoir”, “river” and “reflectance”, indicating the use of UAVs to monitor various types of water bodies by leveraging water reflectance. Finally, the yellow cluster is associated with terms like “linear regression”, inland water”, “hyperspectral imaging” and “unmanned aerial vehicles”. This indicates that UAVs equipped with hyperspectral imaging technology commonly estimate chl-a levels in inland water bodies, often utilising linear regression models for analysis.

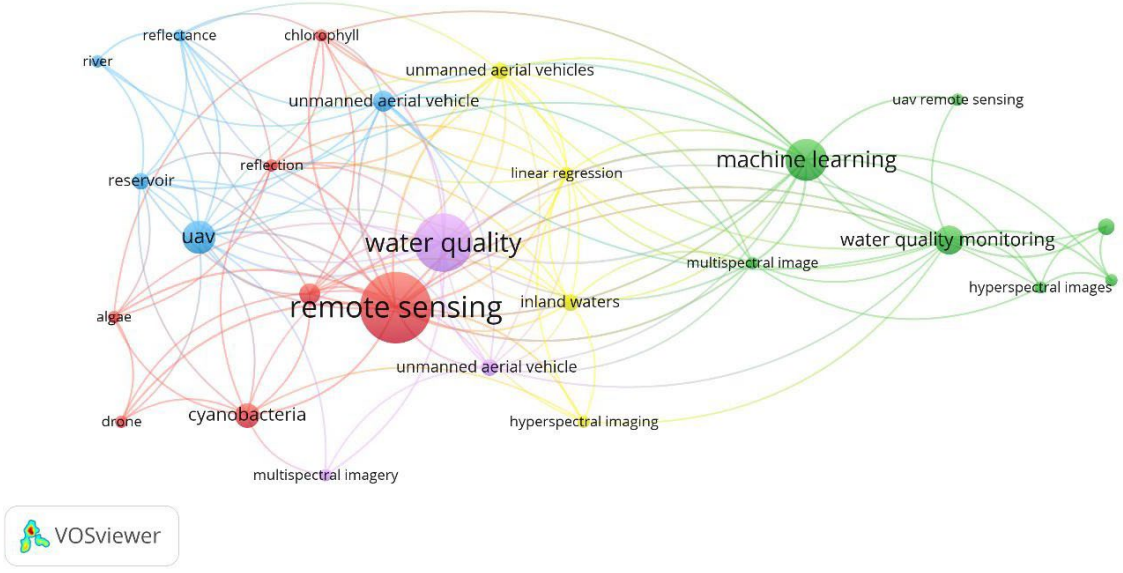

Figure 3.3: Topical concepts in mapping and monitoring of chl-a in small water bodies

3.4.2 Spatial, Temporal Distribution and Trends of Publications

To assess trends in articles published on the use of UAV-acquired remotely sensed data for monitoring chl-a, this review revealed that the first study was conducted in 2015 (Su, 2015). A notable surge in research activity was then observed in 2021 and 2023, accounting for 21% and 25% of the studies, respectively, focusing primarily on rivers, lakes, and reservoirs (Ahn, 2021; Lu, 2021; Hong, 2022; Xiao, 2022; Cai, 2023). A slight decline (22%) in research articles was observed between 2015 and 2019 (Jang, 2016; Guimarães, 2017; Choo, 2018; Arango, 2019; Pyo, 2022). However, from 2019 to 2023, the adoption of UAVs for chl-a monitoring became increasingly popular, as evidenced by the gradual increase in published studies, as shown in Figure 3.4.

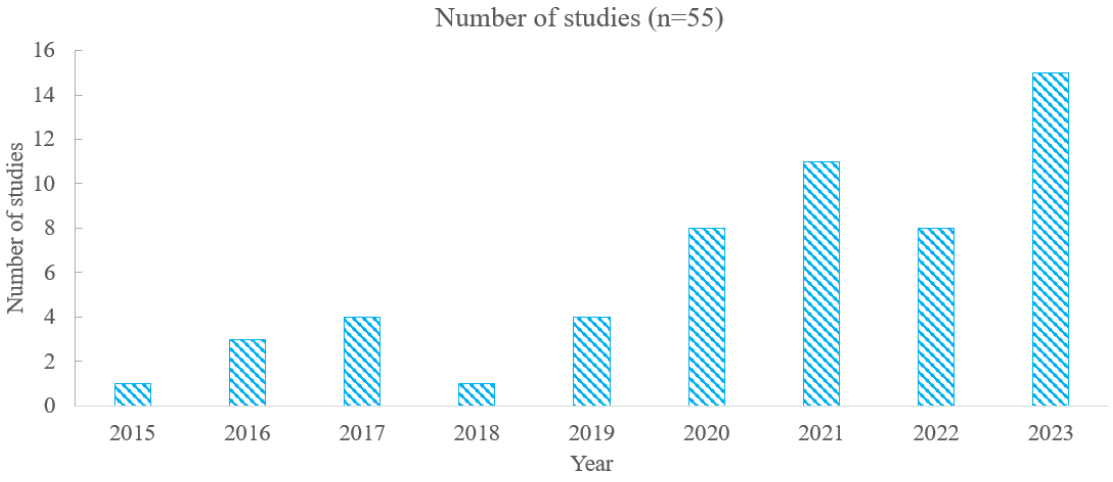

Figure 3.4: Annual frequency of UAV-based studies that monitored chl-a in inland open water bodies

In terms of the spatial distribution, the retrieved studies were conducted across thirteen different countries, with 66% in Asia, 19% in North America, 9% in Europe and 6% in South America (Figure 3.5). In Asia, most of the studies were conducted in China (42%) (Zhang, 2020a; Chen, 2021; El-Alem, 2021; Liu, 2021; Song, 2022; Zhao, 2022b; Xiao, 2023), followed by South Korea (23%) (Kim, 2016; Kwon, 2020; Hong, 2023). In North America, 12% of the studies were done in the United States of America (USA), while Canada and Brazil (South America) had a limited number of studies, 5% and 7%, respectively (Zeng, 2017; Silveira Kupssinskü, 2020; El-Alem, 2021). Only 2% of studies were conducted per country in the remaining countries of Asia and Europe. The high volume of studies in China can be attributed to several factors. China has extensive and diverse water bodies, including numerous large rivers, lakes, and reservoirs, providing ample opportunities for water quality monitoring

research using UAV technology. Additionally, China has invested heavily in UAV technology and remote sensing research, leading to more studies. The fewer studies in other regions could be due to various reasons, including less availability of advanced UAV and remote sensing technology and limited research funding. Notably, no studies in the retrieved literature were undertaken in Africa.

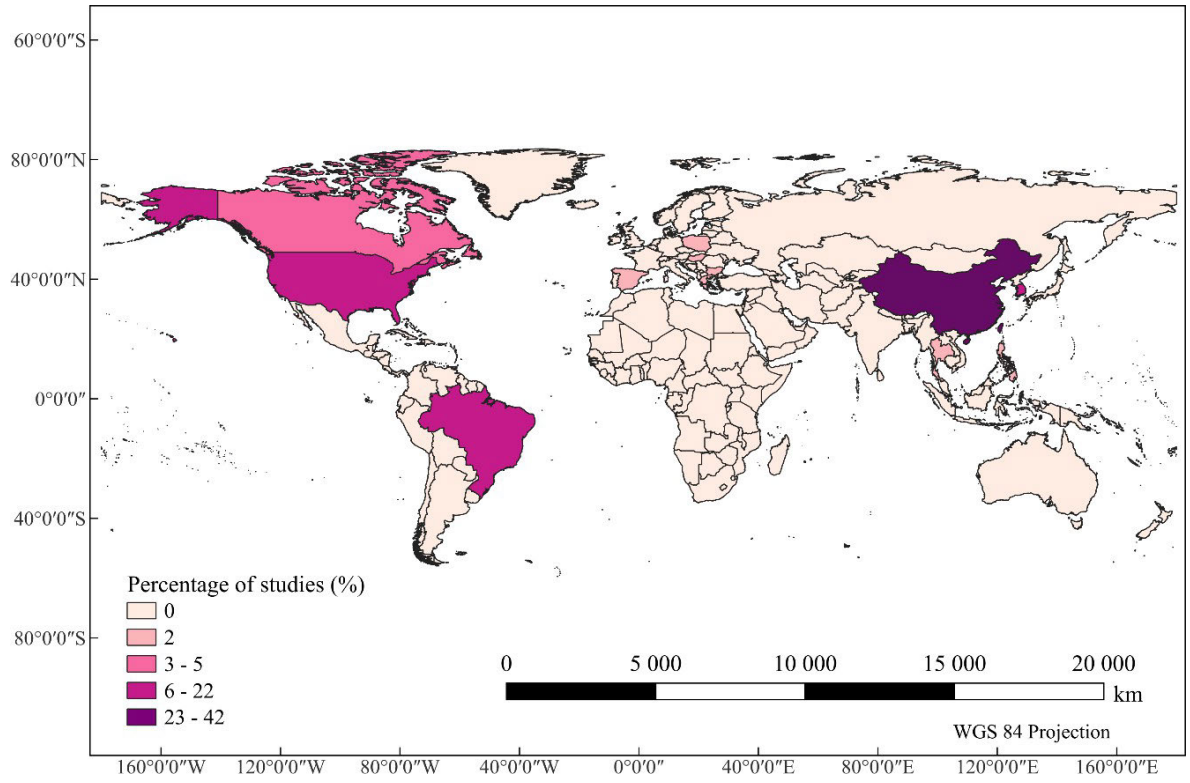

Figure 3.5: Global spatial distribution of studies that utilised UAVs for chl-a monitoring in inland water bodies

Regarding temporal distribution, most (75%) of the selected studies focused exclusively on summer-season research (Su, 2015; Jang, 2016; Kwon, 2020; El-Alem, 2021; Hong, 2022; Lo, 2023). This preference may stem from constraints such as limited funding, shorter research timelines, and the seasonal nature of specific research grants. Despite these limitations, single-season studies can still provide valuable insights, especially during peak periods of algal growth. In contrast, 25% of the studies addressed temporal variations by collecting data across multiple seasons (summer, autumn, and winter) (Arango, 2019; Chen, 2021; Liu, 2021; Sharp, 2021; Zhao, 2022b; Bunyon, 2023; Ciężkowski, 2023). Such multi-season studies are advantageous as they provide a more comprehensive view of seasonal patterns and trends in water quality.

3.4.3 Chl-a and Associated Water Quality Parameters in Various Water Bodies

The included articles focused on various aspects of algal dynamics, including chl-a, cyanobacteria, harmful algal blooms (HABs), and phytoplankton, often examining these parameters individually or, in some cases combined with other eutrophication parameters. As shown in Figure 3.6a, 60% of the articles exclusively focused on the chl-a, underscoring its importance as a key indicator of algal biomass, while 20% examined both chl-a and nutrients such as total nitrogen (TN) and total phosphorus (TP) (Arango, 2019; Cillero Castro, 2020; Zhang, 2020b; Chen, 2023). These nutrients are primary drivers of eutrophication, which leads to increased algal growth and potential HABs (Rankinen *et al.*, 2019). Additionally, 9% of the articles explored the relationship between chl-a and dissolved oxygen (DO) (Bunyon, 2023; Hong, 2023; Yang, 2023). This relationship is important because excessive algal growth, indicated by high chl-a levels, can lead to oxygen depletion. Regarding correlations between chl-a and other water quality parameters, 9% of the studies indicated a positive correlation between chl-a and TP (Arango, 2019; Zhang, 2020a; Zhang, 2022), 5% showed a positive correlation between chl-a and TN (Arango, 2019; Zhang, 2020a; Zhang, 2020b), and 2% revealed a positive correlation between chl-a and DO (Morgan, 2020).

Regarding the type of water bodies, 39% of the retrieved studies were conducted in rivers (Jang, 2016; Choo, 2018; Son, 2020; Ahn, 2021; Liu, 2021; Xiao, 2022), 25% on lakes (Guimarães, 2017; Silveira Kupssinskü, 2020; El-Alem, 2021) and 14% on reservoirs (Stoyneva-Gärtner, 2019; Lu, 2021; Pokrzywinski, 2022). Interestingly, 2% of the studies focused on a dam, highlighting a significant gap in literature. Based on the findings (Figure 3.6b), approximately 26% of the studies focused on water bodies for potable water supply (Su, 2015; Stoyneva-Gärtner, 2019; Son, 2020; Zhao, 2022b; Xiao, 2023), 15% on multi-purpose use (industrial, agricultural, living and drinking purposes) (Kim, 2016; Becker, 2019; Pokrzywinski, 2022) and, 11% directed their focus towards water bodies designated for multi-purpose and or irrigation purposes (Morgan, 2020; Hong, 2022; Ciężkowski, 2023). This gives an understanding of the practical applications and relevance of the research findings. It also shows how UAVs are being utilised in different sectors. A considerable portion of studies (28%) did not articulate the intended purpose of the water bodies under investigation, revealing a significant gap in the literature.

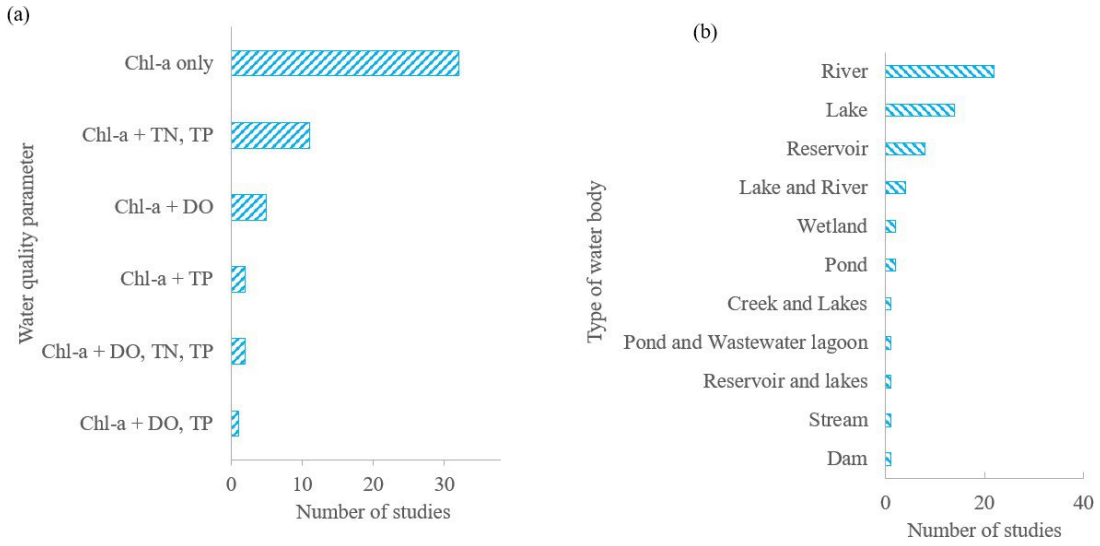

Figure 3.6: (a) Water quality parameters, particularly those related to eutrophication, monitored with chl-a using UAVs and their study frequency (b) Types of inland water bodies studied for chl-a monitoring and their study frequency

3.4.4 In Situ Methods of Measuring and Analysing Chl-a Data in Small Water Bodies

The results in Figure 3.7, reveal that 22% of the included articles employed spectrophotometers for chl-a analysis in a laboratory environment (Su, 2015; Morgan, 2020; Tóth, 2021). While 22% of the studies utilised both spectroradiometers and spectrophotometers to gather in situ data (Kwon, 2020; Zhang, 2021; Hong, 2022). 11% of the articles used spectroradiometers only (Lu, 2021; De Keukelaere, 2023), and 9% of the studies used a variety of multiparameter probes, including the YSI EXO-2 and HX-200 meters (Hong, 2022; Zhao, 2022b; Lo, 2023). The rest of the studies used an integration of either a multiprobe or a spectroradiometer to allow for versatile, comprehensive, enhanced accuracy, automated measurements, and real-time data collection.

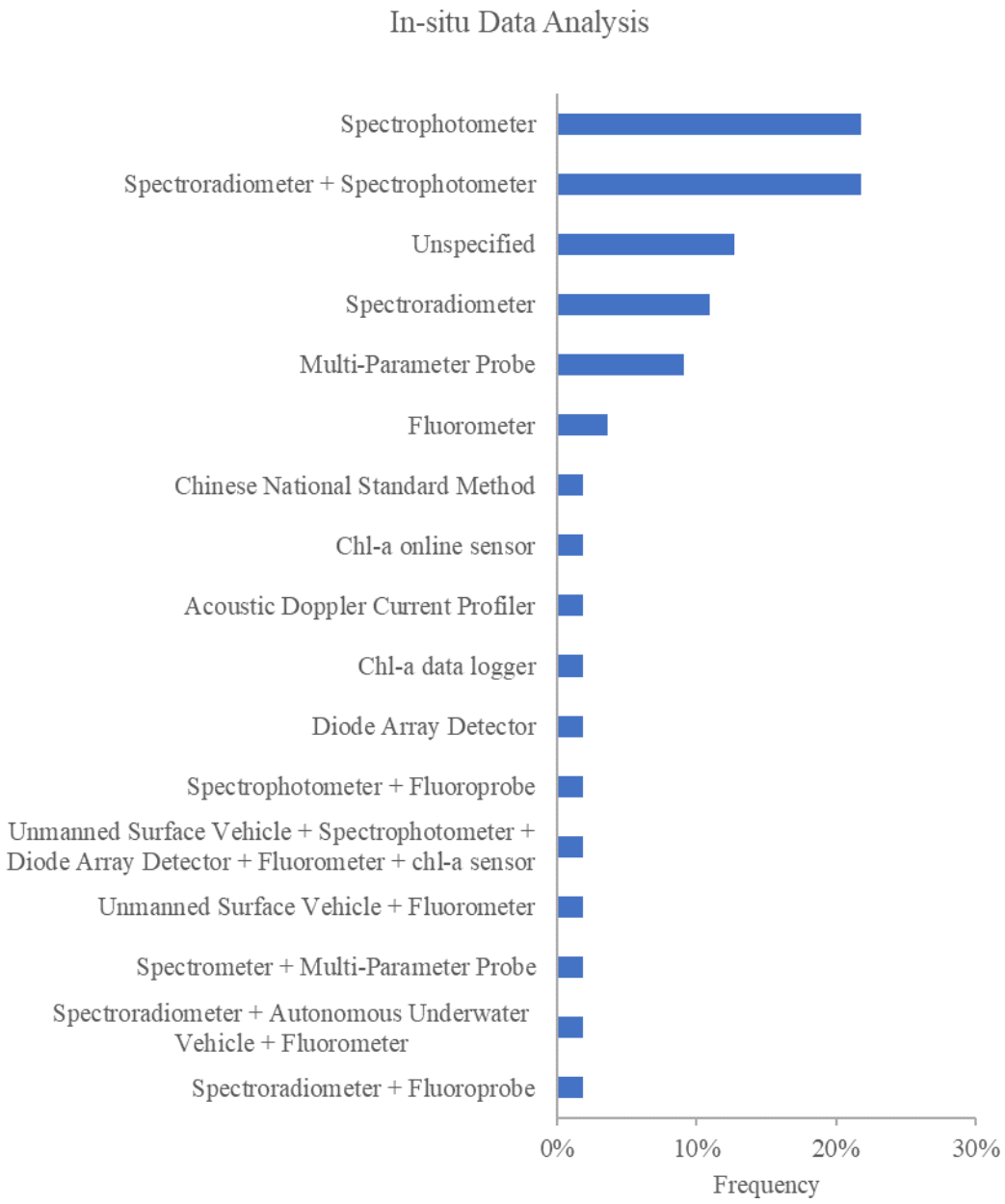

Figure 3.7: Instruments and methods for measuring in situ chl-a data, including field and laboratory techniques, and their frequency of use in the selected studies

3.4.5 UAV Characteristics and Platforms

This review identified two primary UAV platform types used for chl-a monitoring: fixed-wing and multicopters. Multicopters dominated, with 75% of studies employing them, followed by fixed-wing drones (21%) and 4% unspecified. DJI platforms (60%) were the predominant choice among multicopter platforms (Choo, 2018; Zhang, 2020a; Song, 2022; De Keukelaere, 2023), while SenseFly eBee (13%) platforms accounted for a significant share of the fixed-

wing vehicles (Jang, 2016; Su, 2017; Silveira Kupssinskü, 2020). Fixed-wing UAVs offer aerodynamic benefits, enabling longer flight times, larger bloom surveillance, and multiple sensor deployment for enhanced chl-a concentration accuracy. They suit mapping wider spatial extents. Multicopters excel in closer proximity analysis due to their vertical take-off and landing (VTOL) capabilities (Zaludin and Harituddin, 2019). This capability makes them easily employed in different environments than fixed-wing platforms, which require substantially flat and dry areas to deploy and launch successfully near water bodies. Other UAV platforms included Aytges (2%) (Cillero Castro, 2020), FireFLY BirdsEyeView (2%) (Choo, 2018), Begren RC (2%) (Becker, 2019), G4 SkyCrane (2%) (Pokrzywinski, 2022), ATI AgBot (2%) (Arango, 2019), 3DR Solo(2%) (Morgan, 2020), and Remo-M (2%) (Kim, 2021). Additionally, 23% of the reviewed studies combined UAV and satellite acquired data from sensors which include Sentinel-2 & 3, Landsat 7, 8 & 9, PlanetScope, GF-1 (Gaofen-1), Orbita Hyperspectral Satellite (OHS), and ZY-3 satellite (Jung, 2017; Cillero Castro, 2020; El-Alem, 2021; Fu, 2023; Yang, 2023). This synergistic approach improves spatial and temporal coverage, enhances data accuracy, and allows for continuous monitoring, event detection, and more comprehensive analysis.

3.4.6 Sensors and Spectral Bands

In remote sensing, the characteristics of sensors play a pivotal role in estimating water quality parameters. They impact the monitoring system's accuracy, reliability, and effectiveness (Modiegi *et al.*, 2020). Thirteen different sensors and cameras were used in the reviewed studies (Figure 3.8). These sensors comprised multispectral and hyperspectral types, catering to various spectral bands. Approximately 55% of the studies utilised multispectral sensors, spanning the visible to near-infrared spectrum, including red, green, blue, red edge, and near-infrared bands (Su, 2015; Guimarães, 2017; Morgan, 2020; Chen, 2021; Zhao, 2022b; Lo, 2023). These sensors predominantly utilised the near-infrared (NIR; 708-842 nm) and red (640-668 nm) bands as the optimal bands for detecting chl-a. Some studies also incorporated the green band (560 nm) and blue band (475-497 nm), and very few used the red-edge band (730-740 nm) (Xiao, 2022; Zhao, 2022a). The most commonly used multispectral sensor was the MicaSense Rededge, utilised by 18% of the studies (Figure 3.8). On the other hand, 36% of the studies employed hyperspectral sensors, which captured data across a wavelength range of 350 nm to 1700 nm (Jang, 2016; Kwon, 2020; Pokrzywinski, 2022; Cai, 2023), with the 400-755 nm band being the most utilised segment for chl-a detection. A significant number of the studies (16%) used the Nano-Hyperspec hyperspectral sensor (Figure 3.8) making it highly effective for

detecting chl-a in various ecosystem environments. Notably, two studies (Wu, 2023; Xiao, 2023) employed a synergistic approach by concurrently utilising multispectral and hyperspectral sensors. This approach leveraged the strengths of both types of sensors: the broad spectral coverage and high spatial resolution of the multispectral sensors, detailed spectral information, and high precision offered by hyperspectral sensors. By combining these sensors, the studies enhanced the precision and reliability of chl-a monitoring and mapping.

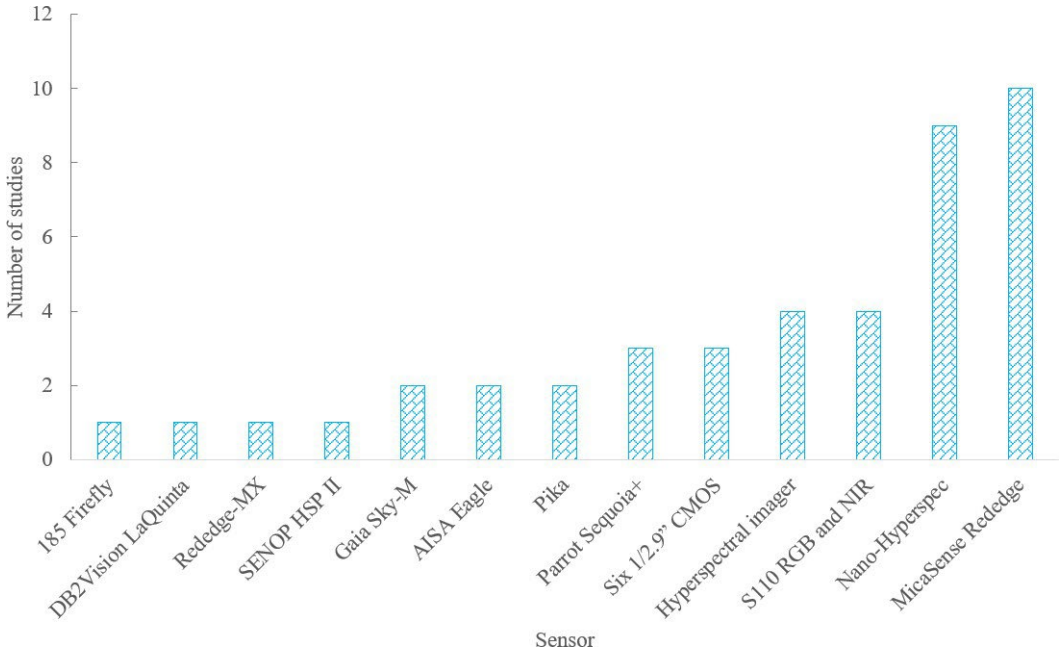

Figure 3.8: Types of sensors used in chl-a monitoring, showing their frequency in the selected studies

3.4.7 Algorithms Utilised for Detecting Chl-a Concentrations in Small Water Bodies

3.4.7.1 Spectral Indices and Band Combinations

This study observed a variety of indices and band combinations for chl-a estimation in small water bodies (Table 3.2). The indices comprise the normalised difference vegetation index (NDVI) (Douglas Greene, 2021), normalised difference red-edge index (NDRE) (Kim, 2021), normalised difference chlorophyll index (NDCI) (Mishra and Mishra, 2012; Pokrzywinski, 2022), surface algal bloom index (SABI) (Douglas Greene, 2021). Although each of these indices was customised for the specific water bodies for which it was developed, the fluorescence line height blue (FLH B), three-band algorithms (3BDA), and the NDCI indices were observed to be more effective, each gave a coefficient of determination, R^2 value of greater

than 0.700. Also, the results showed that 34% of the studies utilised two-band algorithms (2BDA) while 15% utilised 3BDA.

The NDVI index was the most employed (25%) spectral index; however, its R^2 values ranged from as low as 0.040 to 0.720. The NDVI was the most utilised index because it uses NIR and red bands, which are suitable for estimating chl-a. However, the NDCI index, which combines the red and Rededge bands, demonstrated moderately higher accuracy than the NDVI index. This is because varying depths can affect the reflectance in the red and NIR bands, leading to lower accuracy and lower R^2 values for NDVI. Hence, alternative indices like the NDCI index (Mishra and Mishra, 2012; Olivetti, 2023) offer a solution as they are specially designed for chlorophyll estimation in water. The red and red edge bands of the NDCI index exhibit stronger and more reliable correlations, yielding higher R^2 values. The NDCI's targeted sensitivity to chlorophyll reduces the impact of confounding factors such as water turbidity and suspended particles (Chien *et al.*, 2016), hence the higher accuracy.

Additionally, the literature revealed that 3BDA gave a higher precision than 2BDA. 3BDA remarkably exhibited R^2 values, averaging at 0.765, in comparison to 2BDA, which yielded an average of 0.646 for R^2 values. This is because 3BDA leverages extra spectral information from the extra band, enhancing its ability to discern target parameter characteristics. Also, the interaction between different water components can be slightly eliminated using multiple bands (Gitelson 2003). Therefore, indices like the FLH B and INDEX demonstrate improved performance (Table 3.2) but only when hyperspectral sensors capture a broad range of the electromagnetic spectrum. Additionally, poor-performing indices (R^2: 1×10^{-4} - 0.160) were computed from the green, red, and blue bands, for example, the visible atmospherically resistant index (VARIGREEN) and green–red ratio index (GRRI), while the moderate-performing indices (R^2: 0.400 - 0.600) computed from the red and NIR bands, vegetation indices such as NDVI, DVI and green NDVI.

Table 3.2: Accuracy measure for chl-a vegetation indices and band algorithms

Index name	Abbreviation	Formula	Equation number	Metric (R^2)	References
Fluorescence line height blue	FLHB	$G - (R + (B - R))$	3.1	0.750-0.860, average 0.805	Pokrzywinski (2022); Olivetti (2023)
Three band algorithms	3BDA			0.670-0.860, average 0.765	Pokrzywinski (2022); Cai (2023); Olivetti (2023)
Normalised Difference Chlorophyll Index	NDCI	$\frac{708 - 665}{708 + 665}$	3.2	0.500-0.820, average 0.707	Pokrzywinski (2022); Olivetti (2023); Xiao (2023)
	INDEX	$\frac{SR_{665}{}^{-1} - SR_{708}{}^{-1}}{[\![SR_{753}{}^{-1} + SR_{708}{}^{-1})}$	3.3	0.670	Olivetti (2023)
Two band algorithms	2BDA			0.630-0.960, average 0.646	Hong (2022); Logan (2023); Xiao (2023)
Ratio normalised difference vegetation index	RNDVI	$(\frac{NIR - R}{NIR + R}) \times (\frac{NIR}{R})$	3.4	0.611	Zhao (2022b)
	NFH560	$\frac{700}{560\ or\ 675}$	3.5	0.610	Xiao (2023)
Red, Rededge and NIR band ratio				0.586	Maravilla (2019)
Excess green minus excess red	EXGR	$EXG - 1.4 * R - G$ (3.6)	3.6	0.580	Zhao (2022b)
Brute-Force Method		$\frac{684}{674}$	3.7	0.570	Logan (2023)
Brute-Force Method Normalised difference		$\frac{684 - 674}{684 + 674}$	3.8	0.570	
Fluorescence line height violet	FLH Violet	530 – (644 + [430 – 644] * SS (0.467))	3.9	0.550	Pokrzywinski (2022)
	Ocx	$\frac{443\ or\ 490\ or\ 510}{555}$	3.10	0.550	Xiao (2023)
Green Normalised Difference Vegetation Index	GNDVI	$\frac{NIR - G}{NIR + G}$	3.11	0.312-0.740, average 0.519	Kim (2021); Zhao (2022b); Olivetti (2023)
Ratio vegetation index	RVI	$\frac{NIR}{R}$	3.12	0.508	Zhao (2022b)

Table 3.2 continued

Index name	Abbreviation	Formula	Equation number	Metric (R^2)	References
Two-band enhanced vegetation index	EVI2	$\frac{2.5 * (NIR - R)}{NIR + 2.4 * R + 1}$	3.13	0.440	
Normalised difference vegetation index	NDVI	$\frac{(NIR - Red)}{(NIR + Red)}$	3.14	0.040-0.720, average 0.497	Zhao (2022b)
Green Two Band blue	G2B			0.470	
Normalised difference red-edge index	NDRE	$\frac{NIR - RE}{NIR + RE}$	3.15	0.040-0.042, average 0.041	Kim (2021); Zhao (2022b)

B, blue; G, green; NIR, near-infrared; R, red; RE, red edge, SR – spectral reflectance, SS = Spectral Shape coefficient calculated as $(\lambda - \lambda\hat{}-)/(\lambda\hat{} + -\lambda\hat{}-)$

3.4.7.2 Machine Learning

This study revealed that linear regression (LR), followed by random forest (RF), extreme gradient boosting (XGBoost), and support vector machine (SVM) were the most widely used algorithms for the prediction of chl-a from UAV imagery (Figure 3.9). Linear regression was used in 40% of the studies due to its simplicity in computation. While 22% of the studies employed RF, which offers several significant advantages. It is quicker than bagging and highly accurate, effective in handling large data dimensionality and multicollinearity, making it suitable for complex datasets. As a non-parametric algorithm, RF does not assume a specific data distribution, adding to its versatility and ability to work with diverse sample types. Its built-in feature selection mechanism reduces overfitting, improving predictive performance. RF is also robust to outliers and noise, enhancing reliability, and can effectively handle imbalanced data. It is also easy to implement, can be parallelised, and significantly speeds up the training process (Breiman, 2001; Pal, 2005; Belgiu and Drăguţ, 2016; Herrera *et al.*, 2019).

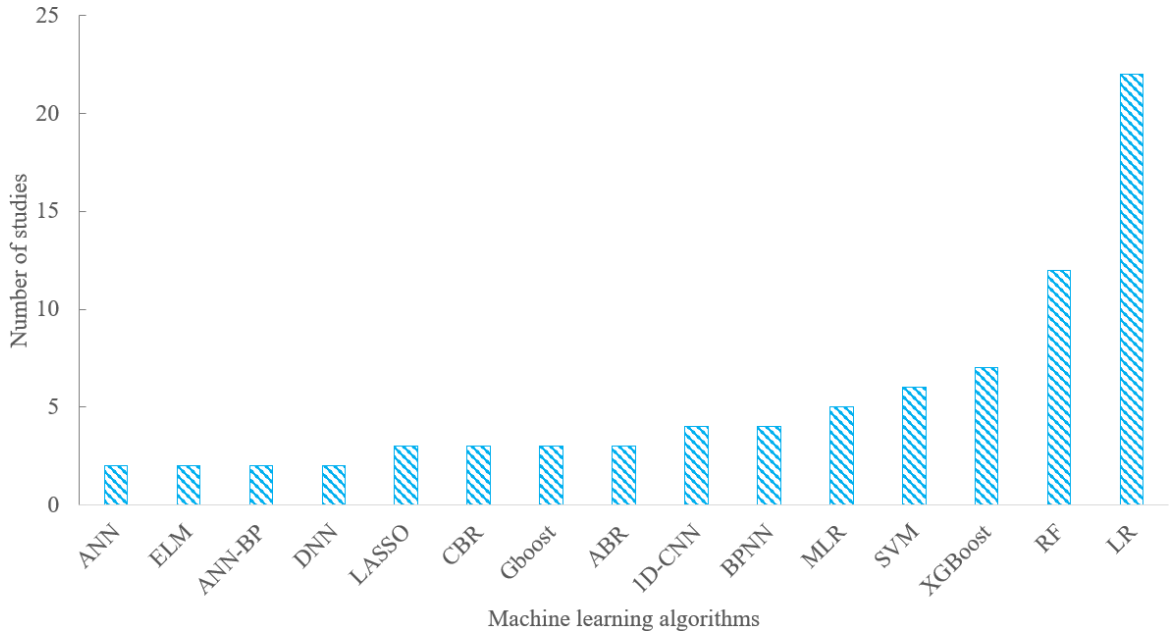

Figure 3.9: Machine learning algorithms used by the selected studies to estimate chl-a concentration from UAV data

Regarding the performance of these algorithms (Table 3.3), the Catboost, Adaboost regression, Artificial Neural Network (ANN), Deep Neural Network (DNN), and K-Nearest Neighbors (KNN) demonstrated high R^2 values over 0.800. It were used in more than three studies, establishing them as high-performing techniques. LR, RF, XGBoost, and Extreme Learning Machine (ELM) had average R^2 values greater than 0.700, positioning them as strong

performers. Despite being used by numerous studies, multiple linear regression (MLR) yielded an average R^2 value of 0.620. This performance can be considered moderate compared to other high-performing algorithms and indicates limited performance in chl-a mapping. Conversely, Self-Adapting Selection of Multiple Neural Networks (SSNN), Ensemble-Based System (EBS), Hybrid Feedback Deep Factorisation Machine (HF-DFM), the Chen method (2023) and Gradient Boost Regression Tree (GBRT) achieved R^2 values exceeding 0.900, while Genetic Algorithm_AdaBoost Regression (GA_ABR), Ensemble Learning Regression (ELR), Genetic Algorithm_XGBoost, and Extremely Randomised Trees (ERT) surpassed 0.800. However, comparing these models is challenging due to their use in singular studies. Notably, Neural Networks (NN) emerged as a low-performing algorithm, with an accuracy of 0.093, rendering it challenging to assess its efficacy in chl-a estimation.

One of the methods used by the reviewed literature to estimate chl-a from UAV images was the use of stacked models. The Artificial Neural Network_Bayesian probabilistic (ANN-BP) stacked model exhibited the highest performance, achieving an average R^2 value of 0.840 (Zhang, 2020a; Zhang, 2020b). This was followed by the Random Forest_XGBoost (RF_XGB) model which gave an R^2 value of 0.504 for the testing data and a near-perfect score of 0.999 for its training data (Xiao, 2022). Additionally, other estimation models including Environmental Fluid Dynamics Code - Recursive Least Squares (Ahn, 2021; Hong, 2023), the Bio-optical algorithm approach (Hong, 2022), and the matching pixel-by-pixel (MPP) algorithm (Su, 2017) were found in the reviewed literature. These methods demonstrated moderately high accuracies, ranging from 0.700 to 0.850.

Table 3.3: Accuracy measure for chl-a machine learning and predictive modelling methods

Algorithm	Abbreviation	Metric (R^2)	References
Self-Adapting Selection of Multiple Neural Networks	SSNN	0.984	Zhang (2020b)
Ensemble-Based System	EBS	0.940	El-Alem (2021)
Hybrid Feedback Deep Factorisation Machine	HF-DFM	0.930	Zhang (2021)
Chen Method 2023		0.917	Chen (2023)
Gradient Boost Regression Tree	GBRT	0.900	(Lu, 2021)
Catboost Regression	CBR	0.808-0.960, average 0.880	Chen (2021); Lu (2021); Fu (2023)
Extremely Randomised Trees	ERT	0.870	Lu (2021)
Genetic Algorithm_XGBoost	GA _XGBoost	0.855	Chen (2023)
Genetic Algorithm_AdaBoost Regression	GA_ABR	0.826	
AdaBoost Regression	ABR	0.784-0.890, average 0.819	Chen (2021); Lu (2021); Chen (2023)
Artificial Neural Network	ANN	0.730-0.901, average 0.816	Silveira Kupssinskü (2020); Wu (2023)
Adaptive Ensemble Learning Regression	AELR	0.814	Fu (2023)
Deep Neural Network	DNN	0.805-0.817, average 0.811	Chen (2021); Chen (2023)
K-Nearest Neighbors	KNN	0.703-0.896, average 0.800	Silveira Kupssinskü (2020); Chen (2021)
Particle Swarm Optimisation Algorithm	PSO–LSSVM	0.778	Liu (2021)
Regression trees	RT	0.770	Morgan (2020)
Partial Least Squares Algorithm	PLS	0.764	Liu (2021)
Extreme Learning Machine	ELM	0.730-0.761, average 0.745	Zhao (2022b); Zhao (2022a)
Extreme Gradient Boosting	XGBoost	0.415-0.920, average 0.737	Chen (2021); Lu (2021); Xiao (2022); Chen (2023)
Genetic Algorithm Partial Least Squares	GA-PLS	0.730	Zhang (2021)
Random Forest	RF	0.317-0.874, average 0.705	Chen (2021); Xiao (2022); Fu (2023); Yang (2023)
Linear regression	LR	0.203-0.980, average 0.700	Su (2017); Silveira Kupssinskü (2020); Yi (2023)
1 Dimensional - Convolutional Neural Network	1D-CNN	0.193-0.910, average 0.691	Hong (2022); Pyo (2022); Zhao (2022a); Lo (2023)
Transformer		0.650	Yang (2023)
Mixture Density Network	MDN	0.650	

Table 3.3 continued

Algorithm	Abbreviation	Metric (R^2)	References
Support Vector Machine	SVM	0.481-0.759, average 0.623	Silveira Kupssinskü (2020); Lu (2021); Zhao (2022a)
Multi-Layer Perceptron Regression	MLPR	0.620	Lu (2021)
Integrated Data Fusion and Mining	IDFM	0.620	Zhang (2021)
Multiple Linear Regression	MLR	0.101-0.860, average 0.620	Arango (2019); Zhang (2020b); Xiao (2023)
ResNet-182		0.610	Hong (2022)

3.5 Discussion

3.5.1 Progress in the Mapping Monitoring of Chl-a using UAVs

The reviewed studies reveal that between 2015 and 2018, the use of UAV applications in small water bodies was limited. This could be attributed to the high cost of UAVs (Sibanda *et al.*, 2021) during this period, limiting access for research purposes. However, the usage of UAVs has gained traction over the last five years, which can be attributed to several factors such as improved UAV technologies, miniaturing of sensors, cost efficiency, increase in research funding, high-resolution data, and real-time monitoring.

The findings showed that most studies were conducted in China, South Korea, and the USA (Figure 3.5). This stems from the fact that UAV technology in these countries/regions evolved as far back as the 20th century (Sibanda *et al.*, 2021). Also, the world's leading UAV manufacturer, DJI, is based in Shenzhen, China, and this platform emerged as the most used from the reviewed studies. This proximity and ease of access to UAV technology have likely contributed to the region's high concentration of research studies. Additionally, South Korea's strong technology industry and innovative culture have facilitated the adoption and application of UAVs in various fields, such as water quality monitoring, leading to more studies in the area. Overall, these countries are well-developed and can fund water quality monitoring programs.

Using a spectrophotometer in situ data collection (Figure 3.7) indicates a preference for controlled, precise measurements, as laboratory settings allow for meticulous calibration and control of experimental conditions, leading to highly reliable data. While spectrophotometers provide high precision, their use is often limited by the need to transport samples to the laboratory, which can introduce delays and potential sample degradation. This justifies why 21% of the studies utilised both spectroradiometers and spectrophotometers to gather in situ data. Spectroradiometers are capable of rapid, non-destructive measurements directly in the field and allow for real-time monitoring and immediate data availability (Guimarães, 2017). Unlike spectrophotometers, spectroradiometers determine chl-a concentration indirectly using radiances computed in an equation. The combined use of spectroradiometers and spectrophotometers reflects an approach that balances field applicability with data accuracy.

Regarding platforms and sensors, multi-copters were most commonly used in mapping chl-a. According to Zaludin and Harituddin (2019), multi-copters are preferred to fixed-wing drones in water quality mapping because of their cost-effectiveness. In this review, multispectral sensors were adopted by most of the studies relative to hyperspectral sensors because of their cost-effectiveness (Adjovu *et al.*, 2023). The MicaSense sensor was widely used in chl-a monitoring in small water bodies because it can capture images in five distinct bands: red, green, blue, near-infrared, and Rededge. These bands are crucial in the estimation of chl-a.

On the other hand, according to Shafique *et al.* (2003), hyperspectral sensors exhibit high spectral resolution, which allows them to provide detailed and accurate information on the quality of surface waters. As a result, hyperspectral sensors are highly valued in water quality monitoring, as they can detect changes in water quality more effectively than multispectral sensors. Despite these merits, hyperspectral sensors have drawbacks, including high costs associated with sensor procurement and operational maintenance, limited depth penetration and sensing capabilities due to water absorption and scattering, and complex data processing and analytical requirements (Bangira *et al.*, 2024). Some reviewed studies utilised both the multispectral and hyperspectral sensors, to achieve comprehensive datasets leveraging the wide range of the electromagnetic spectrum and cost-effective solutions (Topp *et al.*, 2020; Yang *et al.*, 2022).

3.5.2 Application of Chl-a Estimation Algorithms

The findings of this review highlight the strengths and limitations of various algorithms used for chl-a estimation in UAV remote sensing applications. While linear regression is widely used due to its simplicity, it has limitations in accuracy evaluation. As Arias-Rodriguez *et al.* (2021) noted, linear regression assumes a linear relationship between independent variables and the dependant variable, which is not necessarily true in all instances. If the actual relationship is non-linear, linear regression may fail to capture the true pattern, leading to poor accuracy.

In this study, random forest was the most popular machine learning algorithm but exhibited inconsistent performance. Despite an average R^2 value of 0.700, it showed good results in training data ($R^2 > 0.700$) but poor generalisation in testing data (R^2 as low as 0.300) (Su, 2015;

Xiao, 2022; Lo, 2023). This inconsistency may be attributed to the weak correlation between chl-a and spectral indices, which limits model performance (Lo, 2023). In contrast, algorithms like XGBoost demonstrate high accuracy due to their operational efficiency, flexibility, and ability to handle small sample sizes, control model complexity, and reduce bias. For instance, Chen (2021), Lu (2021), Chen (2023), and (Fu, 2023) achieved R^2 values greater than 0.800 using sample sizes of 44, 33, 59, and 31, respectively, showcasing the superior performance of XGBoost in chl-a estimation. The SVM algorithm was also widely used owing to its robustness, ability to handle non-linear relationships, and accuracy in predicting results with small sample sizes (Deka, 2014; Zhao, 2022a). However, its moderate accuracy ($R^2 = 0.620$) highlights the need for alternative approaches.

Probabilistic methods such as BPNN are suitable for large study areas, as they can accurately estimate water quality parameters even with imbalanced datasets and handle non-linear relationships. For example, Zhang (2020a) successfully applied BPNN to a 0.420 km^2 river section with 35 samples. However, BPNN has drawbacks like convergence issues and local minimisation. Liu (2021) observed significant deviations between predicted and true values with the BPNN algorithm, reducing model accuracy and performance. Convolutional Neural Networks (CNN) were the most adopted deep learning method, with reliable feature extraction capabilities from multi-dimensional data (Sothe *et al.*, 2020). However, deep learning algorithms rely on black-box models, which makes it challenging to interpret their outputs (Koh and Liang, 2017; Lee *et al.*, 2021).

Neural networks and supervised machine learning algorithms performed strongly due to their stability, speed, and limited overfitting. Stacked machine learning models achieved higher R^2 values than single models (Zhang, 2020a; Zhang, 2020b), but may be susceptible to overfitting. This overfitting issue suggests that stacked models may become overly specialised in the training data, failing to generalise effectively to new data. Therefore, using stacked models with caution on small datasets is crucial to avoid becoming too focused on specific dataset characteristics rather than learning underlying patterns and relationships (Rocha *et al.*, 2017; Wang *et al.*, 2019).

3.5.3 Gaps, Challenges, and Opportunities

Research on mapping chl-a in small water bodies using UAVs has been gaining momentum in recent years, driven by advancements in UAV sensor technologies. This study extensively reviewed existing literature and identified several key gaps, challenges, and opportunities related to using UAVs for chl-a mapping in small water bodies.

Previous studies of chl-a estimation using UAV-remotely sensed have not done any work in Africa. This may have been impeded by the high costs of UAVs and piloting licenses, as well as legal restrictions on UAV usage in many African countries (Rhee *et al.*, 2018a; Wang *et al.*, 2020b; Sibanda *et al.*, 2021). Most affordable UAVs are also designed for recreational use rather than research (Sibanda *et al.*, 2021).

In addition to the geographical gap, the literature showed that the mapping and monitoring of chl-a in small inland reservoirs is still rudimentary. This is because small inland reservoirs are too small, making them challenging to map using satellite remote sensing with coarse-resolution sensors. However, UAV-borne hyperspectral and multispectral sensors could address this gap by acquiring ultra-high resolution suitable for mapping chl-a in small reservoirs.

Moreover, several studies have successfully used UAVs to monitor chl-a in small water bodies. However, several challenges hinder the effectiveness of UAVs in chl-a mapping, such as the lack of robust models that can be trusted across multiple studies. While several models (EBS, Chen method, PSO-LSSVM, GA_ABR, GA_XGB, AELR, GBRT, ERT, GA_PLS, and SSNN) have shown strong predictive power ($R^2 > 0.700$), each has only been evaluated in a single study, raising concerns about their reliability and generalisability. Furthermore, the limited number of comparative studies makes it difficult to determine the best-performing algorithm.

The use of thirteen different cameras, ten different UAV platforms, several different algorithms, and overall methodology study by study highlights UAVs' flexibility and customised application in estimating chl-a for different geographical settings. While this is a merit, it also reveals a lack of standardisation in the processes involved in UAV-based remote

sensing of chl-a. A solution to this will be to provide a standardised framework and simplified inversion models (Shen *et al.*, 2012) for different case scenarios (based on the type of water body and size of the water body). This will assist in reducing the time spent testing and evaluating multiple UAVs, sensors, and algorithms.

The performance of some algorithms may have been affected by single-date or single-image approach disadvantages because a small sample size can affect the algorithm's accuracy (Wasehun *et al.*, 2024). Few studies collected data across multiple times or seasons, highlighting the need for more robust datasets to improve model accuracy. This review emphasises the importance of multi-temporal data collection to enhance the reliability of water quality predictions.

3.5.4 Limitations of the Study

Some articles were unavailable in full text/length, limiting the review's comprehensiveness. Non-English articles were excluded, which may negatively impact the total number of studies reviewed on estimating chl-a levels. The accuracy of remote sensing data is crucial for reliability. This review used R^2 values as the primary measure for accuracy, which was limiting. Different studies used various accuracy measures with non-universal and variable International System of Units (SI unit). Additionally, R^2 values are influenced by factors such as sample size, sensor type, algorithm used, and vegetation indices applied. These factors should be considered in the final analysis. However, since only peer-reviewed studies were included, it is assumed that the accuracy measures used in each study have been verified and deemed credible by peer reviewers.

3.6 Conclusion

This chapter aimed to perform a systematic literature review on the global application of UAVs for chl-a monitoring in small water bodies. The study provided insights into current progress, trends, algorithms, sensors, wavelengths, and platforms, as well as challenges, gaps, and opportunities. The use of UAVs for monitoring chl-a in small water bodies has shown promising results, with an exponential increase in global studies. However, a significant gap remains in African research, where no studies have been conducted. Multispectral and

hyperspectral sensors have proven essential for high-resolution mapping, while machine learning methods offer cost-effective solutions for chl-a estimation from UAV imagery. Less application was observed with hyperspectral sensors, owing to their high costs. While certain chl-a estimation algorithms, such as stacked machine learning models, show great promise in achieving high performance, they also pose a significant risk of overfitting. Therefore, future research should focus on collecting more sample data to build robust and accurate water quality inversion models. This presents an opportunity to enhance model performance by addressing the current data limitations, ultimately improving the accuracy and reliability of chl-a estimation. Overall, UAV-based remote sensing technology has the potential to revolutionise water resource management strategies, and its application should be further explored and developed.

CHAPTER 4: ASSESSING CYANOBACTERIA IN A SMALL RESERVOIR USING UNMANNED AERIAL VEHICLE SYSTEMS (UAVS): A CASE STUDY OF HIGH FLIGHT FARM DAM [2]

4.1 Abstract

Agricultural intensification often introduces nutrients such as nitrogen and phosphorus into nearby water bodies through runoff, degrading water quality. Smallholder farmers rely on small reservoirs for irrigation. However, the limited spatial resolution of conventional satellite-based remote sensing makes it inadequate for monitoring these small water bodies. Unmanned Aerial Vehicles (UAVs), with their high spatial resolution, offer a promising solution to this challenge by enabling accurate, detailed and localized monitoring of small water bodies The objectives of the study were to employed an unmanned aerial vehicle (UAV) based multispectral imaging system to monitor chlorophyll-a (chl-a) concentrations as a proxy indicator of cyanobacteria within a small reservoir in South Africa and to test if chl-a can be used as a reliable proxy for nutrient concentrations in aquatic systems. In-situ measurements of chl-a, total nitrogen (TN), total phosphorus (TP), and dissolved oxygen (DO) were collected during three field campaigns in April, June, and July 2024. The study integrated remote sensing with machine learning models, including Random Forest (RF), Support Vector Machine (SVM), Artificial Neural Networks (ANN), and Extreme Gradient Boost (XGBoost), to estimate chl-a levels. The green, red and red-edge bands were identified as the most sensitive for chl-a retrieval. Results showed that ANN consistently achieved the highest R^2 values (0.949, 0.991, and 0.734 for April, June, and July, respectively), outperforming other models. High chl-a concentrations of 34.25 µg/L in April were driven by nutrient-enriched runoff, while declines in June and July (13.230 µg/L, 6.328 µg/L respectively) reflected reduced nutrient availability and temperature changes. NIR and red-edge bands were particularly effective in detecting chl-a dynamics, correlating well particularly with TP ($R^2 = 0.879$) and TN ($R^2 = 0.711$) in July. Spatial analysis revealed nutrient hotspots in inlet and periphery regions. This study highlights the advantages of UAV-based remote sensing for high-resolution water quality monitoring in small reservoirs. The findings

[2] **Ngwenya, N**., Bangira, T., Sibanda, M., Gurmessa, S.K., Gokool, S. and Mabhaudhi, T. (2025), (*in press*). Assessing cyanobacteria in a small reservoir using unmanned aerial vehicle systems (UAVs).

emphasise the for accurate, localized water quality assessments, as changing environmental conditions can quickly affect water quality. The proposed approach can be tailored to similar environments, providing a versatile solution for proactive water resource management.

Keywords*: remote sensing, chlorophyll-a, machine learning, multispectral image, drones, inland lakes*

4.2 Introduction

Small water bodies play an essential role in agricultural water supply (Wisser *et al.*, 2010b). In South Africa, the population has surpassed 60 million (Worldometers.info, 2023), increasing the demand for agricultural production and leading to higher usage of fertilisers and pesticides (Baiphethi and Jacobs, 2009; Davis *et al.*, 2017). This intensified agricultural activity contributes to nutrient-rich runoff entering reservoirs, causing eutrophication, the process by which excessive nutrients degrade water quality and promote excessive algae growth. Eutrophication is particularly evident in the Umgeni catchment, where high nutrient levels from agricultural, industrial, and urban sources result in harmful algal blooms (HABs), notably cyanobacteria (Downing *et al.*, 2001; Falconer, 2001). Cyanobacteria growth is exacerbated by rising temperatures and erratic rainfall patterns (Rankinen *et al.*, 2019. Its proliferation in reservoirs can clog irrigation systems, hinder crop growth, and contaminate food crops (Jeong *et al.*, 2016; NSWG, 2017; Singh *et al.*, 2018).

Recognising the challenges posed by eutrophication, water authorities encourage monitoring cyanobacteria over time and across regions (Palmer *et al.*, 2015; Banda and Kumarasamy, 2020). In the Umgeni Catchment, the Department of Water and Sanitation of South Africa conducts physical monitoring of water quality at multiple points. However, this method is time-consuming, costly, and lacks sufficient spatial coverage, making it difficult to capture changes across all affected areas. This limitation highlights the need for more efficient and comprehensive solutions. Remote sensing provides a valuable alternative for water quality monitoring, offering advantages in temporal, spatial, and dynamic coverage (Yang *et al.*, 2022; Tian *et al.*, 2023; Bangira *et al.*, 2024).

Chlorophyll-a (chl-a), a green pigment found in algae, is an effective indicator of phytoplankton biomass and a proxy for the presence of cyanobacteria. (Liu *et al.*, 2019; Morgan *et al.*, 2020). Chl-a exhibits unique optical characteristics, absorbing red and blue light while reflecting green and near-infrared wavelengths, making it detectable through remote sensing (Wu *et al.*, 2010; Gao *et al.*, 2015). Various Earth observation platforms, including handheld hyperspectral, satellite-borne, and airborne sensors, can effectively detect chl-a concentrations. Among these, hyperspectral sensors offer high accuracy in measuring chl-a, as demonstrated by Cao *et al.* (2021), who achieved optimal accuracy (RMSE = 4.770 μg/L, R^2 = 0.880) for a river in China. However, despite their accuracy, hyperspectral data is expensive and computationally intensive, limiting its practicality for widespread use. This challenge underscores the need to balance sensor precision with affordability and accessibility for large-scale water quality monitoring.

To address these limitations, multispectral satellite systems like Landsat and Sentinel-2 offer a more accessible approach, providing sufficient resolution for detecting chl-a at a lower cost (Toming *et al.*, 2016; Saberioon *et al.*, 2020). Despite their utility, satellite data can be limited by coarse resolution and lack of control over data collection timing (Yang *et al.*, 2022). Alternatively, unmanned aerial vehicles (UAVs) offer a promising solution for monitoring smaller water bodies with high spatial resolution, flexible data collection timing, and cost-effectiveness (Xiang *et al.*, 2019; Yao *et al.*, 2019). UAVs address the shortcomings of satellite data, offering enhanced precision and flexibility in data collection for more effective monitoring of cyanobacteria in small water bodies.

Numerous studies have successfully utilised machine learning algorithms (MLAs) to construct, train, and choose the best chl-a estimation models using UAV-derived multispectral images. For instance, Silveira Kupssinskü (2020) used MLAs such as Random Forest (RF), Least Absolute Shrinkage and Selection Operator (LASSO), Artificial Neural Networks (ANN), K-Nearest Neighbors (KNN), and Support Vector Regression (SVR) to estimate chl-a in a lake and a dam. The ANN and RF performed best and yielded R^2 of 0.901 and 0.823, respectively. Chen (2021), used several MLAs including Deep Neural Networks (DNN), RF, Adaboost, Genetic algorithm_Random Forest (GA_ RF), and Genetic algorithm_Extreme

Gradient Boost (GA_XGBoost) to train chl-a estimation models. The GA_XGBoost stability was tested using different numbers of training data (25%, 50%, 75%) and the results showed that 75% of training data gives the best model ($R^2 = 0.855$). These studies highlight the potential and promise of UAV-acquired remote sensing data and a combination of MLAs in detecting and monitoring water quality parameters, such as chl-a, in small water reservoirs with higher accuracies. Literature has revealed that different studies utilise different MLAs and depending on the study area characteristics, each algorithm is site-specific and data-dependent.

Therefore, the main aims of this study are to (i) estimate the spatiotemporal variability of chl-a concentrations in a small reservoir using UAV data and different machine learning algorithms and (ii) assess the potential of remotely sensed chl-a as a proxy for estimating not optically active parameters namely total nitrogen (TN), total phosphorus (TP), and dissolved oxygen (DO) using multispectral UAV remotely sensed data.

4.3 Materials and Methods

4.3.1 Study Area

The study area, High Flight Farm Dam, is in the upper Midmar Dam sub-catchment of the Umgeni catchment, KwaZulu-Natal, South Africa (-29.454537°, 29.902512°) (Figure 4.1a-c). This catchment receives 400–1000 mm of precipitation annually, primarily during the summer months (October to April), with occasional winter rains. The average annual temperature ranges from 12°C to 14°C, with cooler conditions in June and July and warmer temperatures from December to February. Potential evaporation, recorded at the A-pan, averages 1600–1800 mm per year (UmgeniWater, 2016). The reservoir, covering 20 hectares, replenishes through rainfall and natural springs and serves as a critical water source for irrigating crops such as potatoes, maize, sugar, eggplant, and beans, along with fruits like pears, apples, and lemons. Livestock, including goats, sheep, cows, and horses, also rely on this reservoir. Primary irrigation methods include canal systems and some centre-pivot systems, which farmers maintain regularly to prevent clogging, cleaning at least four times a year. These factors make the dam a good example of a system that needs preventive and periodic monitoring to ensure sustained water quality and system functionality.

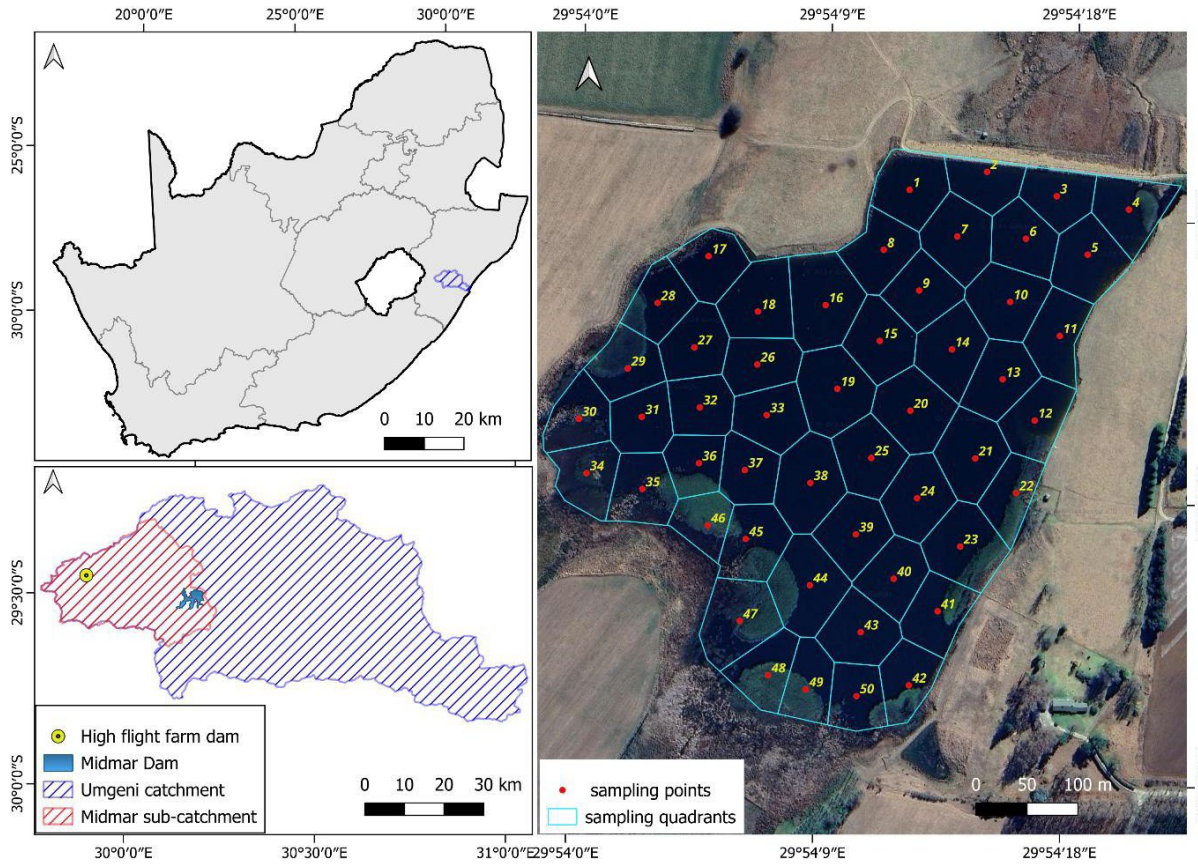

Figure 4.1: Study area location: (a) South Africa, (b) Umgeni and Midmar catchments with High Flight Farm Dam, and (c) High Flight Farm Dam divided into 50 sampling quadrants, with red dots as sampling points.

4.3.2 Data Collection and Processing

UAV images and water samples were collected concurrently during three field campaigns: once in autumn and twice in winter, under clear skies and calm wind conditions. Flights took place between 10 a.m. and 12 p.m. to ensure optimal solar irradiance. Notably, rainfall occurred between the April and June campaigns, potentially influencing water quality results. Agricultural practices within the Midmar sub-catchment involve fertilisers containing nitrogen and phosphorus, which contribute nutrients to nearby rivers, potentially causing eutrophication. For this study area, nutrient loading is reflected in the growth of hyacinth in parts of the dam (Figure 4.2a).

Figure 4.2: (a) Field observation of the dam showing water hyacinth presence, (b) UAV deployed for high-resolution multispectral imaging over the dam, (c) Field team navigating to sampling points within the dam by boat, (d) Laboratory analysis of water samples collected from the field.

4.3.2.1 Water Quality Sample Collection

Water samples were collected on April 15, May 20, June 5, and July 16, 2024, with 50, 50, 41, and 47 samples collected on each respective date. The dam was divided into 50 quadrants using the k-means clustering tool in QGIS (Figure 4.1c), and sampling stations were identified at the centroid of each quadrant. Using a boat and GPS, we navigated to these stations, where a Hanna multiparameter probe measured DO, temperature, pH, turbidity, and electrical conductivity. Water samples were taken 0.500m below the surface using 500ml amber bottles, then immediately transported to the laboratory in ice-filled cooler boxes with ice for analysis chl-a, TN, and TP analysis. Samples were stored at -20°C, with chl-a analysis conducted within 24 hours of collection.

4.3.2.2 UAV Data

Field campaigns were conducted exclusively on the April, June, and July dates. The UAV utilized in this study was a DJI Matrice 300, equipped with a multispectral MicaSense Altum camera and a Downwelling Light Sensor 2 (DLS-2). The camera features five spectral bands: blue, green, red, red-edge, and near-infrared (Table 4.1). It has an 8 mm focal length and a field of view (FOV) of 48° × 37°. The UAV was flown at an altitude of 100 meters, with a ground sample distance (GSD) of 5.2 cm per pixel. An image side overlap of 80% was maintained to assist with post-processing challenges arising from flying over water. A digitised shapefile of the dam was imported into the DJI M-300 smart console to create a flight plan that covered the entire dam surface. This enabled the UAV to complete the flight mission autonomously. Prior to the flight, the MicaSense Altum was calibrated using a reflectance panel, and an image was captured directly over the panel to assess the lighting conditions specific to the flight's time, date, and location. The total UAV flight duration was approximately 90 minutes.

Table 4.1: The wavelengths and bandwidths captured by the MicaSense sensor

Band	Centre	Band Width	Range
Blue	475 nm	32 nm	443–507 nm
Green	560 nm	27 nm	533–587 nm
Red	668 nm	16 nm	652–684 nm
Red Edge	717 nm	12 nm	705–729 nm
Near Infrared (NIR)	842 nm	57 nm	785–899 nm

4.3.3 Data Processing

In-situ and UAV data were processed according to the framework shown in Figure 4.3.

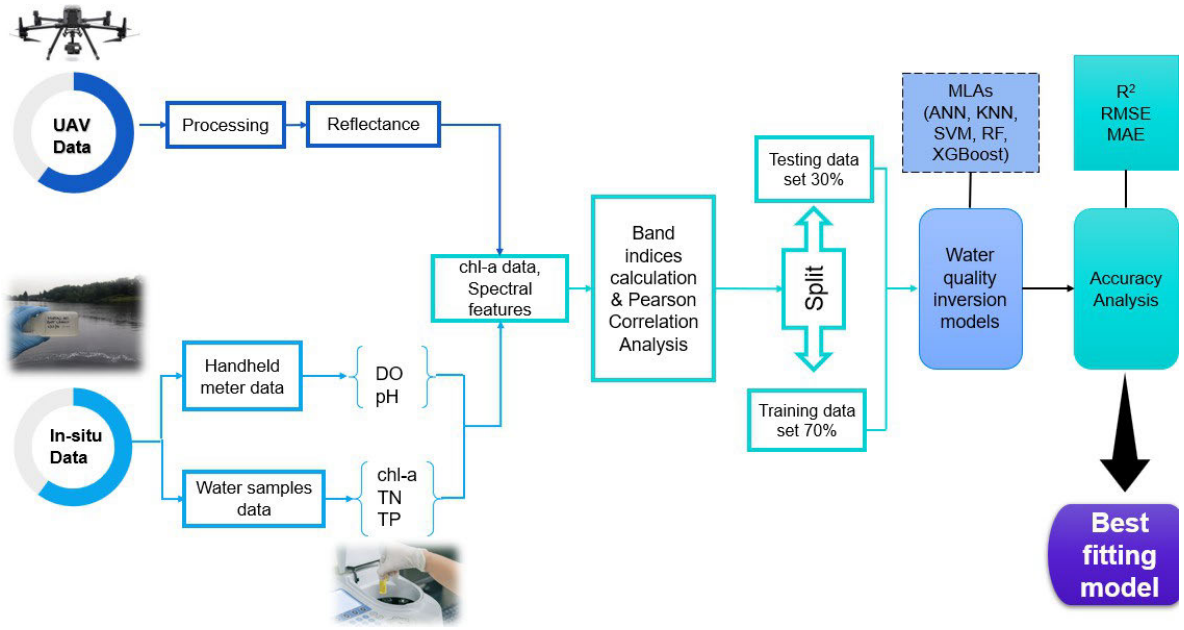

Figure 4.3: Methodological framework for chl-a estimation using UAV-derived data

4.3.3.1 In situ Data Processing

Chl-a was derived in the laboratory using the acetone extraction method under subdued light as explained in Arar (1997). The following steps were followed: i) samples were stored in the dark at -20ºC, ii) 400ml of the sample was filtered using 0.450µm GF/F 151 microfiber glass filters within 24 hours of sampling time, iii) 10ml of 90% acetone was added to filtered samples in 15ml centrifuge tubes, iv) the filtered paper was then mechanically ground by hand using a pestle for 10 to 15 seconds, v) the ground filter paper was allowed to extract for 2 to 24 hrs, vi) followed by 15 minutes of centrifuging at 600G to separate the materials, , and vii) finally analysis using a spectrophotometer at the 750 nm, 665 nm, 664 nm, 647 nm, and 630 nm (Shimadzu UV-1800, Spectrophotometer). Chl-a concentration was computed using Jeffrey and Humphrey's spectrophotometric equation 4.1 (Jeffrey and Humphrey, 1975):

$$\text{Chl} - \alpha \text{ uncorrected } \left(\frac{\text{ug}}{\text{L}}\right) = \frac{[11.85(664_B) - 1.54(647_B) - 0.8(630_B)] \times V_1}{V_2 \times L} \quad (4.1)$$

Where 664_B = Subtract 750 nm value (turbidity correction) from the absorbance at 664 nm before acidification, 647_B = turbidity corrected absorbance at 647 nm before acidification, 630_B = turbidity corrected absorbance at 630 nm before acidification, V_1 = volume of extract (mL), V_2 = volume of sample filtered (L), L = path length (cm).

Total nitrogen (TN) was measured based on the reaction of the nitrate ion with brucine sulfate in a 13N sulfuric acid solution at 100°C as done by Jenkins and Medsker (1964). The resulting solution was measured at 410 nm using a spectrophotometer (EPA, 1971). On the other hand, total phosphorus (TP) was determined by reacting ammonium molybdate and antimony potassium tartrate in an acidic medium with diluted phosphorus solutions to form an antimony-phospho-molybdate compound. When treated with ascorbic acid, the complex turned a deep blue colour and was subsequently analysed for absorbance at 660 nm and 880 nm using a UV spectrophotometer.(Eleuterio and Neethling, 2010).

4.3.3.2 Image Pre-processing

The image processing step aimed to extract spectral values from each band at each sampling station as captured by the multispectral sensor. First, the images captured by the sensor were uploaded into Pix4DFields software and stitched together to create a single mosaic image. This mosaicked was then imported into QGIS software, where the spectral values for each band were extracted at each sampling point. To mitigate background noise and reduce interference from rough water surfaces, the original spectra were pre-processed using the band ratio method (Huang *et al.*, 2016). Based on the extracted spectral values, a total of 60 band combinations were generated in a GIS environment, including band ratios (10), band differences (20), band sums (10), band products (10), and normalised differences (10). The resulting band combinations were exported to Microsoft Excel for correlation analysis with chl-a data. The coefficient of determination (R^2) was then calculated to determine the key wavelengths for accurately estimating water quality parameter concentrations. The band combination showing the highest correlation with in situ data was selected for model construction.

4.3.3.3 Machine Learning Algorithm Implementation

This study utilised artificial neural networks (ANN), extreme gradient boosting (XGBoost), K-nearest neighbours (KNN), random forest (RF), and support vector machine (SVM) to develop

models for estimating chl-a. The analysis was conducted separately for each field campaign, where each dataset was randomly divided into 70% for building and training the model, and 30% for testing through validating the predictive performance of the model. All models were implemented in RStudio using relevant R packages.

RF is an ensemble machine learning approach combines predictions from many decision trees to produce a final result (Breiman, 2001). It uses the bootstrap aggregation (bagging) technique to generate multiple decision trees, each constructed from a random sample of the original dataset. For each tree, only a subset of the available features is randomly selected at each node split to avoid overfitting and to ensure diversity among trees. The attribute that provides the highest information gain is chosen for the split. The final output is generated by averaging predictions from all trees, making RF particularly robust to overfitting and suitable for noisy or small datasets (Ali *et al.*, 2012). In this study, the optimal band combination, determined via correlation analysis, was used as input to train the RF model. The `randomForest` package in R was used for implementation. This algorithm generated classification and regression trees (CART) to model the relationship between spectral predictors and chl-a concentration.

SVM is a supervised machine learning algorithm designed for classification and regression tasks. It operates by finding the optimal hyperplane that maximises the margin between classes (in classification) or by fitting a line that best captures the relationship between input and output (in regression). SVM can accommodate linear and non-linear relationships using kernel functions, such as radial basis function (RBF) and polynomial kernels (Ghosh *et al.*, 2019).This study used SVM for chl-a prediction, taking advantage of its strong performance on small datasets (Deka, 2014). The `e1071` package in R was used to implement the SVM model, with the RBF kernel applied to account for non-linear relationships between reflectance-based predictors and chl-a concentration.

ANN is a computer model made up of layers of interconnected nodes (neurons) that was inspired by the composition and operation of the human brain. (Maier *et al.*, 2010). The ANN algorithm was used for chl-a estimation, leveraging its ability to model intricate, non-linear

relationships between input features and output variables (Zhao *et al.*, 2019). The architecture used in this study included an input layer, with nodes representing selected spectral indices, one or more hidden layers for capturing complex patterns in the data, and an output layer for generating chl-a predictions. The ANN model was implemented using the `neuralnet` package in R. Backpropagation was used to train the network by iteratively adjusting connection weights to minimise the prediction error.

KNN is a non-parametric, instance-based machine learning algorithm. It predicts the value of a target variable by averaging the outcomes of the k-nearest neighbours in the feature space. It measures the Euclidean distance between a given sample and other points in the dataset (Modaresi and Araghinejad, 2014). The `class` package in R was used to implement the KNN model. The number of neighbours (k) was fixed to five, and predictions were based on the average chl-a values of the nearest data points.

XGBoost is a high-performance, tree-based ensemble algorithm that builds models sequentially, where each new tree is trained to correct the residuals (errors) from the previous model. It uses gradient boosting, where residuals from earlier predictions are minimised to improve the model's performance iteratively. XGBoost is known for its speed and ability to prevent overfitting through regularisation techniques, making it suitable for small datasets (Nasir *et al.*, 2022). This research used XGBoost to predict chl-a concentrations, benefiting from its flexibility to handle complex feature interactions and its efficiency in working with limited samples. This model was implemented using the `xgboost` package in R. XGBoost was applied to predict chl-a, leveraging its flexibility to model complex feature interactions and its speed and accuracy even with limited training data.

4.3.4 Accuracy Assessment

Three statistical metrics were used to evaluate the agreement between the estimated $\hat{y}_i$ and measured y_i; the coefficient of determination (R^2), the root-mean-square error (RMSE), and the mean absolute error (MAE) of the response and predictor variables. The greater the R^2 value the stronger the performance of the model. These metrics are defined as follows:

$$R^2 = 1 - \frac{\sum_{i=1}^{n}(y_{i-}\ \hat{y}_i)^2}{\sum_{i=1}^{n}(y_i - \bar{y})^2} \quad (4.2)$$

$$RMSE = \sqrt{\frac{1}{n}\sum_{i=1}^{n}(\hat{y}_i - y_i)^2} \quad (4.3)$$

$$MAE = \frac{1}{n}\sum_{i=1}^{n}|\hat{y}_i - y_i| \quad (4.4)$$

Where n is the number of sampling points, $\hat{y}_i$ represent predicted values of the chl-a, y_i represents the response of measured chl-a. Total nitrogen will be determined by oxidising it with potassium persulfate, followed by measurement using a UV spectrophotometer. Total phosphorus will be digested with a 5% potassium persulfate solution and molybdenum-antimony reagent, and then analysed in a UV spectrophotometer to measure absorbance (O'Dell, 1993).

4.4 Results

4.4.1 Temporal and Spatial Variation of In Situ Data

Periodic monitoring revealed significant differences in water quality across different months. Chl-a levels were highest in April, with a mean value of 24.947 µg/L, suggesting a potential algal bloom. The concentrations decreased steadily over the study period, reaching the lowest mean value of 1.956 µg/L in July. Spatial variability was most pronounced in April, as indicated by the range of 12.200–34.250 µg/L, whereas July showed the most uniform conditions with a range of 0.392–6.328 µg/L. TN concentrations were highest in April (0.191 mg/L) and July (0.150 mg/L), while June recorded the lowest concentration at $1\times\ 10^{-4}$ mg/L. The widest variability in TN was observed in April, with values ranging from 0.063 to 0.315 mg/L, indicating spatial heterogeneity in nitrogen availability across the sampling sites. TP concentrations displayed notable variability, with the highest mean value of 0.644 mg/L in July and the lowest of 0.024 mg/L in June. These results highlight temporal differences in phosphorus dynamics during the study period. DO concentrations peaked in May with a mean value of 1.595 mg/L, while the lowest mean concentration of 1.345 mg/L was recorded in April. The range of DO values was greater in May (0.190–3.870 mg/L) than in April (0.110–2.360 mg/L), reflecting higher spatial or temporal heterogeneity in May. Then in early winter (June)

reduced chl-a, TN, and TP concentrations suggest decreased nutrient availability and lower algal productivity. Mid-winter (July) results showed the lowest mean for chl-a likely due to colder temperatures and lower nutrient inputs. Also, the dam's condition changed significantly due to lower water levels. This variability in space and time highlights the dynamic nature of the irrigation dam, underscoring the importance of continuous monitoring. Detailed statistics of the in situ water quality data are provided in **Error! Reference source not found.**.

Table 4.2: Summary of in situ water quality results collected in April, June, and July 2024

		15 April 2024	20 May 2024	5 June 2024	16 July 2024
	Sample size	**50**	**50**	**41**	**47**
Chl-a (µg/L)	Mean	24.947	4.503	8.218	1.956
	Min	12.200	2.020	0.504	0.392
	Max	34.250	9.790	13.230	6.328
TN (mg/L)	Mean	0.191	0.064	1×10^{-4}	0.150
	Min	0.063	0.025	1×10^{-5}	0.054
	Max	0.315	0.165	2.4×10^{-4}	0.356
TP (mg/L)	Mean	0.056	0.298	0.024	0.644
	Min	0.014	0.095	0.001	0.011
	Max	0.099	0.852	0.055	1.644
DO (mg/L)	Mean	1.345	1.595		
	Min	0.110	0.190		
	Max	2.360	3.870		

The temporal analysis of chl-a levels based on UAV-derived reflectance data demonstrates notable variability across different water body sections over three months. In April, reflectance values were highest in the inlet and periphery sections, particularly in the NIR and Red edge bands, with NIR reflectance exceeding 0.300 sr^{-1}. These elevated values suggest significant chl-a presence, indicative of potential algal blooms. The shallow, deep, and outlet sections exhibited lower reflectance, with values below 0.100 sr^{-1} in most bands. By June, reflectance values decreased across all sections, with the inlet still showing relatively higher reflectance, particularly in the NIR and Red edge bands. The decline continued into July, where reflectance

values were uniformly low across all sections, suggesting minimal chl-a concentrations due to low temperatures that lower phytoplankton growth. The deep and outlet sections consistently exhibited the lowest reflectance throughout the period, while the inlet and periphery demonstrated greater variability and higher overall reflectance levels. Figure 4.4 shows the results of the temporal profile of chl-a.

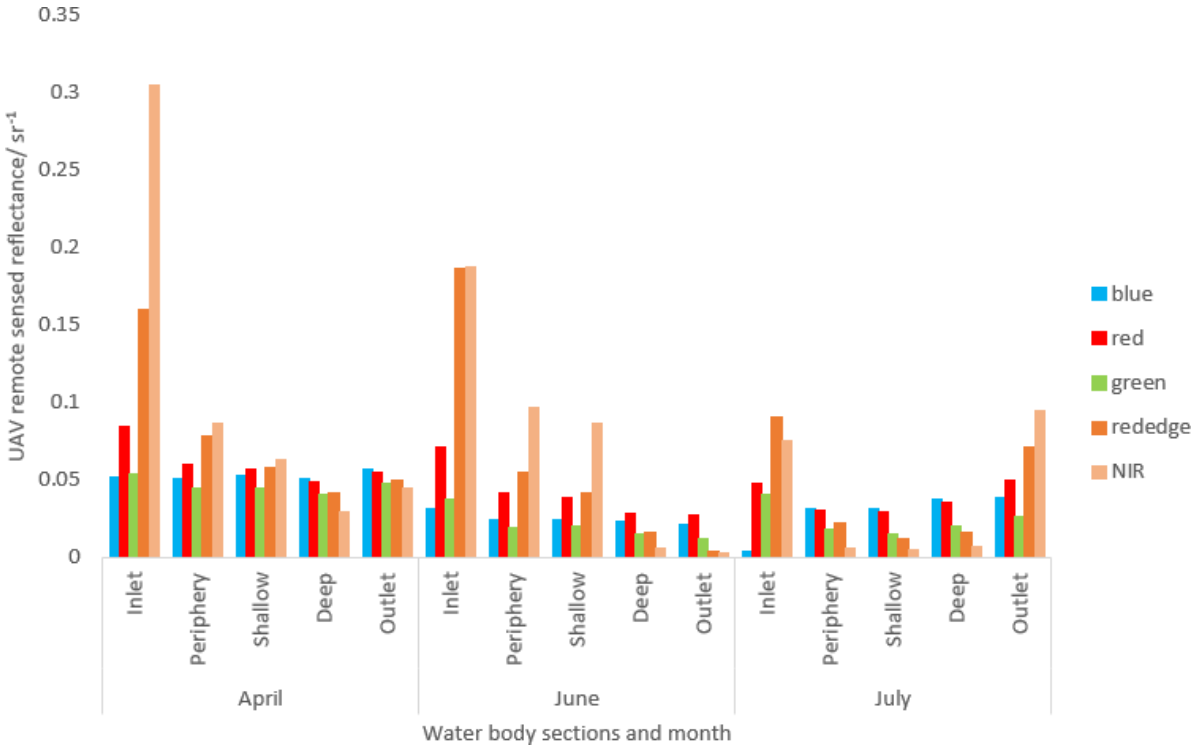

Figure 4.4: Temporal profile of chl-a across different positions of the dam, showing April, May, June, and July 2024 data

4.4.2 Correlation Between In Situ Chl-a and TP, TN, and DO

Correlation analysis showed strong positive relationships between chl-a and key water quality parameters (Figure 4.5 - Figure 4.7). For the April data, the scatter plot in Figure 4.5a shows a positive correlation between chl-a and TN, with an R^2 value of 0.734. This suggests that higher TN concentrations are associated with increased chl-a levels, indicating that nitrogen availability supports algal growth. Figure 4.5b illustrates a positive correlation between chl-a and TP, with an R^2 value of 0.773, highlighting phosphorus as a significant factor influencing chl-a concentrations. The relationship between chl-a and DO in Figure 4.5c shows a moderate

positive correlation ($R^2 = 0.680$), which may reflect the influence of algal photosynthesis on DO levels through oxygen production.

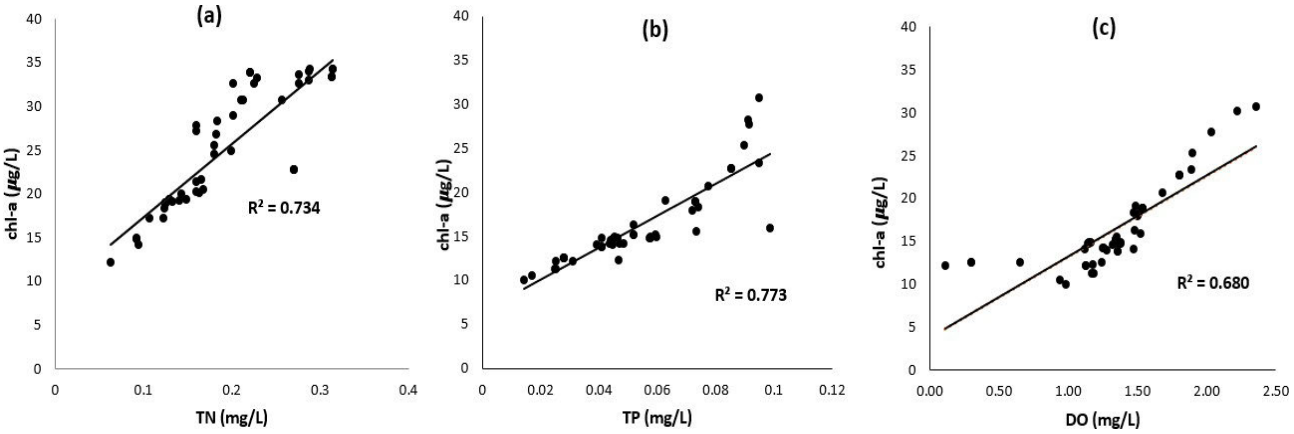

Figure 4.5: Relationships between chl-a concentrations and key water quality parameters: (a) TN, (b) TP, and (c) DO based on April field data

In May, the scatter plot in Figure 4.6a show a positive correlation between chl-a and TN, with an R^2 value of 0.620. This indicates that higher TN levels are associated with increased chl-a concentrations, suggesting that nitrogen availability supports algal growth, although the relationship is moderate. Figure 4.6b depicts a strong positive correlation between chl-a and Total TP, with an R^2 value of 0.716. This suggests that phosphorus availability plays a significant role in influencing chl-a concentrations in the water body. The scatter plot in Figure 4.6c illustrates a moderate positive correlation between chl-a and DO with an R^2 value of 0.670. This relationship may reflect the effect of algal photosynthetic activity on DO levels, where increased chl-a concentrations contribute to higher oxygen production.

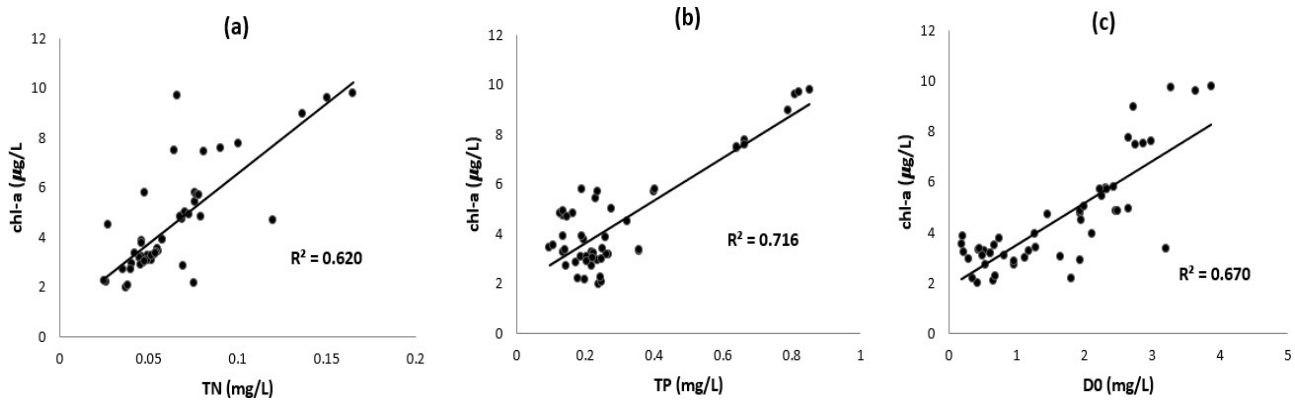

Figure 4.6: Relationships between chl-a concentrations and key water quality parameters: (a) TN, (b) TP, and (c) DO based on May field data

For samples collected in July, chl-a showed strong correlations with TN ($R^2 = 0.711$) and TP ($R^2 = 0.879$) as shown in Figure 4.7, emphasising the influence of nutrient availability on algal concentrations. The results for July highlight the continued importance of nutrient availability, particularly phosphorus, in driving chl-a concentrations. The stronger correlations in July compared to May suggest that nutrient dynamics may shift seasonally, emphasising the need for ongoing monitoring to capture these variations and inform water quality management strategies effectively. The R^2 value for July (0.711) is similar to April's (0.734) but stronger than May's (0.620). This consistency indicates that TN remains an important factor for chl-a dynamics across the three months. The R^2 value for July (0.879) is the highest among the three months (April: 0.773, May: 0.716). This suggests that TP plays a more significant role in regulating chl-a concentrations in July, potentially due to seasonal changes in nutrient availability.

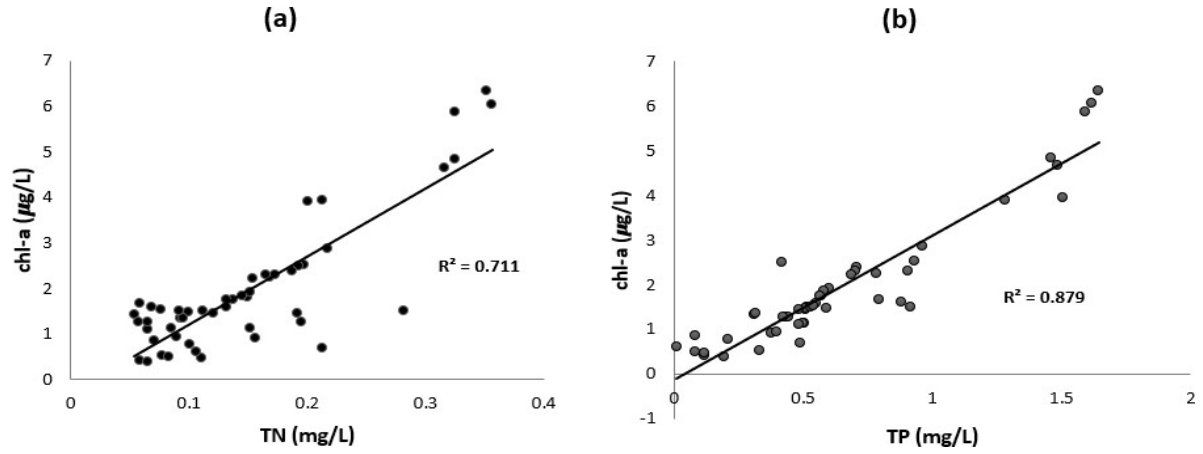

Figure 4.7: Relationships between chl-a concentrations and key water quality parameters: (a) TN and (b) TP based on July field data

4.4.3 Spectral Reflectance Profile of the Water Body

Chl-a exhibits a distinct spectral signature, marked by high absorption in the blue (443 nm) and red (around 675 nm) wavelengths, alongside high reflectance in the green (550–555 nm) and red-edge (685–710 nm) regions (Beck *et al.*, 2016; Buma and Lee, 2020; He *et al.*, 2020). The spectral reflectance of the water body under study was quantitively analysed across five different wavelengths (475 nm, 560 nm, 668 nm, 717 nm, and 842 nm). The spectral curves for the sampled data from the pre-processed UAV-borne multispectral imagery are presented in Figure 4.8. Reflection peaks were observed at 560 nm and 717 nm, while an absorption peak was formed at 668 nm. From these results, a high reflection peak was observed at 717 nm for all three datasets (Song *et al.*, 2013). In terms of different locations in the water body, we observed that the inlet had higher reflection peaks compared to other sections. This may be due to the high amount of nutrient loading in the inlet of the dam. Lower reflectance was observed in July (Figure 4.8c), owing to the reduced water levels in the dam.

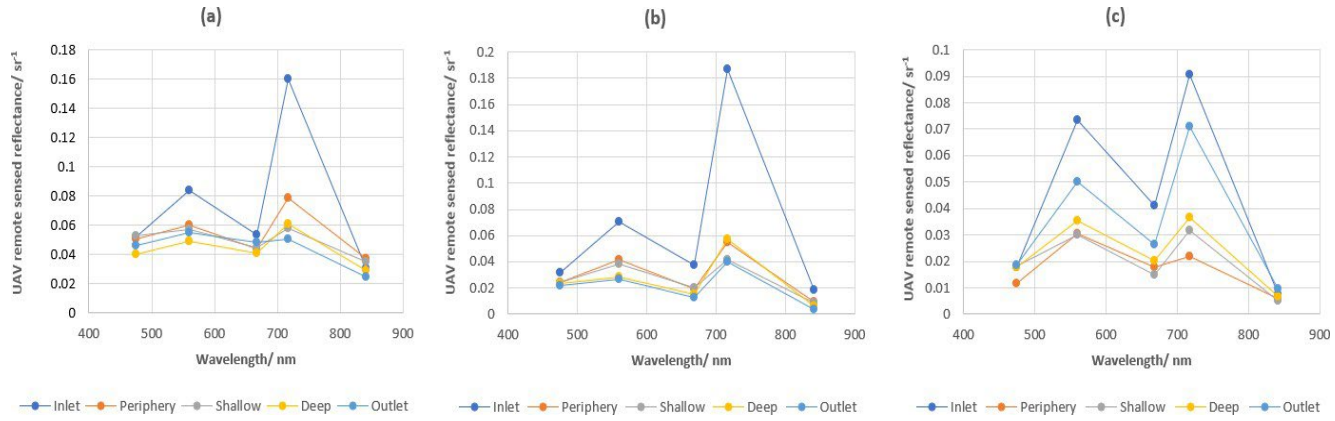

Figure 4.8: Spectral profile for the study water body across different sections of the water body a) April b) June and c) July 2024 data

4.4.4 Inverted Chl-a Results

This study utilised the band ratio method to determine chl-a concentrations, from the five bands, 60 band combinations were calculated. The spectral analysis from UAV images revealed that certain specific band combinations performed better for chl-a estimation (Appendix A, Table A.1). The correlation results are provided in Appendix B, Table B.1 for April 2024, the ratio of green to red-edge bands (G/RE) showed the best performance. In June 2024, the ratio of the green and red bands (G/R) was most effective, while in July 2024, the difference between the red and green band combination (R-G) bands was more suitable. These findings suggest that the green, red, and red-edge bands are the most effective for chl-a retrieval using the MicaSense multispectral sensor for this water body. The machine learning models (RF, SVM, ANN, KNN, and XGBoost) were calibrated using field data from April (50 points), June (41 points), and July (47 points). Table 4.3 presents the evaluation metrics for training and testing datasets. The ANN consistently gave the highest R^2 values: 0.949, 0.991, and 0.734 for April, June, and July testing data respectively.

Table 4.3: Evaluation metrics in the cross-validation phase. The highest values for R^2 are highlighted in bold

		Training			Testing		
	MLA	**R^2**	**RMSE**	**MAE**	**R^2**	**RSME**	**MAE**
15 April 2024	RF	0.970	1.175	0.354	0.826	7.784	2.919
	SVM	0.921	1.831	0.628	0.527	10.703	4.246
	XGBoost	0.994	0.663	0.190	0.859	6.776	2.449
	KNN	0.646	8.882	7.788	0.512	10.306	8.76
	ANN	0.999	0.020	0.013	**0.949**	3.882	1.082
05 June 2024	MLA						
	RF	0.991	0.222	0.121	0.860	1.785	0.796
	SVM	0.989	0.343	0.240	0.300	3.198	1.430
	XGBoost	0.999	0.002	0.001	0.896	1.513	0.742
	KNN	0.829	9.280	7.672	0.857	10.614	9.628
	ANN	0.999	0.009	0.007	**0.991**	0.590	0.235
16 July 2024	MLA						
	RF	0.904	1.835	1.461	0.697	3.028	2.446
	SVM	0.760	2.846	2.127	0.638	3.357	2.585
	XGBoost	0.975	0.987	0.772	0.703	3.315	2.653
	KNN	0.667	13.084	11.656	0.124	15.489	13.087
	ANN	0.815	2.488	1.940	**0.734**	3.044	2.456

Figure 4.9 shows scatter plots illustrating the relationship between observed and predicted chl-a concentrations for 15 April, 5 June, and 16 July 2024. A balanced distribution of data points around the regression line indicates good prediction accuracy. For April and June, the data points are symmetrically distributed on either side of the regression line, demonstrating that the predicted values closely match the observed values. However, for July, there is a noticeable deviation between the predicted and observed values, resulting in a reduced model accuracy of 0.734.

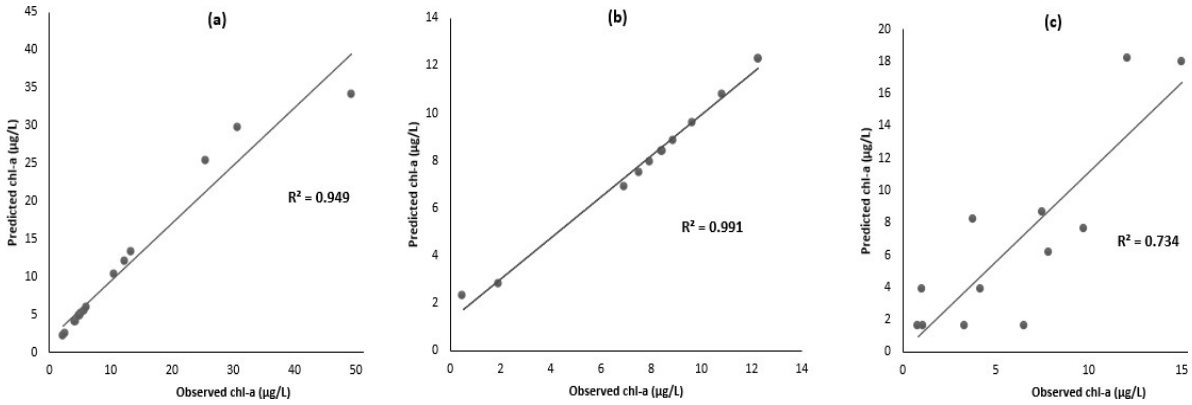

Figure 4.9: Relationship between the observed and predicted chl-a concentration based on the best-performing model (ANN) a) 15 April b) 5 June c) 16 July 2024 data.

Based on the above results, the ANN model was applied to retrieve chl-a concentration for the study area, producing the distribution maps shown in Figure 4.10a-c. White patches in the images are attributed to factors such as sun glint caused by the reflection of sunlight on the water surface and GPS inaccuracies during the UAV flight, which led to the gaps in the captured imagery. Figure 4.10a shows a relatively uniform distribution of chl-a concentrations ranging from 1.644 to 18.289 µg/L in April, a period characterised by rainfall. The elevated chl-a levels observed in most parts of the dam suggest enhanced nutrient inflow from surface runoff. However, lower concentrations around the periphery, despite the rains, may indicate the influence of other limiting factors. For instance, intense rainfall events could have induced water mixing, diluting nutrient concentrations or increasing turbidity, both which can reduce light availability and suppress algal growth.

In Figure 4.10b, chl-a concentrations in June appear strongly concentrated around the dam's periphery (approximately 17.651 µg/L), while the central areas show much lower values. June marks the onset of winter, characterised by cooler temperatures and changes in hydrological conditions. The general decline in chl-a compared to April may be due to more stable water conditions, slower nutrient turnover, and suppressed algal activity resulting from cooler temperatures. The high concentrations along the periphery could be attributed to localised nutrient accumulation or residual runoff effects.

Figure 4.10c illustrates the chl-a distribution in July, during mid-winter. High concentrations (up to 18.289 µg/L) are observed along the periphery, inlet, and shallow areas of the water body, while lower concentrations (1.644 µg/L) appear in deeper and outlet sections. Similar to June, the overall chl-a levels remain relatively low, reflecting the continued influence of winter conditions, such as reduced temperatures and diminished biological activity. Nonetheless, the localised high concentrations suggest the influence of factors such as nutrient retention in shallow zones and reduced water flow. These findings highlight the complex and dynamic nature of chl-a distribution, shaped by seasonal variability and environmental interactions.

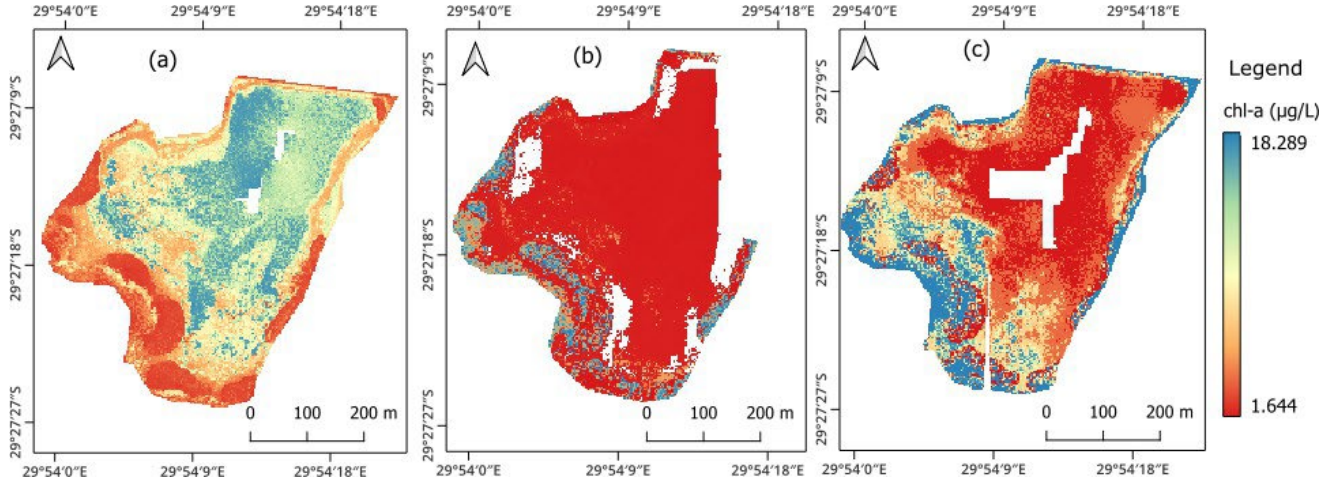

Figure 4.10: Spatial distribution of chl-a concentration for (a) 15 April (b) 5 June and (c) 16 July of 2024 based on the ANN model

4.5 Discussion

The study successfully predicted chl-a concentrations at the irrigation dam site using UAV-based remote sensing and machine learning algorithms, achieving high R^2 values (> 0.700) across multiple models. The ANN model consistently outperformed others, achieving R^2 values of 0.949, 0.991, and 0.734 for April, June, and July, respectively. These results underscore the robustness of the methodology and its potential for scalable chl-a monitoring. However, several critical aspects of seasonal variation, spatial heterogeneity, and MLA performance need further discussion.

4.5.1 Seasonal Variation and Temporal Analysis

The study highlighted distinct seasonal variations in chl-a concentrations. Chl-a levels reached 34.250µg/L in April, the highest observed during the study period, likely driven by nutrient enrichment driven by surface runoff during the rainy season. This period also coincided with elevated TN and TP levels (>0.300 mg/L), critical drivers of algal growth (Pérez-Ruzafa *et al.*, 2005; Filstrup and Downing, 2017). Chl-a and nutrient concentrations declined by June, reflecting reduced external inputs and a transition to drier conditions. In July, chl-a levels sharply declined due to reduced water levels, nutrient depletion, and colder temperatures, which are less favourable for algal productivity (Bakker and Hilt, 2016).

DO levels exhibited seasonal variation, with higher levels in May potentially linked to increased photosynthesis during moderate algal growth. In contrast, lower DO levels in April may result from oxygen consumption during algal bloom decomposition. Variability in May indicates dynamic oxygenation processes influenced by mixing or localised algal activity (Kazbar *et al.*, 2019; Lauguico *et al.*, 2020).

Temporal reflectance patterns supported these trends. High reflectance in April, particularly in the NIR and red-edge bands, indicated algal blooms, especially in the inlet and periphery sections. Reduced reflectance in June and July corresponded with lower chl-a concentrations, suggesting nutrient depletion and increased water mixing. These findings underscore the sensitivity of UAV-acquired reflectance data to seasonal changes in chl-a concentrations and their environmental drivers.

4.5.2 Spatial Patterns and Implications

The spatial distribution of chl-a and nutrient levels revealed significant heterogeneity across the water body. High chl-a reflectance in the inlet and periphery sections in April suggested localised nutrient enrichment, likely driven by agricultural runoff or point-source pollution. In contrast, the deep and outlet sections consistently exhibited low reflectance and nutrient concentrations, indicating reduced algal activity and nutrient influx. By June, moderate reflectance in shallow and peripheral areas suggested wider algal distribution, whereas July's patterns reflected the concentration of nutrients and algal growth in the outlet due to lower water

levels. These spatial trends highlight the importance of targeted nutrient management strategies to mitigate eutrophication and its impacts on water quality.

4.5.3 UAV-based Monitoring for Water Quality Parameters

The study demonstrated the utility of UAV-acquired chl-a data as a proxy for TN, TP, and DO. High correlations between chl-a and nutrient levels reinforced the pivotal role of these nutrients in driving algal growth (Zhou *et al.*, 2016). Additionally, UAV-derived reflectance effectively captured temporal and spatial variations in chl-a, providing insights into nutrient dynamics and hydrodynamic processes.

Chl-a's strong correlation with TP compared to TN in some periods underscored the dominant role of phosphorus as a limiting nutrient in freshwater systems. Moderate correlations with DO suggested that while oxygen levels are influenced by algal activity, they also depend on factors like temperature and microbial processes. These findings emphasise the capability of UAV-based approaches to monitor water quality comprehensively and efficiently.

The red-edge bands proved particularly effective for detecting chl-a peaks, enhancing the accuracy of remote sensing for water quality assessment (Yang *et al.*, 2017; Bramich *et al.*, 2021). The consistent spatial and temporal trends captured by UAVs underscore their potential for high-resolution, scalable monitoring of aquatic ecosystems. Future studies should expand temporal coverage and integrate high-resolution datasets to address challenges such as nutrient hotspots, sediment interactions, and hydrodynamic influences.

4.5.4 Machine Learning Models

The testing data for MLAs showed that the ANN model consistently outperformed other models, achieving the highest R^2 values for April (0.949), June (0.991), and July (0.734). The superior performance of the ANN can be attributed to its ability to capture non-linear relationships (Abrahart and See, 2007) between spectral indices and chl-a levels. The use of UAV-acquired spectral data particularly the green, red-edge and red bands was crucial, as these bands are sensitive to chl-a. However, the lower accuracy observed in July could be explained by the reduced water levels, which may have altered the optical properties of the water and limited the representativeness of the spectral indices. In addition, variability in environmental

conditions such as cloud cover, shadows, or vegetation growth along the dam's edges could have further impacted the model's accuracy. This study applied several MLAs including RF, SVM, XGBoost, KNN, and ANN; alongside cross-validation and data-splitting techniques (70% training and 30% testing). These strategies helped address potential issues like overfitting and bias, particularly by leveraging models with ensemble and iterative weighting mechanisms (e.g., Random Forest and XGBoost) (Salzberg, 1997). Although ANN emerged as the best performer, the other models provided complementary insights into the robustness of the prediction framework.

The limited number of spectral bands used (five bands) ensured a compact feature space, which reduced the dimensionality of the dataset and improved computational efficiency. This study highlights that even with a small number of bands, UAV sensors can provide reliable data for chl-a monitoring, making the approach applicable to similar small water bodies. Given the promising results of this study, the methodology can be extended to other dams or water bodies of similar size. The flexibility of UAV-based data acquisition allows for scalable monitoring, especially in areas where traditional water sampling may be challenging. Additionally, incorporating more spectral bands or fusing UAV data with satellite imagery could improve model performance by capturing more detailed information about the water column.

Despite the soundness of the approach, future studies should explore the use of other algorithms and larger datasets to further validate the findings. Furthermore, longer-term monitoring across different seasons will provide deeper insights into the temporal variability of chl-a and its relationship with water quality parameters, especially in dynamic environments.

4.5 Conclusion

This study demonstrated the effectiveness of UAV-acquired remote sensing images combined with machine learning algorithms (MLAs) for estimating chl-a concentrations in a small irrigation dam. The models achieved high prediction accuracy, with R^2 values exceeding 0.900 for April and June, confirming the suitability of the proposed approach for chl-a monitoring. Seasonal variations were evident, with chl-a levels increasing after rainfall events and decreasing in July as water levels dropped, highlighting the impact of environmental factors on

chl-a dynamics. Among the tested MLAs, the artificial neural network (ANN) outperformed other models, proving adept at capturing non-linear relationships between spectral indices and chl-a. However, moderate accuracy in July emphasised the challenges posed by fluctuating water levels and environmental conditions, which influence the optical properties of water. Seasonal variations indicated higher chl-a and nutrient levels in April, followed by declines in June and July due to reduced nutrient availability and temperature changes. UAV-based monitoring using red, green and red-edge bands effectively captured chl-a dynamics and correlated well with TN, TP, and DO levels. Spatial analysis identified nutrient hotspots in inlet and periphery regions, emphasising the need for localised management strategies. This methodology, though limited to five spectral bands, proved effective and can be scaled to other small water bodies using UAV platforms. Future studies can build on this work by incorporating additional spectral bands, exploring other MLAs, and conducting long-term monitoring to improve predictive accuracy and capture seasonal variability more comprehensively. The flexibility of UAV-based remote sensing provides a reliable framework for cyanobacteria assessment, enabling effective monitoring and management of freshwater systems.

CHAPTER 5: CONCLUSIONS AND RECOMMENDATIONS FOR FURTHER RESEARCH

5.1 Introduction

Water quality monitoring is essential for sustainable water resource management, particularly in small reservoirs that support agriculture and local livelihoods. This study explored the impacts of eutrophication on water quality in small water bodies within the Umgeni catchment using UAV-based remote sensing. Through systematic literature review, field campaigns, and machine learning, the study addressed the challenges of monitoring chl-a concentrations, a key proxy for assessing eutrophication. The findings contribute to advancing UAV applications in environmental management, demonstrating their potential for high-resolution, real-time data collection and analysis.

5.2 Revisiting the Aims and Objectives

This study successfully achieved its primary aim of assessing the impacts of eutrophication on water quality in small reservoirs using UAV data. The specific objectives were met as follows:

i. To conduct a systematic review of the literature on UAV-based remote sensing of chlorophyll-a concentrations in inland water bodies - The first objective was accomplished through a systematic review conducted using the PRISMA method, which identified 55 relevant studies that utilised UAVs to monitor chl-a in small water bodies (**Section 3.3**). These studies were further analysed, focusing on bibliographic trends, methodologies, and applications (**Section 3.4**).

ii. To estimate the spatiotemporal variability of chlorophyll-a concentrations in a reservoir using UAV data and different machine learning algorithms – This objective was fulfilled by collecting field data, including water samples, and acquiring UAV-based remote sensing imagery over the reservoir (**Section 4.3.2**). The spatiotemporal variations in chl-a concentrations were then estimated using machine learning algorithms such as ANN, RF, KNN, SVM, and XGBoost, with field data used for model training and validation (**Section 4.3.3).** The results of this analysis are presented in **Section 4.4**.

iii. To assess the potential of remotely sensing chlorophyll-a as a proxy for TN, TP, and DO using drone remotely sensed data – The final objective was achieved by examining the

relationships and correlations between chl-a and water quality parameters, including Total Nitrogen (TN), Total Phosphorus (TP), and Dissolved Oxygen (DO). This analysis was conducted in Microsoft Excel, with the coefficient of determination (R^2) calculated to quantify the strength of these relationships. The results are detailed in **Sections 4.4.1 and 4.4.2**.

5.3 Contributions of the Study

This research has significantly expanded the understanding of UAV applications in chl-a monitoring in small water bodies that are used for irrigation by:

- Highlighting the ability of UAVs to provide high-resolution data for small reservoirs as this it is challenging to use the freely available multispectral satellite-based remote sensing.
- Validating the ANN model as the most reliable machine learning approach for chl-a retrieval.
- Establishing chl-a's strong correlation with nutrients, particularly in peripheral and inlet water samples, enhances its value as a proxy for nutrient monitoring.
- Providing insights into seasonal variations in water quality, emphasising the role of environmental factors in eutrophication dynamics.

5.4 Challenges

The study encountered the following major challenges:

- Regulatory constraints on UAV operations significantly influenced the selection of study sites, limiting the freedom to choose locations based solely on scientific objectives. Factors such as airspace regulations, proximity to restricted zones, and safety protocols necessitated selecting sites where UAV flights were both legally and logistically feasible.
- Weather dependency posed challenges for in-situ data collection. Adverse weather conditions could delay or prevent fieldwork, and cloudy conditions were unsuitable for UAV operations, as they could obscure water surfaces and reduce the accuracy of reflectance measurements. Data collection schedules had to be aligned with favourable

weather forecasts to ensure the quality and consistency of both UAV and ground measurements.

- Technical issues with the UAV's in-built GPS affected some flights. These issues resulted in poor geolocation accuracy and incomplete orthomosaic images, leaving certain sections of the water body unmapped. This limitation impacted the completeness of the dataset.

5.5 Recommendations

To address the challenges encountered in this study, the following recommendations are proposed:

- Obtaining an aviation license for UAV operation could reduce regulatory limitations and allow access to a wider range of sites, improving flexibility in future studies while ensuring compliance with legal requirements.
- Careful planning around weather forecasts should continue to be prioritised for future data collection campaigns. Developing a flexible field schedule can reduce weather-related disruptions.
- To minimise GPS-related issues, future UAV missions should include additional ground control points (GCPs) and conduct thorough pre-flight checks to ensure GPS accuracy and optimal flight conditions. Use of high-precision Real-Time Kinematics (RTK) or Post-Processed Kinematic (PPK) GPS systems is also encouraged to enhance image alignment and mapping precision.

5.6 Future Possibilities

The findings from this study pave the way for several future research directions:

- Development of cost-effective UAV platforms such as UAV technologies can improve accessibility for resource-limited regions, particularly in Africa.
- Standardised and transferable chl-a retrieval algorithms will enhance the scalability of UAV-based monitoring methods.
- Real-time data from UAVs can be linked with Internet of Things (IoT) sensors for continuous and automated water quality monitoring.

- Beyond chl-a, UAVs can be used to monitor additional indicators of water quality, such as turbidity, nitrogen, phosphorus, and harmful algal blooms.
- Applying UAV-based methods to smaller water bodies or regions can validate their applicability in diverse environments.

5.7 Final Comments and Summary Conclusions

This study demonstrated the potential of UAV-based remote sensing as an innovative and practical approach to managing water quality in small reservoirs. By integrating high-resolution imaging with advanced machine learning models, the research provides a robust framework for monitoring chl-a and related parameters. Despite challenges, the insights gained highlight the necessity of continuous monitoring and adaptive management strategies to address the dynamic nature of water quality issues. Ultimately, this study establishes a foundation for future advancements in UAV applications, contributing to sustainable water resource management in small, yet vital, aquatic systems.

REFERENCES

Abrahart, RJ and See, L. 2007. Neural network modelling of non-linear hydrological relationships. *Hydrology and Earth System Sciences* 11 (5): 1563-1579.

Adejimi, OE, Sadhasivam, G, Schmilovitch, Ze, Shapiro, OH and Herrmann, I. 2023. Applying hyperspectral transmittance for inter-genera classification of cyanobacterial and algal cultures. *Algal Research* 71 103067.

Adjovu, GE, Stephen, H, James, D and Ahmad, S. 2023. Overview of the Application of Remote Sensing in Effective Monitoring of Water Quality Parameters. *Remote Sensing* 15 (7): 1938.

Ahn, JMK, Byungik; Jong, Jaehun; Nam, Gibeom; Park, Lan Joo; Park, Sanghyun; Kang, Taegu; Lee, Jae-Kwan; Kim, Jungwook. 2021. Predicting cyanobacterial blooms using hyperspectral images in a regulated river. *Sensors* 21 (2): 530.

Ali, J, Khan, R, Ahmad, N and Maqsood, I. 2012. Random forests and decision trees. *International Journal of Computer Science Issues (IJCSI)* 9 (5): 272.

Ali, K, Abiye, T and Adam, E. 2022. Integrating in Situ and Current Generation Satellite Data for Temporal and Spatial Analysis of Harmful Algal Blooms in the Hartbeespoort Dam, Crocodile River Basin, South Africa. *Remote Sensing* 14 (17): 4277.

Anderson, DM. 2009. Approaches to monitoring, control and management of harmful algal blooms (HABs). *Ocean & coastal management* 52 (7): 342-347.

Anderson, K and Gaston, KJ. 2013. Lightweight unmanned aerial vehicles will revolutionize spatial ecology. *Frontiers in Ecology and the Environment* 11 (3): 138-146.

Aranda, YN, Bhatt, P, Ates, N, Engel, BA and Simsek, H. 2023. Cyanophage-cyanobacterial interactions for sustainable aquatic environment. *Environmental Research* 229 115728.

Arango, JGN, Robert W. 2019. Prediction of optical and non-optical water quality parameters in oligotrophic and eutrophic aquatic systems using a small unmanned aerial system. *Drones* 4 (1): 1.

Arar, EJ. 1997. *Method 446.0, In vitro determination of chlorophylls a, b, c1, +c2 and pheopigments in marine and freshwater algae by visible spectrophotometry.* Environmental Protection Agency, Washington, DC: U. S.

Arias-Rodriguez, LF, Duan, Z, Díaz-Torres, JdJ, Basilio Hazas, M, Huang, J, Kumar, BU, Tuo, Y and Disse, M. 2021. Integration of remote sensing and Mexican water quality monitoring system using an extreme learning machine. *Sensors* 21 (12): 4118.

Baiphethi, MN and Jacobs, PT. 2009. The contribution of subsistence farming to food security in South Africa. *Agrekon* 48 (4): 459-482.

Bakker, ES and Hilt, S. 2016. Impact of water-level fluctuations on cyanobacterial blooms: options for management. *Aquatic ecology* 50 485-498.

Banda, TD and Kumarasamy, M. 2020. Development of a universal water quality index (UWQI) for South African river catchments. *Water* 12 (6): 1534.

Banerjee, A, Chakrabarty, M, Rakshit, N, Bhowmick, AR and Ray, S. 2019. Environmental factors as indicators of dissolved oxygen concentration and zooplankton abundance: Deep learning versus traditional regression approach. *Ecological indicators* 100 99-117.

Bangira, T, Matongera, TN, Mabhaudhi, T and Mutanga, O. 2024. Remote sensing-based water quality monitoring in African reservoirs, potential and limitations of sensors and algorithms: A systematic review. *Physics and Chemistry of the Earth, Parts A/B/C* 134 103536.

Bashir, I, Lone, FA, Bhat, RA, Mir, SA, Dar, ZA and Dar, SA. 2020. Concerns and threats of contamination on aquatic ecosystems. *Bioremediation and biotechnology: sustainable approaches to pollution degradation* 1-26.

Batur, E and Maktav, D. 2018. Assessment of surface water quality by using satellite images fusion based on PCA method in the Lake Gala, Turkey. *IEEE Transactions on Geoscience and Remote Sensing* 57 (5): 2983-2989.

Beck, R, Zhan, S, Liu, H, Tong, S, Yang, B, Xu, M, Ye, Z, Huang, Y, Shu, S and Wu, Q. 2016. Comparison of satellite reflectance algorithms for estimating chlorophyll-a in a temperate reservoir using coincident hyperspectral aircraft imagery and dense coincident surface observations. *Remote Sensing of Environment* 178 15-30.

Becker, RH, Sultan, MI, Boyer, GL, Twiss, MR and Konopko, E. 2009. Mapping cyanobacterial blooms in the Great Lakes using MODIS. *Journal of Great Lakes Research* 35 (3): 447-453.

Becker, RHS, Michael; Dehm, Dustin; Shuchman, Robert; Quintero, Kaydian; Bosse, Karl; Sawtell, Reid. 2019. Unmanned aerial system based spectroradiometer for monitoring harmful algal blooms: A new paradigm in water quality monitoring. *Journal of Great Lakes Research* 45 (3): 444-453.

Beires, L. 2010. A study of urbanisation in the province of Kwazulu Natal. *Durban: Department of economic development and tourism, Kwazulu Natal Provincial Government*.

Belgiu, M and Drăguţ, L. 2016. Random forest in remote sensing: A review of applications and future directions. *ISPRS Journal of Photogrammetry and Remote Sensing* 114 24-31.

Biggs, J, Williams, P, Whitfield, M, Nicolet, P and Weatherby, A. 2005. 15 years of pond assessment in Britain: results and lessons learned from the work of Pond Conservation. *Aquatic conservation: marine and freshwater ecosystems* 15 (6): 693-714.

Bramich, J, Bolch, CJ and Fischer, A. 2021. Improved red-edge chlorophyll-a detection for Sentinel 2. *Ecological Indicators* 120 106876.

Breiman, L. 2001. Random forests. *Machine learning* 45 5-32.

Brion, G, Brye, K, Haggard, B, West, C and Brahana, J. 2011. Land-use effects on water quality of a first-order stream in the Ozark Highlands, mid-southern United States. *River Research and Applications* 27 (6): 772-790.

Bulcock, H and Jewitt, G. 2012. Field data collection and analysis of canopy and litter interception in commercial forest plantations in the KwaZulu-Natal Midlands, South Africa. *Hydrology and Earth System Sciences* 16 (10): 3717-3728.

Buma, WG and Lee, S-I. 2020. Evaluation of sentinel-2 and landsat 8 images for estimating chlorophyll-a concentrations in lake Chad, Africa. *Remote Sensing* 12 (15): 2437.

Bunyon, CL, Fraser, BT, McQuaid, A and Congalton, RG. 2023. Using Imagery Collected by an Unmanned Aerial System to Monitor Cyanobacteria in New Hampshire, USA, Lakes. *Remote Sensing* 15 (11): 2839.

Bunyon, CLF, Benjamin T; McQuaid, Amanda; Congalton, Russell G. 2023. Using Imagery Collected by an Unmanned Aerial System to Monitor Cyanobacteria in New Hampshire, USA, Lakes. *Remote Sensing* 15 (11): 2839.

Cai, XW, Luyao; Li, Yunmei; Lei, Shaohua; Xu, Jie; Lyu, Heng; Li, Junda; Wang, Huaijing; Dong, Xianzhang; Zhu, Yuxing. 2023. Remote sensing identification of urban water pollution source types using hyperspectral data. *Journal of Hazardous Materials* 459 132080.

Cao, Q, Yu, G and Qiao, Z. 2023. Application and recent progress of inland water monitoring using remote sensing techniques. *Environmental Monitoring and Assessment* 195 (1): 125.

Cao, Q, Yu, G, Sun, S, Dou, Y, Li, H and Qiao, Z. 2021. Monitoring water quality of the Haihe River based on ground-based hyperspectral remote sensing. *Water* 14 (1): 22.

Cao, Z, Ma, R, Duan, H, Pahlevan, N, Melack, J, Shen, M and Xue, K. 2020. A machine learning approach to estimate chlorophyll-a from Landsat-8 measurements in inland lakes. *Remote Sensing of Environment* 248 111974.

Carlberg, C and Carlberg, CG. 2014. *Statistical analysis: Microsoft excel 2013*. Pearson Education.

Carnie, T. 2019. Toxic farm chemicals: emerging threat to South Africa's surface waters. *Water Wheel* 18 (6): 40-43.

Chebud, Y, Naja, GM, Rivero, RG and Melesse, AM. 2012. Water quality monitoring using remote sensing and an artificial neural network. *Water, Air, & Soil Pollution* 223 4875-4887.

Chen, BM, Xi; Chen, Peng; Wang, Biao; Choi, Jaewan; Park, Honglyun; Xu, Sheng; Wu, Yanlan; Yang, Hui. 2021. Machine learning-based inversion of water quality parameters in typical reach of the urban river by UAV multispectral data. *Ecological Indicators* 133 108434.

Chen, PW, Biao; Wu, Yanlan; Wang, Qijun; Huang, Zuoji; Wang, Chunlin. 2023. Urban river water quality monitoring based on self-optimizing machine learning method using multi-source remote sensing data. *Ecological Indicators* 146 109750.
Chien, W-H, Wang, T-S, Yeh, H-C and Hsieh, T-K. 2016. Study of NDVI application on turbidity in reservoirs. *Journal of the Indian Society of Remote Sensing* 44 829-836.
Choo, YK, G.; Kim, D.; Lee, S. 2018. A study on the evaluation of water-bloom using image processing. *Environmental Science and Pollution Research* 25 (36): 36775-36780.
Chung, W-Y and Yoo, J-H. 2015. Remote water quality monitoring in wide area. *Sensors and Actuators B: Chemical* 217 51-57.
Ciężkowski, WF, Magdalena; Kardel, Ignacy; Pełka, Wiktoria; Chormański, Jarosław.2023. Cyanobacteria Risk and Water Quality Assessment in Inland Głuszyńskie Lake Poland Using Field and UAV Spectroscopy. *IGARSS 2023-2023 IEEE International Geoscience and Remote Sensing Symposium*, 3752-3754. IEEE.
Cillero Castro, C, Domínguez Gómez, JA, Delgado Martín, J, Hinojo Sánchez, BA, Cereijo Arango, JL, Cheda Tuya, FA and Díaz-Varela, R. 2020. An UAV and satellite multispectral data approach to monitor water quality in small reservoirs. *Remote Sensing* 12 (9): 1514.
Cillero Castro, CDG, Jose Antonio; Delgado Martín, Jordi; Hinojo Sánchez, Boris Alejandro; Cereijo Arango, Jose Luis; Cheda Tuya, Federico Andrés; Díaz-Varela, Ramon. 2020. An UAV and satellite multispectral data approach to monitor water quality in small reservoirs. *Remote Sensing* 12 (9): 1514.
Cook, KV, Beyer, JE, Xiao, X and Hambright, KD. 2023. Ground-based remote sensing provides alternative to satellites for monitoring cyanobacteria in small lakes. *Water Research* 242 120076.
Davis, KF, Rulli, MC, Seveso, A and D'Odorico, P. 2017. Increased food production and reduced water use through optimized crop distribution. *Nature Geoscience* 10 (12): 919-924.
De Keukelaere, LM, R.; Knaeps, E.; Sterckx, S.; Reusen, I.; De Munck, D.; Simis, S. G. H.; Constantinescu, A. M.; Scrieciu, A.; Katsouras, G.; Mertens, W.; Hunter, P. D.; Spyrakos, E.; Tyler, A. 2023. Airborne Drones for Water Quality Mapping in Inland, Transitional and Coastal Waters-MapEO Water Data Processing and Validation. *Remote Sensing* 15 (5).
Deka, PC. 2014. Support vector machine applications in the field of hydrology: a review. *Applied soft computing* 19 372-386.
Dekker, AG. 1993. Detection of optical water quality parameters for eutrophic waters by high resolution remote sensing.
Ding, J, Jiang, Y, Liu, Q, Hou, Z, Liao, J, Fu, L and Peng, Q. 2016. Influences of the land use pattern on water quality in low-order streams of the Dongjiang River basin, China: A multi-scale analysis. *Science of the total environment* 551 205-216.
Dlamini, S, Nhapi, I, Gumindoga, W, Nhiwatiwa, T and Dube, T. 2016. Assessing the feasibility of integrating remote sensing and in-situ measurements in monitoring water quality status of Lake Chivero, Zimbabwe. *Physics and Chemistry of the Earth, Parts A/B/C* 93 2-11.
Douglas Greene, SBL, G. H.; Markfort, C. D. 2021. Improving the spatial and temporal monitoring of cyanotoxins in Iowa lakes using a multiscale and multi-modal monitoring approach. *Science of the Total Environment* 760.
Downing, JA, Watson, SB and McCauley, E. 2001. Predicting cyanobacteria dominance in lakes. *Canadian journal of fisheries and aquatic sciences* 58 (10): 1905-1908.
Du Plessis, A. 2017. *Freshwater challenges of South Africa and its Upper Vaal river*. Springer.
DWS. 2022. National Eutrophication Monitoring Programme. [Internet]. Department of Water and Sanitation, Republic of South Africa. Available from: http://www.dwa.gov.za/iwqs/eutrophication/NEMP/default.aspx. [Accessed: 06 September 2023].
Dzurume, T, Dube, T and Shoko, C. 2022. Remotely sensed data for estimating chlorophyll-a concentration in wetlands located in the Limpopo Transboundary River Basin, South Africa. *Physics and Chemistry of the Earth, Parts A/B/C* 127 103193.

El-Alem, AC, K.; Venkatesan, A.; Rachid, L.; Agili, H.; Dedieu, J. P. 2021. How accurate is an unmanned aerial vehicle data-based model applied on satellite imagery for chlorophyll-a estimation in freshwater bodies? *Remote Sensing* 13 (6).

Eleuterio, L and Neethling, J.2010. Low Phosphorus Analytical Measurement Study. *Proceedings of the 83rd Annual Water Environmental Federation Annual Conference and Exposition (WEFTEC). New Orleans, LA*.

Fairbanks, D, Thompson, MW**, Vink, DE***, Newby, TS****, Van den Berg, HM***** and Everard, D. 2000. The South African land-cover characteristics database: a synopsis of the landscape. *South African Journal of Science* 96 (2): 69-82.

Falconer, I, Bartram, J, Chorus, I, Kuiper-Goodman, T, Utkilen, H, Burch, M and Codd, G. 1999. Safe levels and safe practices. *Toxic cyanobacteria in water* 155-178.

Falconer, IR. 2001. Toxic cyanobacterial bloom problems in Australian waters: risks and impacts on human health. *Phycologia* 40 (3): 228-233.

Fan, J, Wang, Y, Zhou, Z, You, N and Meng, J. 2016. Dynamic ecological risk assessment and management of land use in the middle reaches of the Heihe River based on landscape patterns and spatial statistics. *Sustainability* 8 (6): 536.

Fernandez-Figueroa, EG, Wilson, AE and Rogers, SR. 2022. Commercially available unoccupied aerial systems for monitoring harmful algal blooms: A comparative study. *Limnology and Oceanography: Methods* 20 (3): 146-158.

Filstrup, CT and Downing, JA. 2017. Relationship of chlorophyll to phosphorus and nitrogen in nutrient-rich lakes. *Inland Waters* 7 (4): 385-400.

Flynn, KF and Chapra, SC. 2014. Remote sensing of submerged aquatic vegetation in a shallow non-turbid river using an unmanned aerial vehicle. *Remote Sensing* 6 (12): 12815-12836.

Fournier, C, Quesada, A, Cirés, S and Saberioon, M. 2024. Discriminating bloom-forming cyanobacteria using lab-based hyperspectral imagery and machine learning: Validation with toxic species under environmental ranges. *Science of the Total Environment* 932 172741.

Fu, BL, Sunzhe; Lao, Zhinan; Yuan, Bingyan; Liang, Yiyin; He, Wen; Sun, Weiwei; He, Hongchang. 2023. Multi-sensor and multi-platform retrieval of water chlorophyll a concentration in karst wetlands using transfer learning frameworks with ASD, UAV, and Planet CubeSate reflectance data. *Science of The Total Environment* 901 165963.

Gao, Y, Gao, J, Yin, H, Liu, C, Xia, T, Wang, J and Huang, Q. 2015. Remote sensing estimation of the total phosphorus concentration in a large lake using band combinations and regional multivariate statistical modeling techniques. *Journal of Environmental Management* 151 33-43.

Ghosh, S, Dasgupta, A and Swetapadma, A.2019. A study on support vector machine based linear and non-linear pattern classification. *2019 International Conference on Intelligent Sustainable Systems (ICISS)*, 24-28. IEEE.

Gilerson, AA, Gitelson, AA, Zhou, J, Gurlin, D, Moses, W, Ioannou, I and Ahmed, SA. 2010. Algorithms for remote estimation of chlorophyll-a in coastal and inland waters using red and near infrared bands. *Optics Express* 18 (23): 24109-24125.

Gitelson, A. 1992. The peak near 700 nm on radiance spectra of algae and water: relationships of its magnitude and position with chlorophyll concentration. *International Journal of Remote Sensing* 13 (17): 3367-3373.

Gohin, F, Bryère, P, Lefebvre, A, Sauriau, P-G, Savoye, N, Vantrepotte, V, Bozec, Y, Cariou, T, Conan, P and Coudray, S. 2020. Satellite and in situ monitoring of chl-a, turbidity, and total suspended matter in coastal waters: Experience of the year 2017 along the french coasts. *Journal of Marine Science and Engineering* 8 (9): 665.

Gregor, J and Maršálek, B. 2004. Freshwater phytoplankton quantification by chlorophyll a: a comparative study of in vitro, in vivo and in situ methods. *Water Research* 38 (3): 517-522.

Guimarães, TTV, M. R.; Koste, E. C.; Gonzaga, L.; Bordin, F.; Inocencio, L. C.; Larocca, A. P. C.; de Oliveira, M. Z.; Vitti, D. C.; Mauad, F. F. 2017. An alternative method of spatial autocorrelation for chlorophyll detection in water bodies using remote sensing. *Sustainability (Switzerland)* 9 (3).

Gurlin, D, Gitelson, AA and Moses, WJ. 2011. Remote estimation of chl-a concentration in turbid productive waters—Return to a simple two-band NIR-red model? *Remote Sensing of Environment* 115 (12): 3479-3490.

Harding, W. 2015. Living with eutrophication in South Africa: a review of realities and challenges, Transactions of the Royal Society of South Africa 70 (2) 2015: pp. 155-171. *Transactions of the Royal Society of South Africa* 70 (3): 299-303.

Harvey, ET, Kratzer, S and Philipson, P. 2015. Satellite-based water quality monitoring for improved spatial and temporal retrieval of chlorophyll-a in coastal waters. *Remote Sensing of Environment* 158 417-430.

He, J, Chen, Y, Wu, J, Stow, DA and Christakos, G. 2020. Space-time chlorophyll-a retrieval in optically complex waters that accounts for remote sensing and modeling uncertainties and improves remote estimation accuracy. *Water research* 171 115403.

Herrera, VM, Khoshgoftaar, TM, Villanustre, F and Furht, B. 2019. Random forest implementation and optimization for Big Data analytics on LexisNexis's high performance computing cluster platform. *Journal of Big Data* 6 1-36.

Hong, SMA, Ather; Kim, Soobin; Kwon, Do Hyuck; Yoon, Nakyung; Yun, Daeun; Lee, Sanguk; Pachepsky, Yakov; Pyo, JongCheol; Cho, Kyung Hwa. 2023. Autonomous calibration of EFDC for predicting chlorophyll-a using reinforcement learning and a real-time monitoring system. *Environmental Modelling & Software* 168 105805.

Hong, SMC, Kyung Hwa; Park, Sanghyun; Kang, Taegu; Kim, Moon Sung; Nam, Gibeom; Pyo, JongCheol. 2022. Estimation of cyanobacteria pigments in the main rivers of South Korea using spatial attention convolutional neural network with hyperspectral imagery. *GIScience & Remote Sensing* 59 (1): 547-567.

Horn, S, Pieters, R and Bøhn, T. 2019. A first assessment of glyphosate, 2, 4-D and Cry proteins in surface water of South Africa. *South African Journal of Science* 115 (9-10): 1-7.

Hua, AK. 2017. Land use land cover changes in detection of water quality: a study based on remote sensing and multivariate statistics. *Journal of environmental and public health* 2017 (1): 7515130.

Huang, M, Kim, MS, Delwiche, SR, Chao, K, Qin, J, Mo, C, Esquerre, C and Zhu, Q. 2016. Quantitative analysis of melamine in milk powders using near-infrared hyperspectral imaging and band ratio. *Journal of Food Engineering* 181 10-19.

Hunter, PD, Tyler, AN, Présing, M, Kovács, AW and Preston, T. 2008. Spectral discrimination of phytoplankton colour groups: The effect of suspended particulate matter and sensor spectral resolution. *Remote Sensing of Environment* 112 (4): 1527-1544.

Jang, SWY, Hong Joo; Kwak, Seok Nam; Sohn, Byeong Yong; Kim, Se Geun; Kim, Dae Hyun. 2016. Algal bloom monitoring using UAVs imagery. *Adv. Sci. Technol. Lett* 138 30-33.

Jeffrey, St and Humphrey, G. 1975. New spectrophotometric equations for determining chlorophylls a, b, c1 and c2 in higher plants, algae and natural phytoplankton. *Biochemie und physiologie der pflanzen* 167 (2): 191-194.

Jenkins, D and Medsker, LL. 1964. Brucine Method for the Determination of Nitrate in Ocean, Estuarine, and Fresh Waters. *Analytical Chemistry* 36 (3): 610-612.

Jeong, H, Kim, H and Jang, T. 2016. Irrigation water quality standards for indirect wastewater reuse in agriculture: a contribution toward sustainable wastewater reuse in South Korea. *Water* 8 (4): 169.

Joehnk, KD, Huisman, J, Sharples, J, Sommeijer, B, Visser, PM and Stroom, JM. 2008. Summer heatwaves promote blooms of harmful cyanobacteria. *Global change biology* 14 (3): 495-512.

Johan, FB, Jafri, MZBM, San, LH, Omar, WMW and Ho, TC.2018. Chlorophyll a concentration of fresh water phytoplankton analysed by algorithmic based spectroscopy. *Journal of Physics: Conference Series*, 012015. IOP Publishing.

Jung, SC, Hoon; Kim, Donghoon; Kim, Kyukwang; Han, Jong-In; Myung, Hyun. 2017. Development of algal bloom removal system using unmanned aerial vehicle and surface vehicle. *IEEE Access* 5 22166-22176.

Kabbara, N, Benkhelil, J, Awad, M and Barale, V. 2008. Monitoring water quality in the coastal area of Tripoli (Lebanon) using high-resolution satellite data. *ISPRS Journal of Photogrammetry and Remote Sensing* 63 (5): 488-495.

Kazbar, A, Cogne, G, Urbain, B, Marec, H, Le-Gouic, B, Tallec, J, Takache, H, Ismail, A and Pruvost, J. 2019. Effect of dissolved oxygen concentration on microalgal culture in photobioreactors. *Algal Research* 39 101432.

Kim, EJN, S. H.; Koo, J. W.; Hwang, T. M. 2021. Hybrid Approach of Unmanned Aerial Vehicle and Unmanned Surface Vehicle for Assessment of Chlorophyll-a Imagery Using Spectral Indices in Stream, South Korea. *Water* 13 (14).

Kim, H-MY, Hong-Joo; Jang, Seon Woong; Kwak, Seok Nam; Sohn, Byeong Yong; Kim, Se Geun; Kim, Dae Hyun. 2016. Application of unmanned aerial vehicle imagery for algal bloom monitoring in river basin. *International Journal of Control and Automation* 9 (12): 203-220.

Kim, K-M and Ahn, J-H. 2022. Machine learning predictions of chlorophyll-a in the Han river basin, Korea. *Journal of Environmental Management* 318 115636.

Kirk, JT. 1994. *Light and photosynthesis in aquatic ecosystems*. Cambridge university press.

Koh, PW and Liang, P.2017. Understanding black-box predictions via influence functions. *International conference on machine learning*, 1885-1894. PMLR.

Kolluru, S, Gedam, SS, Chander, S and Sahay, A. 2023. Development of chlorophyll-a concentration estimation algorithm for turbid productive inland waters in India. *Geocarto International* 2171143.

Kolluru, S and Tiwari, SP. 2022. Modeling ocean surface chlorophyll-a concentration from ocean color remote sensing reflectance in global waters using machine learning. *Science of the Total Environment* 844 157191.

Koparan, C, Koc, AB, Privette, CV, Sawyer, CB and Sharp, JL. 2018. Evaluation of a UAV-assisted autonomous water sampling. *Water* 10 (5): 655.

Kuhn, C, de Matos Valerio, A, Ward, N, Loken, L, Sawakuchi, HO, Kampel, M, Richey, J, Stadler, P, Crawford, J and Striegl, R. 2019. Performance of Landsat-8 and Sentinel-2 surface reflectance products for river remote sensing retrievals of chlorophyll-a and turbidity. *Remote Sensing of Environment* 224 104-118.

Kutser, T. 2009. Passive optical remote sensing of cyanobacteria and other intense phytoplankton blooms in coastal and inland waters. *International Journal of Remote Sensing* 30 (17): 4401-4425.

Kutser, T, Metsamaa, L, Strömbeck, N and Vahtmäe, E. 2006. Monitoring cyanobacterial blooms by satellite remote sensing. *Estuarine, Coastal and Shelf Science* 67 (1-2): 303-312.

Kwon, YSP, J.; Kwon, Y. H.; Duan, H.; Cho, K. H.; Park, Y. 2020. Drone-based hyperspectral remote sensing of cyanobacteria using vertical cumulative pigment concentration in a deep reservoir. *Remote Sensing of Environment* 236.

Lade, OO, Fullen, MA, Oloke, D, Subedi, M and Booth, CA. 2014. Urban Precipitation: Measurements, Monitoring and Processes. *Water Resources in the Built Environment: Management Issues and Solutions* 197-210.

Lai, Y, Zhang, J, Song, Y and Gong, Z. 2021. Retrieval and evaluation of chlorophyll-a concentration in reservoirs with main water supply function in Beijing, China, based on landsat satellite images. *International journal of environmental research and public health* 18 (9): 4419.

Lauguico, S, Concepcion, R, Tobias, RR, Alejandrino, J, Macasaet, D and Dadios, E.2020. Indirect measurement of dissolved oxygen based on algae growth factors using machine learning models. *2020 IEEE 8th R10 Humanitarian Technology Conference (R10-HTC)*, 1-6. IEEE.

Lee, J, Kim, M, Im, J, Han, H and Han, D. 2021. Pre-trained feature aggregated deep learning-based monitoring of overshooting tops using multi-spectral channels of GeoKompsat-2A advanced meteorological imagery. *GIScience & Remote Sensing* 58 (7): 1052-1071.

Li, R and Li, J. 2004. Satellite remote sensing technology for lake water clarity monitoring: an overview. *Environmental Informatics Archives* 2 893-901.

Li, Z, Zhu, X, Wu, Z, Sun, T and Tong, Y. 2023. Recent advances in cyanotoxin synthesis and applications: a comprehensive review. *Microorganisms* 11 (11): 2636.

Lillesand, T, Kiefer, RW and Chipman, J. 2015. *Remote sensing and image interpretation*. John Wiley & Sons.

Lins, RC, Martinez, J-M, Motta Marques, DD, Cirilo, JA and Fragoso Jr, CR. 2017. Assessment of chlorophyll-a remote sensing algorithms in a productive tropical estuarine-lagoon system. *Remote Sensing* 9 (6): 516.

Liu, HY, Tao; Hu, Bingliang; Hou, Xingsong; Zhang, Zhoufeng; Liu, Xiao; Liu, Jiacheng; Wang, Xueji; Zhong, Jingjing; Tan, Zhengxuan. 2021. Uav-borne hyperspectral imaging remote sensing system based on acousto-optic tunable filter for water quality monitoring. *Remote Sensing* 13 (20): 4069.

Liu, W and Qiu, R. 2007. Water eutrophication in China and the combating strategies. *Journal of Chemical Technology & Biotechnology: International Research in Process, Environmental & Clean Technology* 82 (9): 781-786.

Liu, X, Feng, J and Wang, Y. 2019. Chlorophyll a predictability and relative importance of factors governing lake phytoplankton at different timescales. *Science of the Total Environment* 648 472-480.

Lo, YF, Lang; Lu, Tiancheng; Huang, Hong; Kong, Lingrong; Xu, Yunqing; Zhang, Cheng. 2023. Medium-Sized Lake Water Quality Parameters Retrieval Using Multispectral UAV Image and Machine Learning Algorithms: A Case Study of the Yuandang Lake, China. *Drones* 7 (4): 244.

Logan, RDT, Madison A; Feijó-Lima, Rafael; Colman, Benjamin P; Valett, H Maurice; Shaw, Joseph A. 2023. UAV-Based Hyperspectral Imaging for River Algae Pigment Estimation. *Remote Sensing* 15 (12): 3148.

Lu, QS, Wei; Wei, Lifei; Li, Zhongqiang; Xia, Zhihong; Ye, Song; Xia, Yu. 2021. Retrieval of water quality from UAV-borne hyperspectral imagery: A comparative study of machine learning algorithms. *Remote Sensing* 13 (19): 3928.

Maier, HR, Jain, A, Dandy, GC and Sudheer, KP. 2010. Methods used for the development of neural networks for the prediction of water resource variables in river systems: Current status and future directions. *Environmental modelling & software* 25 (8): 891-909.

Malahlela, OE, Oliphant, T, Tsoeleng, LT and Mhangara, P. 2018. Mapping chlorophyll-a concentrations in a cyanobacteria-and algae-impacted Vaal Dam using Landsat 8 OLI data. *South African Journal of Science* 114 (9-10): 1-9.

Maravilla, RMGQ, J. P.; Blanco, A. C.; Candido, C. G.; Gubatanga, E. V.; Ticman, K. D. V.2019. Estimation of chlorophyll-a concentration in sampaloc lake using uas multispectral remote sensing and regression. *International Archives of the Photogrammetry, Remote Sensing and Spatial Information Sciences - ISPRS Archives*, 297-303. International Society for Photogrammetry and Remote Sensing.

Markogianni, V, Kalivas, D, Petropoulos, GP and Dimitriou, E. 2018. An appraisal of the potential of Landsat 8 in estimating chlorophyll-a, ammonium concentrations and other water quality indicators. *Remote Sensing* 10 (7): 1018.

Matthews, MW. 2011. A current review of empirical procedures of remote sensing in inland and near-coastal transitional waters. *International Journal of Remote Sensing* 32 (21): 6855-6899.

Matthews, MW. 2014. Eutrophication and cyanobacterial blooms in South African inland waters: 10 years of MERIS observations. *Remote Sensing of Environment* 155 161-177.

Matthews, MW. 2017. Bio-optical modeling of phytoplankton chlorophyll-a. In: *Bio-optical modeling and remote sensing of inland waters*. Elsevier.

Matthews, MW and Bernard, S. 2015. Eutrophication and cyanobacteria in South Africa's standing water bodies: A view from space. *South African journal of science* 111 (5): 1-8.

Matthews, MW, Bernard, S and Winter, K. 2010. Remote sensing of cyanobacteria-dominant algal blooms and water quality parameters in Zeekoevlei, a small hypertrophic lake, using MERIS. *Remote sensing of environment* 114 (9): 2070-2087.

McEliece, R, Hinz, S, Guarini, J-M and Coston-Guarini, J. 2020. Evaluation of nearshore and offshore water quality assessment using UAV multispectral imagery. *Remote Sensing* 12 (14): 2258.
Meneses, BM, Reis, R, Vale, MJ and Saraiva, R. 2015. Land use and land cover changes in Zêzere watershed (Portugal)—Water quality implications. *Science of the Total Environment* 527 439-447.
Mishra, S and Mishra, DR. 2012. Normalized difference chlorophyll index: A novel model for remote estimation of chlorophyll-a concentration in turbid productive waters. *Remote Sensing of Environment* 117 394-406.
Mobley, C. 1994. Light and Water: Radiative Transfer in Natural Waters' Academic Press. *San Diego, California*.
Modaresi, F and Araghinejad, S. 2014. A comparative assessment of support vector machines, probabilistic neural networks, and K-nearest neighbor algorithms for water quality classification. *Water resources management* 28 4095-4111.
Modiegi, M, Rampedi, IT and Tesfamichael, SG. 2020. Comparison of multi-source satellite data for quantifying water quality parameters in a mining environment. *Journal of Hydrology* 591 125322.
Morgan, BJ, Stocker, MD, Valdes-Abellan, J, Kim, MS and Pachepsky, Y. 2020. Drone-based imaging to assess the microbial water quality in an irrigation pond: A pilot study. *Science of the Total Environment* 716 135757.
Morgan, BJS, M. D.; Valdes-Abellan, J.; Kim, M. S.; Pachepsky, Y. 2020. Drone-based imaging to assess the microbial water quality in an irrigation pond: A pilot study. *Science of The Total Environment* 716 135757.
Moses, WJ, Gitelson, AA, Perk, RL, Gurlin, D, Rundquist, DC, Leavitt, BC, Barrow, TM and Brakhage, P. 2012. Estimation of chlorophyll-a concentration in turbid productive waters using airborne hyperspectral data. *Water research* 46 (4): 993-1004.
Namugize, JN, Jewitt, G and Graham, M. 2018. Effects of land use and land cover changes on water quality in the uMngeni river catchment, South Africa. *Physics and Chemistry of the Earth, Parts a/b/c* 105 247-264.
Nasir, N, Kansal, A, Alshaltone, O, Barneih, F, Sameer, M, Shanableh, A and Al-Shamma'a, A. 2022. Water quality classification using machine learning algorithms. *Journal of Water Process Engineering* 48 102920.
NSWG. 2017. Farm water quality and treatment: Algae. [Internet]. NSW Department of Primary Industries. Available from: https://www.mirrigation.com.au/ArticleDocuments/215/Farm%20water%20quality%20and%20treatment.pdf.aspx?embed=Y. [Accessed: 31 October].
O'Reilly, JE, Maritorena, S, Mitchell, BG, Siegel, DA, Carder, KL, Garver, SA, Kahru, M and McClain, C. 1998. Ocean color chlorophyll algorithms for SeaWiFS. *Journal of Geophysical Research: Oceans* 103 (C11): 24937-24953.
O'Reilly, JE and Werdell, PJ. 2019. Chlorophyll algorithms for ocean color sensors-OC4, OC5 & OC6. *Remote sensing of environment* 229 32-47.
O'Dell, J. 1993. Method 365.1, Revision 2.0: Determination of phosphorus by semi-automated colorimetry. *EPA-United States Environ Prot Agency* 1-15.
O'Reilly, JE, Maritorena, S, Siegel, DA, O'Brien, MC, Toole, D, Mitchell, BG, Kahru, M, Chavez, FP, Strutton, P and Cota, GF. 2000. Ocean color chlorophyll a algorithms for SeaWiFS, OC2, and OC4: Version 4. *SeaWiFS postlaunch calibration and validation analyses, Part* 3 9-23.
Olivetti, DC, Rejane; Martinez, Jean-Michel; Almeida, Tati; Casari, Raphael; Borges, Henrique; Roig, Henrique. 2023. Comparing Unmanned Aerial Multispectral and Hyperspectral Imagery for Harmful Algal Bloom Monitoring in Artificial Ponds Used for Fish Farming. *Drones* 7 (7): 410.
Omer, NH. 2019. Water quality parameters. *Water quality-science, assessments and policy* 18 1-34.
Otieno, FA and Ochieng, GM. 2004. Water management tools as a means of averting a possible water scarcity in South Africa by the year 2025. *Water Sa* 30 (5): 120-124.

Paerl, HW and Barnard, MA. 2020. Mitigating the global expansion of harmful cyanobacterial blooms: Moving targets in a human-and climatically-altered world. *Harmful Algae* 96 101845.
Paerl, HW, Hall, NS and Calandrino, ES. 2011. Controlling harmful cyanobacterial blooms in a world experiencing anthropogenic and climatic-induced change. *Science of the total environment* 409 (10): 1739-1745.
Pal, M. 2005. Random forest classifier for remote sensing classification. *International journal of remote sensing* 26 (1): 217-222.
Pamula, AS, Gholizadeh, H, Krzmarzick, MJ, Mausbach, WE and Lampert, DJ. 2023. A remote sensing tool for near real-time monitoring of harmful algal blooms and turbidity in reservoirs. *JAWRA Journal of the American Water Resources Association* 59 (5): 929-949.
Peace, N and Muhammad, H. 2020. World Population Variability and Heat Bias Prediction: An Approach to Global Heat Disaster Management. *International Journal of Climate Research* 4 (1): 51-58.
Pérez-Ruzafa, A, Fernández, AI, Marcos, C, Gilabert, J, Quispe, JI and García-Charton, JA. 2005. Spatial and temporal variations of hydrological conditions, nutrients and chlorophyll a in a Mediterranean coastal lagoon (Mar Menor, Spain). *Hydrobiologia* 550 11-27.
Pokrzywinski, KJ, Richard; Reif, Molly; Bourne, Scott; Hammond, Shea; Fernando, Brianna. 2022. Remote sensing of the cyanobacteria life cycle: A mesocosm temporal assessment of a Microcystis sp. bloom using coincident unmanned aircraft system (UAS) hyperspectral imagery and ground sampling efforts. *Harmful Algae* 117 102268.
Pugliesi, D. 2012. Absorbance spectra of free chlorophyll a (blue) and b (red) in a solvent. [Internet]. Available from: https://commons.wikimedia.org/w/index.php?curid=20509583. [Accessed: 1 November 2023].
Pulliainen, J, Kallio, K, Eloheimo, K, Koponen, S, Servomaa, H, Hannonen, T, Tauriainen, S and Hallikainen, M. 2001. A semi-operative approach to lake water quality retrieval from remote sensing data. *Science of the Total Environment* 268 (1-3): 79-93.
Pyo, JC, Ligaray, M, Kwon, YS, Ahn, M-H, Kim, K, Lee, H, Kang, T, Cho, SB, Park, Y and Cho, KH. 2018. High-spatial resolution monitoring of phycocyanin and chlorophyll-a using airborne hyperspectral imagery. *Remote Sensing* 10 (8): 1180.
Pyo, JH, S. M.; Jang, J.; Park, S.; Park, J.; Noh, J. H.; Cho, K. H. 2022. Drone-borne sensing of major and accessory pigments in algae using deep learning modeling. *GIScience and Remote Sensing* 59 (1): 310-332.
Ramnath, A. 2010. Umgeni Water infrastructure master plan, planning services, engineering and scientific service division. *Umgeni Water, Pietermaritzburg*.
Rankinen, K, Bernal, JEC, Holmberg, M, Vuorio, K and Granlund, K. 2019. Identifying multiple stressors that influence eutrophication in a Finnish agricultural river. *Science of the Total Environment* 658 1278-1292.
Rhee, DS, Kim, YD, Kang, B and Kim, D. 2018a. Applications of unmanned aerial vehicles in fluvial remote sensing: An overview of recent achievements. *KSCE Journal of Civil Engineering* 22 (2): 588-602.
Rhee, DS, Kim, YD, Kang, B and Kim, D. 2018b. Applications of unmanned aerial vehicles in fluvial remote sensing: An overview of recent achievements. *KSCE Journal of Civil Engineering* 22 588-602.
Ritchie, JC, Zimba, PV and Everitt, JH. 2003. Remote sensing techniques to assess water quality. *Photogrammetric engineering & remote sensing* 69 (6): 695-704.
Rocha, AD, Groen, TA, Skidmore, AK, Darvishzadeh, R and Willemen, L. 2017. The Naïve Overfitting Index Selection (NOIS): A new method to optimize model complexity for hyperspectral data. *ISPRS journal of photogrammetry and remote sensing* 133 61-74.
Román, A, Tovar-Sánchez, A, Gauci, A, Deidun, A, Caballero, I, Colica, E, D'Amico, S and Navarro, G. 2022. Water-Quality Monitoring with a UAV-Mounted Multispectral Camera in Coastal Waters. *Remote Sensing* 15 (1): 237.

Saberioon, M, Brom, J, Nedbal, V, Souček, P and Císař, P. 2020. Chlorophyll-a and total suspended solids retrieval and mapping using Sentinel-2A and machine learning for inland waters. *Ecological Indicators* 113 106236.

Sagan, V, Peterson, KT, Maimaitijiang, M, Sidike, P, Sloan, J, Greeling, BA, Maalouf, S and Adams, C. 2020. Monitoring inland water quality using remote sensing: Potential and limitations of spectral indices, bio-optical simulations, machine learning, and cloud computing. *Earth-Science Reviews* 205 103187.

Sakuno, Y, Yajima, H, Yoshioka, Y, Sugahara, S, Abd Elbasit, MA, Adam, E and Chirima, JG. 2018. Evaluation of unified algorithms for remote sensing of chlorophyll-a and turbidity in Lake Shinji and Lake Nakaumi of Japan and the Vaal Dam Reservoir of South Africa under eutrophic and ultra-turbid conditions. *Water* 10 (5): 618.

Salmi, P, Eskelinen, MA, Leppänen, MT and Pölönen, I. 2021. Rapid quantification of microalgae growth with hyperspectral camera and vegetation indices. *Plants* 10 (2): 341.

Salzberg, SL. 1997. On comparing classifiers: Pitfalls to avoid and a recommended approach. *Data mining and knowledge discovery* 1 317-328.

Sayyed, A, Medeiros de Araújo, G, Bodanese, JP and Buss Becker, L. 2015. Dual-stack single-radio communication architecture for UAV acting as a mobile node to collect data in WSNs. *Sensors* 15 (9): 23376-23401.

Schaeffer, BA, Schaeffer, KG, Keith, D, Lunetta, RS, Conmy, R and Gould, RW. 2013. Barriers to adopting satellite remote sensing for water quality management. *International Journal of Remote Sensing* 34 (21): 7534-7544.

Schalles, JF. 2006. Optical remote sensing techniques to estimate phytoplankton chlorophyll a concentrations in coastal waters with varying suspended matter and CDOM concentrations. *Remote sensing of aquatic coastal ecosystem processes: Science and management applications* 27-79.

Schürings, C, Feld, CK, Kail, J and Hering, D. 2022. Effects of agricultural land use on river biota: a meta-analysis. *Environmental Sciences Europe* 34 (1): 124.

Serediak, NA, Prepas, EE and Putz, GJ. 2014. 11.8 - Eutrophication of Freshwater Systems. In: eds. Holland, HD and Turekian, KK, *Treatise on Geochemistry (Second Edition)*. Elsevier, Oxford.

Shafique, NA, Fulk, F, Autrey, BC and Flotemersch, J.2003. Hyperspectral remote sensing of water quality parameters for large rivers in the Ohio River basin. *First interagency conference on research in the watershed, Benson, AZ*, 216-221. Citeseer.

Sharp, SLF, Alexander L; Bouma-Gregson, Keith; Jin, Yufang; Cortés, Alicia; Schladow, S Geoffrey. 2021. Quantifying scales of spatial variability of cyanobacteria in a large, Eutrophic lake using multiplatform remote sensing tools. *Frontiers in Environmental Science* 9 612934.

Shen, L, Xu, H and Guo, X. 2012. Satellite remote sensing of harmful algal blooms (HABs) and a potential synthesized framework. *Sensors* 12 (6): 7778-7803.

Shi, K, Zhang, Y, Qin, B and Zhou, B. 2019. Remote sensing of cyanobacterial blooms in inland waters: present knowledge and future challenges. *Science Bulletin* 64 (20): 1540-1556.

Sibanda, M, Mutanga, O, Chimonyo, VG, Clulow, AD, Shoko, C, Mazvimavi, D, Dube, T and Mabhaudhi, T. 2021. Application of drone technologies in surface water resources monitoring and assessment: A systematic review of progress, challenges, and opportunities in the global south. *Drones* 5 (3): 84.

Silveira Kupssinskü, L, Thomassim Guimarães, T, Menezes de Souza, E, C. Zanotta, D, Roberto Veronez, M, Gonzaga Jr, L and Mauad, FF. 2020. A method for chlorophyll-a and suspended solids prediction through remote sensing and machine learning. *Sensors* 20 (7): 2125.

Silveira Kupssinskü, LTG, Tainá; Menezes de Souza, Eniuce; C. Zanotta, Daniel; Roberto Veronez, Mauricio; Gonzaga Jr, Luiz; Mauad, Frederico Fabio. 2020. A method for chlorophyll-a and suspended solids prediction through remote sensing and machine learning. *Sensors* 20 (7): 2125.

Singh, S, Ghosh, N, Gurjar, S, Krishan, G, Kumar, S and Berwal, P. 2018. Index-based assessment of suitability of water quality for irrigation purpose under Indian conditions. *Environmental monitoring and assessment* 190 1-14.

Son, GK, Dongsu; Kim, Young Do; Lyu, Siwan; Kim, Soojeong. 2020. A forecasting method for harmful algal bloom (HAB)-prone regions allowing preemptive countermeasures based only on acoustic doppler current profiler measurements in a large river. *Water* 12 (12): 3488.

Søndergaard, M, Larsen, SE, Jørgensen, TB and Jeppesen, E. 2011. Using chlorophyll a and cyanobacteria in the ecological classification of lakes. *Ecological Indicators* 11 (5): 1403-1412.

Song, K, Li, L, Tedesco, L, Li, S, Duan, H, Liu, D, Hall, B, Du, J, Li, Z and Shi, K. 2013. Remote estimation of chlorophyll-a in turbid inland waters: Three-band model versus GA-PLS model. *Remote Sensing of Environment* 136 342-357.

Song, ZX, Wenxin; Dong, Huilin; Wang, Xiaowei; Cao, Yuqi; Huang, Pingjie; Hou, Dibo; Wu, Zhengfang; Wang, Zhongyi. 2022. Research on cyanobacterial-bloom detection based on multispectral imaging and deep-learning method. *Sensors* 22 (12): 4571.

Sothe, C, De Almeida, C, Schimalski, M, La Rosa, L, Castro, J, Feitosa, R, Dalponte, M, Lima, C, Liesenberg, V and Miyoshi, G. 2020. Comparative performance of convolutional neural network, weighted and conventional support vector machine and random forest for classifying tree species using hyperspectral and photogrammetric data. *GIScience & Remote Sensing* 57 (3): 369-394.

Stengel, VG, Trevino, JM, King, TV, Ducar, SD, Hundt, SA, Hafen, KC and Churchill, CJ. 2023. Near real-time satellite detection and monitoring of aquatic algae and cyanobacteria: how a combination of chlorophyll-a indices and water-quality sampling was applied to north Texas reservoirs. *Journal of Applied Remote Sensing* 17 (4): 044514-044514.

Stoyneva-Gärtner, MPU, Blagoy A; Descy, Jean-Pierre; Gärtner, Georg; Draganova, Petya H; Borisova, Cvetanka I; Pavlova, Vera; Mitreva, Maria. 2019. Pilot application of drone observations and pigment marker detection by HPLC in studies of cyanobacterial harmful algal blooms in Bulgarian inland waters. *Marine and Freshwater Research* 71 (5): 606-616.

Stumpf, RP, Davis, TW, Wynne, TT, Graham, JL, Loftin, KA, Johengen, TH, Gossiaux, D, Palladino, D and Burtner, A. 2016. Challenges for mapping cyanotoxin patterns from remote sensing of cyanobacteria. *Harmful Algae* 54 160-173.

Su, T-C and Chou, H-T. 2015. Application of multispectral sensors carried on unmanned aerial vehicle (UAV) to trophic state mapping of small reservoirs: A case study of Tain-Pu reservoir in Kinmen, Taiwan. *Remote Sensing* 7 (8): 10078-10097.

Su, T-CC, Hung-Ta. 2015. Application of multispectral sensors carried on unmanned aerial vehicle (UAV) to trophic state mapping of small reservoirs: A case study of Tain-Pu reservoir in Kinmen, Taiwan. *Remote Sensing* 7 (8): 10078-10097.

Su, TC. 2017. A study of a matching pixel by pixel (MPP) algorithm to establish an empirical model of water quality mapping, as based on unmanned aerial vehicle (UAV) images. *International Journal of Applied Earth Observation and Geoinformation* 58 213-224.

Sun, X, Zhang, Y, Shi, K, Zhang, Y, Li, N, Wang, W, Huang, X and Qin, B. 2022. Monitoring water quality using proximal remote sensing technology. *Science of The Total Environment* 803 149805.

Tahiru, AA, Doke, DA and Baatuuwie, BN. 2020. Effect of land use and land cover changes on water quality in the Nawuni Catchment of the White Volta Basin, Northern Region, Ghana. *Applied Water Science* 10 (8): 1-14.

Tian, S, Guo, H, Xu, W, Zhu, X, Wang, B, Zeng, Q, Mai, Y and Huang, JJ. 2023. Remote sensing retrieval of inland water quality parameters using Sentinel-2 and multiple machine learning algorithms. *Environmental Science and Pollution Research* 30 (7): 18617-18630.

Toming, K, Kutser, T, Laas, A, Sepp, M, Paavel, B and Nõges, T. 2016. First experiences in mapping lake water quality parameters with Sentinel-2 MSI imagery. *Remote Sensing* 8 (8): 640.

Topp, SN, Pavelsky, TM, Jensen, D, Simard, M and Ross, MR. 2020. Research trends in the use of remote sensing for inland water quality science: Moving towards multidisciplinary applications. *Water* 12 (1): 169.

Torbick, N, Hession, S, Hagen, S, Wiangwang, N, Becker, B and Qi, J. 2013. Mapping inland lake water quality across the Lower Peninsula of Michigan using Landsat TM imagery. *International Journal of Remote Sensing* 34 (21): 7607-7624.

Tóth, VZG, J.; Ladányi, M.; Jung, A. 2021. A new lake algae detection method supported by a drone-based multispectral camera. *Lakes and Reservoirs: Science, Policy and Management for Sustainable Use* 26 (3).

UmgeniWater. 2016. Umgeni Water Infrastructure Master Plan 2016, 2016/2017-2046/2047, vol.1, Umgeni Water, Pietermaritzburg, South Africa, 2016. Volume 1.

Urquhart, EA, Schaeffer, BA, Stumpf, RP, Loftin, KA and Werdell, PJ. 2017. A method for examining temporal changes in cyanobacterial harmful algal bloom spatial extent using satellite remote sensing. *Harmful algae* 67 144-152.

Van Deventer, R, Morris, C, Hill, T and Rivers-Moore, N. 2022. Use of biological and water quality indices to evaluate conditions of the Upper uMngeni Catchment, KwaZulu-Natal, South Africa. *African Journal of Aquatic Science* 47 (1): 11-22.

Van Eck, NJ and Waltman, L.2007. VOS: A new method for visualizing similarities between objects. *Advances in Data Analysis: Proceedings of the 30th Annual Conference of the Gesellschaft für Klassifikation eV, Freie Universität Berlin, March 8–10, 2006*, 299-306. Springer.

Van Ginkel, C. 2011. Eutrophication: Present reality and future challenges for South Africa. *Water Sa* 37 (5): 693-702.

Visser, F, Wallis, C and Sinnott, AM. 2013. Optical remote sensing of submerged aquatic vegetation: Opportunities for shallow clearwater streams. *Limnologica* 43 (5): 388-398.

Wang, EK, Wang, F, Sun, R and Liu, X. 2019. A new privacy attack network for remote sensing images classification with small training samples. *Mathematical Biosciences and Engineering* 16 (5): 4456-4476.

Wang, J, Shi, T, Yu, D, Teng, D, Ge, X, Zhang, Z, Yang, X, Wang, H and Wu, G. 2020a. Ensemble machine-learning-based framework for estimating total nitrogen concentration in water using drone-borne hyperspectral imagery of emergent plants: A case study in an arid oasis, NW China. *Environmental Pollution* 266 115412.

Wang, L, Yue, X, Wang, H, Ling, K, Liu, Y, Wang, J, Hong, J, Pen, W and Song, H. 2020b. Dynamic inversion of inland aquaculture water quality based on UAVs-WSN spectral analysis. *Remote Sensing* 12 (3): 402.

Wang, S, He, S, Wang, J, Li, J, Zhong, X, Cole, J, Kurbanov, E and Sha, J. 2023. Analysis of Land Use/Cover Changes and Driving Forces in a Typical Subtropical Region of South Africa. *Remote Sensing* 15 (19): 4823.

Wang, W, Shi, K, Zhang, Y, Li, N, Sun, X, Zhang, D, Zhang, Y, Qin, B and Zhu, G. 2022. A ground-based remote sensing system for high-frequency and real-time monitoring of phytoplankton blooms. *Journal of Hazardous Materials* 439 129623.

Warren, MA, Simis, SGH and Selmes, N. 2021. Complementary water quality observations from high and medium resolution Sentinel sensors by aligning chlorophyll-a and turbidity algorithms. *Remote Sensing of Environment* 265 112651.

Wasehun, ET, Hashemi Beni, L and Di Vittorio, CA. 2024. UAV and satellite remote sensing for inland water quality assessments: a literature review. *Environmental Monitoring and Assessment* 196 (3): 277.

Wisser, D, Frolking, S, Douglas, EM, Fekete, BM, Schumann, AH and Vörösmarty, CJ. 2010a. The significance of local water resources captured in small reservoirs for crop production–A global-scale analysis. *Journal of Hydrology* 384 (3-4): 264-275.

Wisser, D, Frolking, S, Douglas, EM, Fekete, BM, Schumann, AH and Vörösmarty, CJ. 2010b. The significance of local water resources captured in small reservoirs for crop production – A global-scale analysis. *Journal of Hydrology* 384 (3): 264-275.

Worldometers.info. 2023. South Africa Population. [Internet]. Available from: https://www.worldometers.info/world-population/south-africa-population/. [Accessed: 16 October 2023].

Wu, C, Wu, J, Qi, J, Zhang, L, Huang, H, Lou, L and Chen, Y. 2010. Empirical estimation of total phosphorus concentration in the mainstream of the Qiantang River in China using Landsat TM data. *International Journal of Remote Sensing* 31 (9): 2309-2324.

Wu, D, Li, R, Zhang, F and Liu, J. 2019. A review on drone-based harmful algae blooms monitoring. *Environmental monitoring and assessment* 191 1-11.

Wu, DJ, Jie; Wang, Fangyi; Luo, Yunru; Lei, Xiangdong; Lai, Chengguang; Wu, Xushu; Xu, Menghua. 2023. Retrieving Eutrophic Water in Highly Urbanized Area Coupling UAV Multispectral Data and Machine Learning Algorithms. *Water* 15 (2): 354.

Xiang, T-Z, Xia, G-S and Zhang, L. 2019. Mini-unmanned aerial vehicle-based remote sensing: Techniques, applications, and prospects. *IEEE geoscience and remote sensing magazine* 7 (3): 29-63.

Xiao, Y, Chen, J, Xu, Y, Guo, S, Nie, X, Guo, Y, Li, X, Hao, F and Fu, YH. 2023. Monitoring of chlorophyll-a and suspended sediment concentrations in optically complex inland rivers using multisource remote sensing measurements. *Ecological Indicators* 155 111041.

Xiao, Y, Guo, Y, Yin, G, Zhang, X, Shi, Y, Hao, F and Fu, Y. 2022. UAV multispectral image-based urban river water quality monitoring using stacked ensemble machine learning algorithms—A case study of the Zhanghe river, China. *Remote Sensing* 14 (14): 3272.

Xiao, YC, Jiahao; Xu, Yue; Guo, Shihui; Nie, Xingyu; Guo, Yahui; Li, Xiran; Hao, Fanghua; Fu, Yongshuo H. 2023. Monitoring of chlorophyll-a and suspended sediment concentrations in optically complex inland rivers using multisource remote sensing measurements. *Ecological Indicators* 155 111041.

Xiao, YG, Y.; Yin, G.; Zhang, X.; Shi, Y.; Hao, F.; Fu, Y. 2022. UAV Multispectral Image-Based Urban River Water Quality Monitoring Using Stacked Ensemble Machine Learning Algorithms—A Case Study of the Zhanghe River, China. *Remote Sensing* 14 (14).

Yang, H, Kong, J, Hu, H, Du, Y, Gao, M and Chen, F. 2022. A review of remote sensing for water quality retrieval: progress and challenges. *Remote Sensing* 14 (8): 1770.

Yang, WF, Bolin; Li, Sunzhe; Lao, Zhinan; Deng, Tengfang; He, Wen; He, Hongchang; Chen, Zhikun. 2023. Monitoring multi-water quality of internationally important karst wetland through deep learning, multi-sensor and multi-platform remote sensing images: A case study of Guilin, China. *Ecological Indicators* 154 110755.

Yang, Z, Reiter, M and Munyei, N. 2017. Estimation of chlorophyll-a concentrations in diverse water bodies using ratio-based NIR/Red indices. *Remote Sensing Applications: Society and Environment* 6 52-58.

Yao, H, Qin, R and Chen, X. 2019. Unmanned aerial vehicle for remote sensing applications—A review. *Remote Sensing* 11 (12): 1443.

Yi, LZ, G.; Zhang, B. 2023. Application of UAV Push-Broom Hyperspectral Images in Water Quality Assessments for Inland Water Protection: A Case Study of Zhang Wei Xin River in Dezhou Distinct, China. *Remote Sensing* 15 (9).

Yu, G, Yang, W, Matsushita, B, Li, R, Oyama, Y and Fukushima, T. 2014. Remote estimation of Chlorophyll-a in inland waters by a NIR-Red-based algorithm: Validation in Asian lakes. *Remote sensing* 6 (4): 3492-3510.

Zaludin, Z and Harituddin, ASM.2019. Challenges and trends of changing from hover to forward flight for a converted hybrid fixed wing vtol uas from automatic flight control system perspective. *2019 IEEE 9th International Conference on System Engineering and Technology (ICSET)*, 247-252. IEEE.

Zang, W, Lin, J, Wang, Y and Tao, H.2012. Investigating small-scale water pollution with UAV remote sensing technology. *World Automation Congress 2012*, 1-4. IEEE.

Zeng, CR, Murray; King, Douglas J. 2017. The impacts of environmental variables on water reflectance measured using a lightweight unmanned aerial vehicle (UAV)-based spectrometer system. *ISPRS Journal of Photogrammetry and Remote Sensing* 130 217-230.

Zhang, DZ, Lifu; Sun, Xuejian; Gao, Yu; Lan, Ziyue; Wang, Yining; Zhai, Haoran; Li, Jingru; Wang, Wei; Chen, Maming. 2022. A New Method for Calculating Water Quality Parameters by

Integrating Space–Ground Hyperspectral Data and Spectral-In Situ Assay Data. *Remote Sensing* 14 (15): 3652.
Zhang, YW, Lun; Deng, Licui; Ouyang, Bin. 2021. Retrieval of water quality parameters from hyperspectral images using a hybrid feedback deep factorization machine model. *Water Research* 204 117618.
Zhang, YW, Lun; Ren, Huazhong; Deng, Licui; Zhang, Pengcheng. 2020a. Retrieval of water quality parameters from hyperspectral images using hybrid Bayesian probabilistic neural network. *Remote Sensing* 12 (10): 1567.
Zhang, YW, Lun; Ren, Huazhong; Liu, Yu; Zheng, Yongqian; Liu, Yaowen; Dong, Jiaji. 2020b. Mapping water quality parameters in urban rivers from hyperspectral images using a new self-adapting selection of multiple artificial neural networks. *Remote Sensing* 12 (2): 336.
Zhao, N, Fan, Z and Zhao, M. 2021. A new approach for estimating dissolved oxygen based on a high-accuracy surface modeling method. *Sensors* 21 (12): 3954.
Zhao, X, Li, Y, Chen, Y, Qiao, X and Qian, W. 2022. Water Chlorophyll a Estimation Using UAV-Based Multispectral Data and Machine Learning. *Drones* 7 (1): 2.
Zhao, XL, Yanzhou; Chen, Yongli; Qiao, Xi. 2022a. A Method of Cyanobacterial Concentrations Prediction Using Multispectral Images. *Sustainability* 14 (19): 12784.
Zhao, XL, Yanzhou; Chen, Yongli; Qiao, Xi; Qian, Wanqiang. 2022b. Water Chlorophyll a Estimation Using UAV-Based Multispectral Data and Machine Learning. *Drones* 7 (1): 2.
Zhao, Y, Li, T, Zhang, X and Zhang, C. 2019. Artificial intelligence-based fault detection and diagnosis methods for building energy systems: Advantages, challenges and the future. *Renewable and Sustainable Energy Reviews* 109 85-101.
Zhou, Q, Zhang, Y, Lin, D, Shan, K, Luo, Y, Zhao, L, Tan, Z and Song, L. 2016. The relationships of meteorological factors and nutrient levels with phytoplankton biomass in a shallow eutrophic lake dominated by cyanobacteria, Lake Dianchi from 1991 to 2013. *Environmental Science and Pollution Research* 23 15616-15626.

APPENDIX A

A total of 60 band combinations were generated from five bands and are presented in Table A.1.

Table A.1: Spectral band combinations calculated to identify the most suitable band for chl-a retrieval

Band Category	Band combination
Single Bands	B1 - blue, B2 – green, B3 – red, B4 – red edge, B5 – NIR
Band Ratios	B1/B2; B1/B3; B1/B4; B1/B5; B2/B3; B2/B4; B2/B5; B3/B4; B3/B5; B4/B5
Band Differences	B1-B2; B1-B3; B1-B4; B1-B5; B2-B1; B2-B3; B2-B4; B2-B5; B3-B1; B3-B2; B3-B4; B3-B5; B4-B1; B4-B2; B4-B3; B4-B5; B5-B1; B5-B2; B5-B3; B5-B4
Band Sums	B1+B2; B1+B3; B1+B4; B1+B5; B2+B3; B2+B4; B2+B5; B3+B4; B3+B5; B4+B5;
Band products	B1B2; B1B3; B1B4; B1B5; B2B3; B2B4; B2B5; B3B4; B3B5; B4B5
Normalised Differences	(B1-B2)/(B1+B2); (B1-B3)/(B1+B3); (B1-B4)/(B1+B4); (B1-B5)/(B1+B5); (B2-B3)/(B2+B3); (B2-B4)/(B2+B4); (B2-B5)/(B2+B5); (B3-B4)/(B3+B4); (B3-B5)/(B3+B5); (B4-B5)/(B4+B5)

APPENDIX B

Table B.1: Correlation results between in situ data and spectral features at the sampling points

Band name/ combination	April	June	July
		Chl-a	
B1	0,201385	-0,52129	-0,12588
B2	-0,15265	-0,21257	-0,0534
B3	-0,15293	-0,29167	0,09601
B4	-0,24761	-0,16499	0,087021
B5	-0,29929	-0,0407	0,035256
B1/B2	-0,22054	0,051297	0,136266
B1/B3	0,426261	0,130933	-0,09049
B1/B4	0,411656	-0,15677	-0,25849
B1/B5	0,386572	-0,09387	0,048252
B2/B3	-0,17865	0,207335	-0,2291
B2/B4	0,495441	-0,16443	-0,28311
B2/B5	0,380357	-0,0979	0,030426
B3/B4	0,338992	-0,19775	-0,2814
B3/B5	0,355436	-0,10143	0,040151
B4/B5	0,29171	0,054939	0,199257
B1-B2	0,244939	0,112387	-0,02092
B1-B3	0,421866	0,048371	-0,22325
B1-B4	0,28114	0,130086	-0,1225
B1-B5	0,315253	0,011091	-0,06004
B2-B1	-0,24494	-0,11239	0,020919
B2-B3	-0,12646	-0,13915	-0,33252
B2-B4	0,295417	0,134276	-0,14503
B2-B5	0,324281	-0,0132	-0,06713
B3-B1	-0,42187	-0,04837	0,223246
B3-B2	0,126464	0,139152	0,332516
B3-B4	0,249133	0,138108	-0,06207
B3-B5	0,301805	0,008283	-0,00243
B4-B1	-0,28114	-0,13009	0,122497
B4-B2	-0,29542	-0,13428	0,145033
B4-B3	-0,24913	-0,13811	0,062072
B4-B5	0,330763	-0,12057	0,098039
B5-B1	-0,31525	-0,01109	0,060035
B5-B2	-0,32428	0,013198	0,067129
B5-B3	-0,3018	-0,00828	0,002427
B5-B4	-0,33076	0,120567	-0,09804
B1+B2	-0,08469	-0,27517	-0,07997
B1+B3	-0,01428	-0,3749	0,030392
B1+B4	-0,21618	-0,1947	0,056873
B1+B5	-0,2836	-0,06778	0,014885

Table B1 continued

Band name/ combination	April	June Chl-a	July
B2+B3	-0,15984	-0,23857	0,029156
B2+B4	-0,22324	-0,17878	0,05193
B2+B5	-0,28005	-0,07602	0,016045
B3+B4	-0,24393	-0,18405	0,094904
B3 + B5	-0,2962	-0,06747	0,053256
B4 +B5	-0,28434	-0,0947	0,059428
B1B2	-0,04047	-0,27651	0,02552
B1B3	0,013746	-0,33661	0,110193
B1B4	-0,14032	-0,26265	0,084405
B1B5	-0,20701	-0,15261	0,065039
B2B3	-0,10742	-0,19455	0,115565
B2B4	-0,16736	-0,16288	0,070417
B2B5	-0,21981	-0,07424	0,055794
B3B4	-0,17008	-0,207	0,124964
B3B5	-0,23794	-0,11399	0,111566
B4B5	-0,23256	-0,11224	0,029097
B1-B2/B1+B2	0,33287	-0,0474	0,104612
B1-B3/B1+B3	0,428093	0,031576	-0,12086
B1-B4/B1+B4	0,401935	-0,05814	-0,21338
B1-B5/B1+B5	0,400569	-0,11329	-0,03375
B2-B3/B2+B3	-0,10086	-0,03888	-0,25147
B2-B4/B2+B4	0,401949	-0,15991	-0,26353
B2-B5/B2+B5	0,410713	-0,12496	-0,0323
B3-B4/B3+B4	0,328203	-0,17218	-0,25123
B3-B5/B3+B5	0,370797	-0,13303	0,044517
B4-B5/B4+B5	0,353005	-0,13806	0,253172